MECHANICAL RELIABILITY OF POROUS LOW-K DIELECTRICS FOR ADVANCED INTERCONNECT: STUDY OF THE INSTABILITY MECHANISMS IN POROUS LOW-K DIELECTRICS AND THEIR MEDIATION THROUGH INERT PLASMA INDUCED RE-POLYMERIZATION OF THE BACKBONE STRUCTURE

by

YOONKI SA

Presented to the Faculty of the Graduate School of

The University of Texas at Arlington in Partial Fulfillment

of the Requirements

for the Degree of

DOCTOR OF PHILOSOPHY

THE UNIVERSITY OF TEXAS AT ARLINGTON

May 2015

Acknowledgements

First and foremost, I must express the deepest appreciation to my advisor, Prof. Choong-Un Kim for leading me further into the microelectronics society in both academic and industrial aspects, offering me the opportunities to raise the insights of research, providing continuous support and assistance throughout my doctoral research. Without his guidance and persistent help this dissertation would not have been possible. In addition, special thanks are extended to the other committee members Prof. Efstathios I. Meletis, Prof. Fugiang Liu, Dr. Nancy Michael, and Prof. Kyungsuk Yum for their thoughtful questions, encouraging words, and valuable feedback.

Next, although it is very difficult to mention all people who help and advise me during PhD study because there are so many, I would like to thank my all group members including old and current members, the faculties, staffs, students in the Materials Science & Engineering Department, and especially former fellow workers at KITECH, without whose teaching and support none of this would have been possible.

My last thanks should go to my parents. Their infinite encouragement and support have been the cornerstone to my success. I want to dedicate this thesis to them and express all my respects to them.

April 3, 2015

Abstract

MECHANICAL RELIABILITY OF POROUS LOW-K DIELECTRICS FOR ADVANCED INTERCONNECT: STUDY OF THE INSTABILITY MECHANISMS IN POROUS LOW-K DIELECTRICS AND THEIR MEDIATION THROUGH INERT PLASMA INDUCED RE-POLYMERIZATION OF THE BACKBONE STRUCTURE

Yoonki Sa, PhD

The University of Texas at Arlington, 2015

Supervising Professor: Choong-Un Kim

Continuous scaling down of critical dimensions in interconnect structures requires the use of ultralow dielectric constant (k) films as interlayer dielectrics to reduce resistance-capacitance delays. Porous carbon-doped silicon oxide (p-SiCOH) dielectrics have been the leading approach to produce these ultralow-k materials. However, embedding of porosity into dielectric layer necessarily decreases the mechanical reliability and increases its susceptibility to adsorption of potentially deleterious chemical species during device fabrication process. Among those, exposure of porous-SiCOH low-k (PLK) dielectrics to oxidizing plasma environment causes the increase in dielectric constant and their vulnerability to mechanical instability of PLKs due to the loss of methyl species and increase in moisture uptake. These changes in PLK properties and physical stability have been persisting challenges for next-generation interconnects because they are the sources of failure in interconnect integration as well as functional and physical failures appearing later in IC device manufacturing. It is therefore essential to study the fundamentals of the interactions on p-SiCOH matrix induced by plasma exposure and find an effective and easy-to-implement way to reverse such changes by repairing damage in PLK structure.

From these perspectives, the present dissertation proposes 1) a fundamental

understanding of structural transformation occurring during oxidative plasma exposure in PLK matrix structure and 2) its restoration by using silylating treatment, soft x-ray and inert Ar-plasma radiation, respectively. Equally important, 3) as an alternative way of increasing the thermo-mechanical reliability, PLK dielectric film with an intrinsically robust structure by controlling pore morphology is fabricated and investigated.

Based on the investigations, stability of PLK films studied by time-dependent ball indentation tester under the elevated temperature, variation in film thickness and dielectric constant, shows striking difference with small change in the chemical bond structure. Comparison of peak extracted by using FTIR (Fourier transform infrared spectroscopy) reveals that viscoplastic deformation and dielectric constant change correctly reflect the evolution in morphological structure of Si-O-Si peak. It is also found that hydrophilic nature of PLK matrix induced by silanol group is more involved with viscoplastic deformation rate and cage-like crosslinking in Si-O-Si peak is responsible for dielectric constant change. However, the level of instability driven by plasma exposure in PLK matrix is found to recover and desired mechanical and electrical properties are obtained by modifying the chemical bond configuration. Silylation process by HMDS (hexamethyldisilazane) works on recovery of hydrophobicity because it replenishes –C while removing –OH bonds. Contact angle is restored by controlling process temperature, however, the silylating agent cannot penetrate deep into PLK matrix without an adequate medium such as supercritical CO_2, making it difficult to implement. As a way of overcoming the limitation of UV cure, soft x-ray cure with Al Kα target is applied to induce gentle reconfiguration of chemical bond. It is possible to break bond links selectively by controlling x-ray energy level and also reduce thermal curing temperature due to the increased penetration depth. As a result of soft x-ray cure, film thickness loss almost not occurred. However, influence of x-ray radiation on the moisture removal is limited. Basically, oxidative plasma damage appears in two extensive areas. The first is the loss of –C from PLK matrix, and the second is the increase in hydrophilic nature involved with the formation of Si-OH terminal bonds and H_2O. Both alternations

cause the dielectric constant to degrade because of increased density and/or loss of free volume, but the second causes PLK to lose thermal and mechanical stability because Si-OH and H_2O act as catalysts for reactions that break the cross-linked backbone. Clearly, both changes in PLK chemistry and bond structure must be addressed in order for any repair method to be favorable. For this reason, Ar plasma treatment with low energy ions is employed to repair the plasma induced damage by creating the desired changes in the film matrix without a significant loss of other properties. Our approach of using inert plasma as a way for damage recovery is motivated by the realization that there is no possibility of chemical reaction with any organic species, driving the energy transfer only from the plasma species towards the respective film matrix. As results, after applying Ar plasma beam treatment followed by annealing on damaged PLK films, the resistance against thermal instability and viscoplastic deformation is found to be improved. Ball indentation depth of the films with Ar plasma process is drastically reduced at the identical condition. More noticeable is the fact that such alternation is converted towards a dehydration reaction under hydrostatic thermal pressure, which causes dielectric constant to decrease and films shrinkage to restore during reconstruction of polymer chains. It is suggested that the immediate event of an Ar plasma beam radiation is to deposit energy from the plasma species (ions, electrons) and this energy input produces the excited state species because Ar cannot chemically react with the film matrix. As a consequence, the radical sites are generated at the less stable area such as colony boundary or pore surface with the decay of the excited species, leading to the production of free radicals by an energy transfer to the bonds which are to be broken. Then, the activated sites experience chemical bond rearrangement by chain-scission, branching, or cross-linking. In our case, crosslink with C is involved with silylmethylene (Si-$(CH_2)_x$-Si) groups and it is turned out that some of these groups are converted to methyl groups terminally bonded to siloxane backbone structure under 300~400^oC by reaction with –OH, and simultaneously creating a new Si-O-Si crosslink.

As an alternative way of increasing the thermo-mechanical reliability, PLK dielectric film

with an intrinsically robust structure by controlling pore morphology is fabricated. Since pore surface is susceptible to be damaged by BEOL integration damage, pore morphology in terms of size, distribution, and connectivity should be controlled in order to increase the robustness of PLK dielectrics. Generally, pores in PLK matrix are created by depositing organic fragment (called 'porogen') into the film and removed later by thermal and electron beam cure to form porous PLK layer (; Subtractive deposition). However, during the curing Si-O-Si backbone crosslink is broken and pores are easily interconnected, leading to vulnerable structure to the extrinsic damage. Constitutive deposition approach is feasible for the introduction of smaller nano-pores with little or no interconnectivity by steric hindrance. Due to the closed pore system, thermally-induced stress and plasma-induced damage is restricted merely to the surface of the dielectric film. This is attributed to the stable siloxane (Si-O-Si) backbone and the terminally bonded methyl group attached to silicon ($Si-CH_3$), inducing steric hindrance that lowers the density of the films. The low dielectric constant and mechanical stability are closely involved with the formation of the Si-O-Si cage-like structure and an appropriate combination of stable Si-O-Si, $Si-CH_3$ groups. Based on the FTIR and XPS spectra, it is concluded that the formation of the Si-O-Si cage-like structure was enhanced by structural method.

It is believed that all these changes are beneficial for improving PLK stability as will be detailed in this dissertation. Especially, the originality and particular advantage of this study regarding plasma-induced damage repair will be highlighted.

Table of Contents

List of Illustrations

List of Tables

Chapter 1

INTRODUCTION

1.1 Implementation of Cu/low-k interconnect

In the integrated circuit (IC), the interconnect wiring structure serves as an essential function in carrying electrical signals and distributing clock signals that control the timing and synchronize the operation. It includes the metal wires that connect the individual devices (e.g. transistor, capacitor, and resistor) and the interlayer dielectrics (ILD) that isolate and mechanically support the wires. Recently, IC logic chip processor speed reaches several GHz and random access memory (RAM) capacity does several tens GB while critical dimensions of the consumer electronics are continuously miniaturized, driving to ultra-large-scale integration (ULSI) with a hierarchical system containing multilevel of metallization layers. The cross section of a typical interconnect structure is shown in Fig. 1.1 and Fig. 1.2(a). [1]

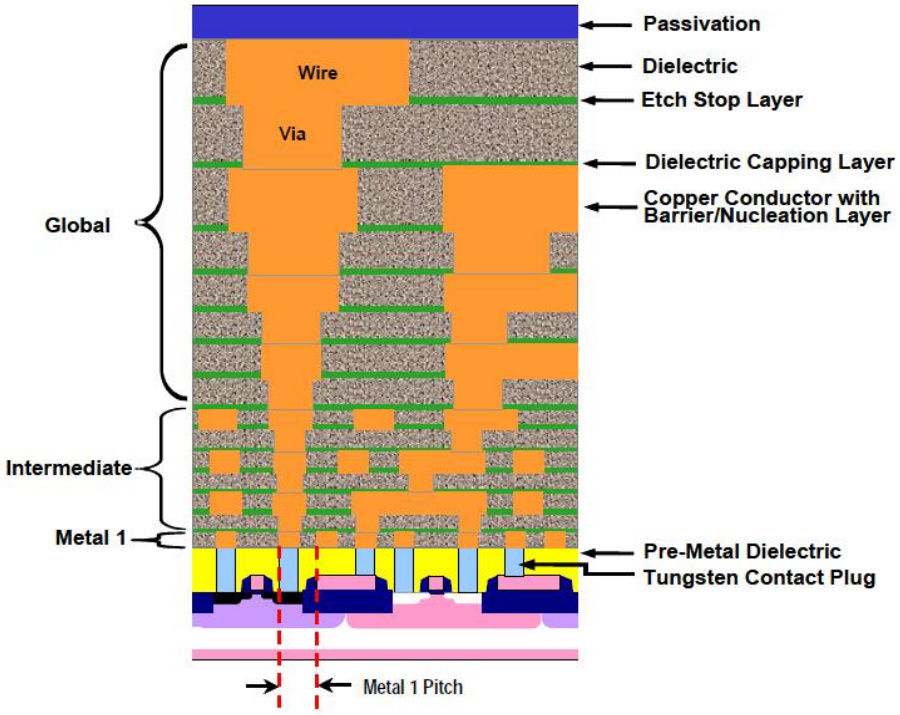

Fig. 1.1 Typical cross-section of the interconnect structure indicating the hierarchical scaling

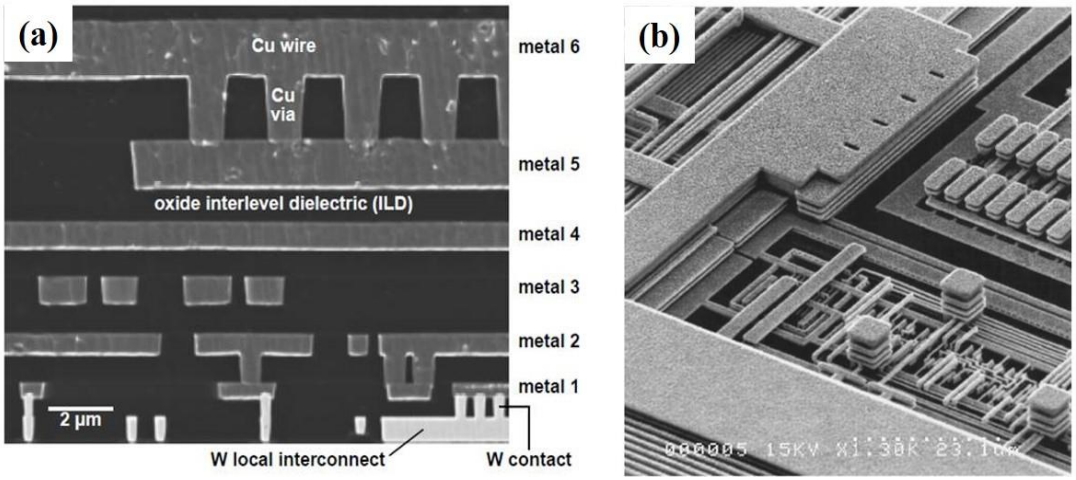

Fig. 1.2 Scanning electron microscopy (SEM) images of interconnect architecture; (a) with Cu wire, Cu via, and ILD, (b) without ILD [2,3]

The important fact is that ULSI with multilevel of metallization layers brings an increase of complexity in IC structure and compels the overall interconnect length to increase and pitch size between metal wires in IC to become finer, which leads the sharp increase of parasitic capacitance as the space between metal wires decreases. Hence, this scaling effect causes the signal propagation to be delayed through the intrinsic gate delay and interconnect delay. Basically, device performance in terms of the response speed in an IC is governed by two components: (1) the switching speed of an individual transistor, known as the transistor gate delay, and (2) the signal propagation time between transistors, known as interconnect or RC delay, where R is metal wire resistance and C is ILD capacitance. The continuous scaling down of the multilevel integrated circuits requires the metal wires to be thinner and closer each other, inducing the increase of the resistance and capacitance in the device. It has been recognized that the delay and power consumption raised by interconnect wires is the limiting factor upon further improvement for system performance. According to Saraswat et al. the RC delay associated to the resistance and the capacitance between the wires is given by

$$RC = 5.53\varepsilon_0 k\rho \frac{A}{F_{min}^2} \quad (1.1)$$

where ε_0 is the permittivity of vacuum, k is dielectric constant of the insulator, ρ is the resistivity of metal wire, A is the area of the chip, F_{min} is minimum feature size in the chip, respectively. [4] Equation (1.1) suggests that the reduction of feature size can lead to a sharp increase in the RC delay time. Therefore IC performance has been relying on the switching speed of transistors over the last decade, however, it is determined by RC delay these days. Fig. 1.2 shows the trend of interconnect delay versus technology generation. To some point (250 nm for Al/SiO_2 interconnect, and 180 nm for Cu/low-k interconnect), gate delay is dominant factor for device performance, however, as the feature size shrinks, interconnect delay dominates. Traditionally, metal wires are made of vapor deposited aluminum and the interlayer dielectrics are silicon dioxide (SiO_2). In order to improve the device performance, therefore, resistance of aluminum metal wire and capacitance of dielectrics should be reduced. The metal resistance is reduced by substituting the traditional aluminum (Al) wire with copper (Cu) wire because of the lower resistance of Cu relative to Al. In addition, the traditional interlayer dielectric SiO_2 (k~4.0) is replaced by low dielectric constant materials (k<3.0). Dielectric constant can be reduced by decreasing the density, polarizability, and permanent dipole moment of dielectric. This is achieved by introducing C, H, and F elements as well as pores to reduce the film density and the polarizability per unit volume of the dielectric material. [5]

Another major concern for interconnects is power consumption. Dynamic power consumption is given by

$$P = \alpha C f V^2 \tag{1.2}$$

where α is the wire activity (i.e., when the wire is really transferring a signal), f is the frequency, V is the power supply voltage, and

$$C = C_{output} + C_{wire} + C_{input} \tag{1.3}$$

where the output and input capacitance of the transistors and the capacitance introduced by the wires are all included. Additionally, to a lesser extent, power dissipates statically through the leakage current between wires. According to equations (1.1) and (1.2), the situation may be

addressed by using metals with lower resistivity as the interconnect wires and dielectrics with lower permittivity as the insulator. The interconnect delay calculated with copper wires and low-k dielectric insulator shows significant decrease as compared traditional interconnect. (see Fig. 1.3) Therefore, with recent decision to replace Al/SiO_2 by Cu/low-k in the integrated circuit IC chips and package, the implementation of low-k dielectric in Cu interconnect structures has become one of the key subjects in the microelectronics industry.

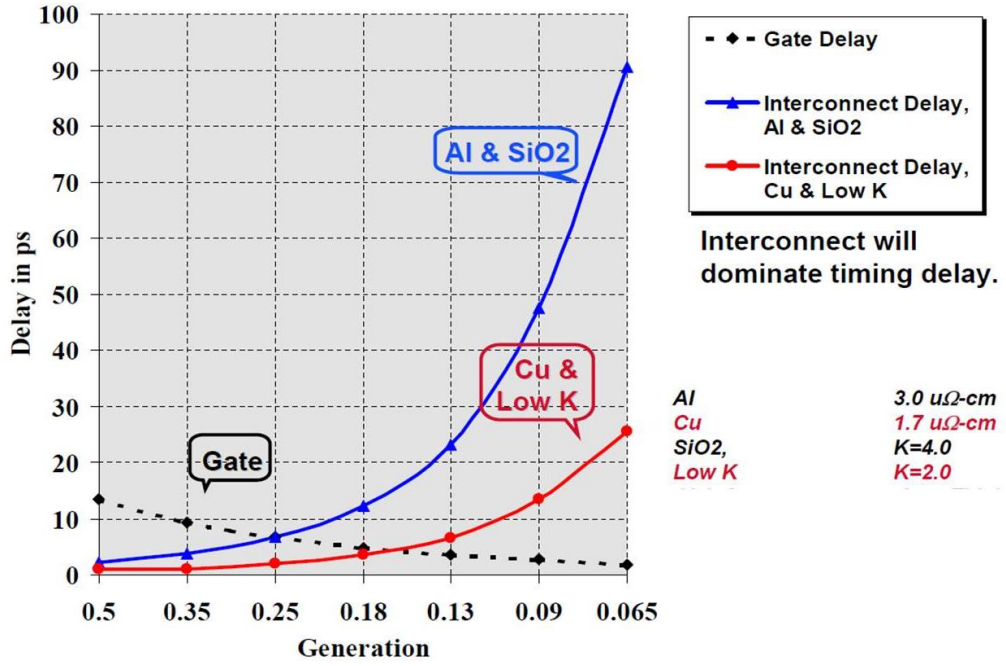

Fig. 1.3 Gate and interconnect delay versus technology generation (unit: um) [6]

1.2 Low dielectric constant (low-k) materials

Generally, low-k dielectrics are defined as the materials with a dielectric constant less than 4.0 which is the value of silicon dioxide dielectric constant. Dielectric constant refers to the permittivity of dielectric with respect to that of vacuum as shown in Fig. 1.4. Since dielectric constant of air or vacuum is defined as 1, the lowest possible dielectric constant is 1, which technology to incorporate the air or vacuum is known as air gap. While Cu is the most probable choice of metal for interconnect to decrease the resistance since no other metal can offer notable

advantages, the choices of low-k dielectrics can be various. Therefore, the further reduction of RC delay depends on the continuous development of low-k material with a dielectric constant lower than SiO_2, the standard dielectric material used for interconnect. As indicated in the roadmap for implementation of low-k dielectrics (Fig. 1.5), the effective dielectric constant is decreasing and expected to reduce to below 2.0 in the future. [1]

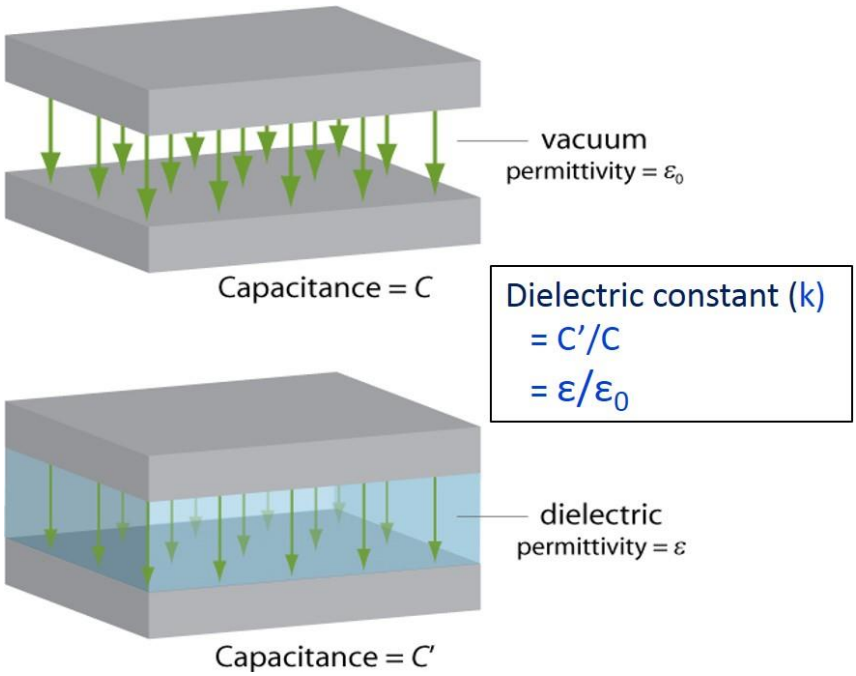

Fig. 1.4 Definition of dielectric constant (k)

Year of Production	2001	2002	2003	2004	2005	2006	2007	2010	2013	2016
MPU 1/2 Metal One Pitch (nm)	150	130	107	90	80	70	65	45	32	22
Interlevel metal insulator (minimum expected) —bulk dielectric constant (k)	<2.7	<2.7	<2.7	<2.4	<2.4	<2.4	<2.1	<1.9	<1.7	<1.6
Interlevel metal insulator - effective dielectric constant (k)	3.0-3.6	3.0–3.6	3.0–3.6	2.6–3.1	2.6–3.1	2.6–3.1	2.3–2.7	2.1	1.9	1.8

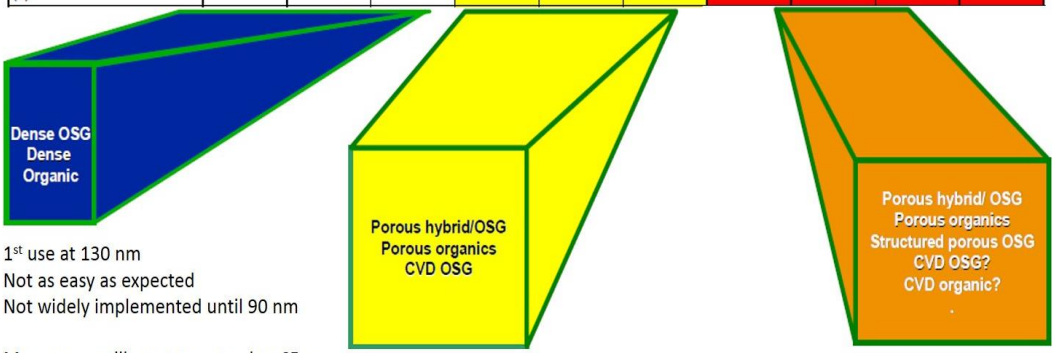

1st use at 130 nm
Not as easy as expected
Not widely implemented until 90 nm

Many users will want to extend to 65 nm node

Many material candidates
Many new problems encountered
(pore sealing, lower mechanical strength, plasma-induced degradation, etc.)

Most current materials are extensions of k > 2.2 versions

Outlook for k ~2.0 uncertain

Fig. 1.5 Roadmap for implementation of low-k dielectric materials

The reduction in dielectric constant of ILD is achieved through the incorporation of atoms and bonds that have a lower polarizability, or the decrease in density of material as described in Clausius-Mossotti-Debye equation. [7]

$$\frac{k-1}{k+2} = \frac{N}{3\varepsilon_0}\left(\alpha_e + \alpha_i + \frac{\mu^2}{3kT}\right) \tag{1.4}$$

where N is the density of the material (number of molecules per cm^3). α_e is the electronic polarization, which describes the displacement of the cloud of bond electrons with reference to the nucleus under an applied electric field. α_i is the ionic polarization, which is induced by the displacement of the nuclei by the applied electric field, thereby stretching or compressing the bond length. The third term in equation (1.4), $(\frac{\mu^2}{3kT})$, describes the dipolar polarization, where μ is the orientation polarizability, k is the Boltzmann constant and T is the temperature. The term $(\frac{\mu^2}{3kT})$ is the thermal averaging of the permanent electric dipole moments in the presence of an applied

field. Depending on the signal frequency of the applied electrical field, the relative dominance of each polarization mechanism varies. The latter two polarization mechanisms contribute to polarization and are important at lower frequencies ($<10^{13}$ Hz), while the electronic polarization dominates in dielectric permittivity at higher frequencies ($\sim10^{15}$ Hz). [8] At typical device operating frequencies, currently $<10^{9}$ Hz, all three polarization mechanisms are important in the dielectric constant and should be minimized for optimum performance. [5] Among all the possible approaches for decreasing the dielectric constant of ILD, the most effective approaches is to reduce the volume density because the reduction of density indicates the decrease of the total number of electronic and ionic dipoles per unit volume. The density can be reduced by using lighter atoms such as C and H atoms and/or by introducing more free space around the atoms. Accordingly, incorporation of pores into the existing SiO_2 is a favorable approach to increase the free space and decrease the ILD density. There are two methods for adding pores into existing low-k materials: subtractive and constitutive method. [5,8] In the subtractive method, a skeleton precursor mixed with an organic precursor (which is called porogen) is introduced by using the PECVD. During curing of the dielectric, the organic precursor burn out from the dielectrics, leaving nano-size pores. [9] The constitutive method for fabricating low-k materials is the porogenless structural approach. The porosity in the film can be obtained by using particular precursors that contain molecular pores when the film cross-links during annealing, leaving behind pores. [10-14] The description of lowering dielectric constant is shown in Fig. 1. 6. The organic polymers were considered at first because they can be formed with non-polar C-C bonds. However, this category of material had many issues, including thermal instability at high temperature, weak mechanical properties and high coefficient of thermal expansions (CTE). These factors present significant difficulties for integration in the existing IC processing technology. This has led to the development of the main approach adopted by the industry which is to use SiO_2-like low-k materials. This category of materials can be easily integrated into existing technology since the SiO_2 integration

is highly developed. The polarizability of SiO_2 can be decreased by introducing less polarized bonds, such as Si-F, Si-H, or $Si-CH_3$, into the silicon network.

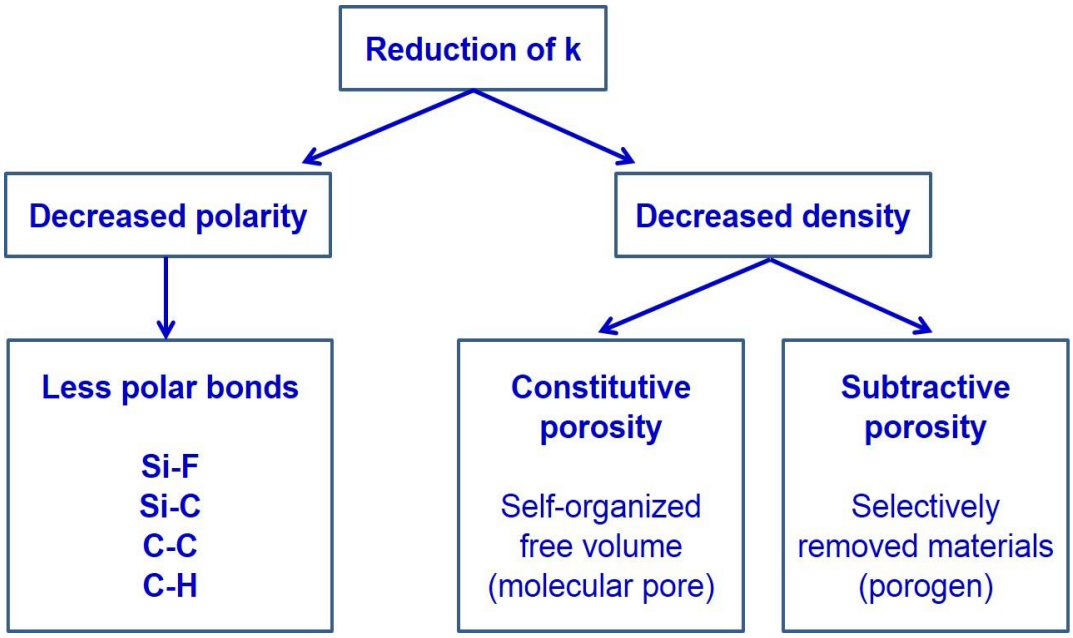

Fig. 1.6 Description of lowering dielectric constant

The effect of porosity on dielectric constant can be predicted by using the Bruggeman effective medium approximation model [15, 16]:

$$f_1 \frac{k_1 - k_e}{k_1 + 2k_e} + f_2 \frac{k_2 - k_e}{k_2 + 2k_e} = 0 \qquad (1.5)$$

where $f_{1,2}$ represents the fraction of the two components, $k_{1,2}$ the dielectric constant of the components, and k_e is the effective dielectric constant of the material. The model assumes two components to the film: the solid dielectric material and pores. Since the dielectric constant of free space is unit, the introduction of pores reduces the dielectric constant by lowering the density of the ILD. However, the drawback of incorporating pores in a material is to reduce the mechanical strength and degrade thermal properties, which leading to potential reliability issues as well as significant integration challenges in advanced Cu/PLK interconnects. Such reliability issues and integration challenges will be reviewed in more details in section 1.4.

As described in Fig. 1.7, from 90 nm technology node, SiCOH materials have been mainly studied and used for interlayer dielectrics. [17] The name “SiCOH” indicates the elemental composition of the material but does not represent the stoichiometry. The SiCOH material is formed by introducing carbon molecular bonds (mainly through CH_3 groups) into a silica matrix, which reduces both the total polarizability as well as the density of the material. The SiCOH materials, therefore, is also called carbon-doped oxide (CDO) or organosilicate glass (OSG).

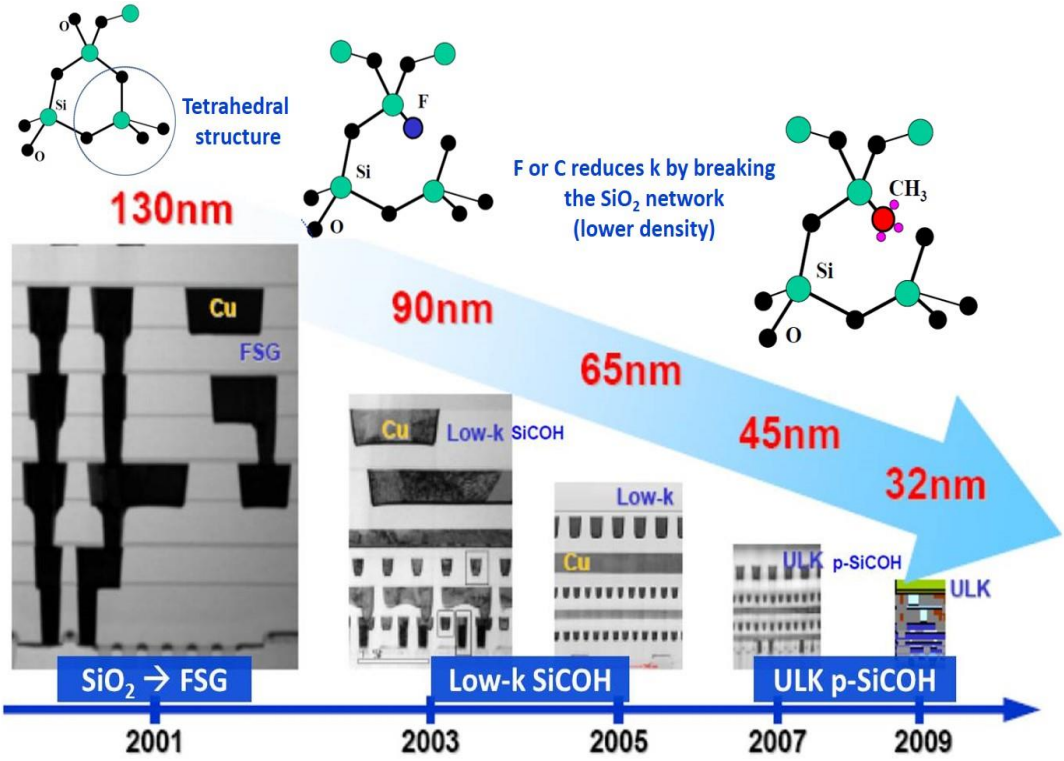

Fig. 1.7 Trend of interlayer dielectric materials

The implementation of SiCOH materials can reduce the effective k value to 2.7. To achieve lower k value, the density of the material needs to be further reduced by introducing porosity in the low-k material. The k value of a porous material with porosity P is expressed by the following equation:

$$\frac{k-1}{k+2} = (1-P)\cdot\frac{k_m-1}{k_m+2} \tag{1.6}$$

where k_m is the dielectric of the matrix material without porosity and all pores are assumed to empty or filled with a substance that has k=1. With the introduction of porosity, the ultralow-k (ULK) material, which is defined as material that has a k value lower than 2.5, was produced. The ULK material used in this dissertation is a porous SiCOH (p-SiCOH) material provided by GLOBALFOUNDRIES and INTEL Corporation.

A porous SiCOH dielectric layer is deposited by using plasma enhanced chemical vapor deposition (PECVD). It is the most used approach in the industry and first introduced by Grill et al. [18] In this process, the film is deposited using at least two precursors in the plasma, where one of them is a pure organic molecule (sacrificial nanoparticle) referred to as a 'porogen'. The other precursor consists of silicon atoms and organic radicals and is called the 'matrix' precursor. The plasma interaction of these precursors forms a "hybrid" film composed of an organosilicate-based matrix enclosing the porogens. Then, the porogens are removed by a post-deposition treatment such as thermal annealing or UV treatment, resulting in a porous SiCOH film with ultralow-k properties.

1.3 Fabrication of low-k dielectrics

Low-k or porous low-k films can be categorized into two, based on the method to obtain these materials. The two methods are spin-on and chemical vapor deposition (CVD). Both the deposition techniques have their advantages and disadvantages and there is very little agreement that which of the two techniques is best suitable for future technology.

For the spin-on deposition, the dielectric precursors mainly consist of organic or inorganic polymer matrixes mixed with solvent along with porogen precursors to make porous films. There are several steps involved in spin coating: first the substrate on which the low-k film has to be coated is placed on the spinner and the precursors are dispensed onto the center of the substrate at room temperature and ambient pressure. The second step is to rotate the spinner to produce a uniform distribution of material on the substrate by the creation of centrifugal force

[8]. The thickness and uniformity of the coated film are dependent on the viscosity of the film, the spinning rate and the evaporation rate of the solvent. The coating is subsequently cured to at temperatures typically around 200ºC to remove the solvent and induce polymerization and cross-linking of the precursors. Lastly, heating to temperatures typically around 400ºC, or using e-beam technology is required to remove organics and porogens. This baking and curing steps result in the final cross-linking of polymer chains which gives desirable mechanical strength to the film.

Chemical vapor deposition has widely gained importance in depositing thin films [19]. The CVD is a process in which chemical components from a gas phase absorb and react on the surface of substrate in a vacuum environment. There are several methods of CVD deposition such as APCVD, done at atmospheric pressure, LPCVD, done at low pressure and PECVD which is a plasma-enhanced CVD process. Recently, most of the low-k films have been deposited by a subtractive PECVD technique. In the subtractive technique, precursor materials such as diethoxymethylsilane (DEMS), octamethylcy-clotetrasiloxane (OMCTS) and tetramethylcyclotetrasiloxane (TMCTS) can be introduced into the PECVD reactor and deposited on the substrate. (see the structure of precursors in Fig. 1.8)

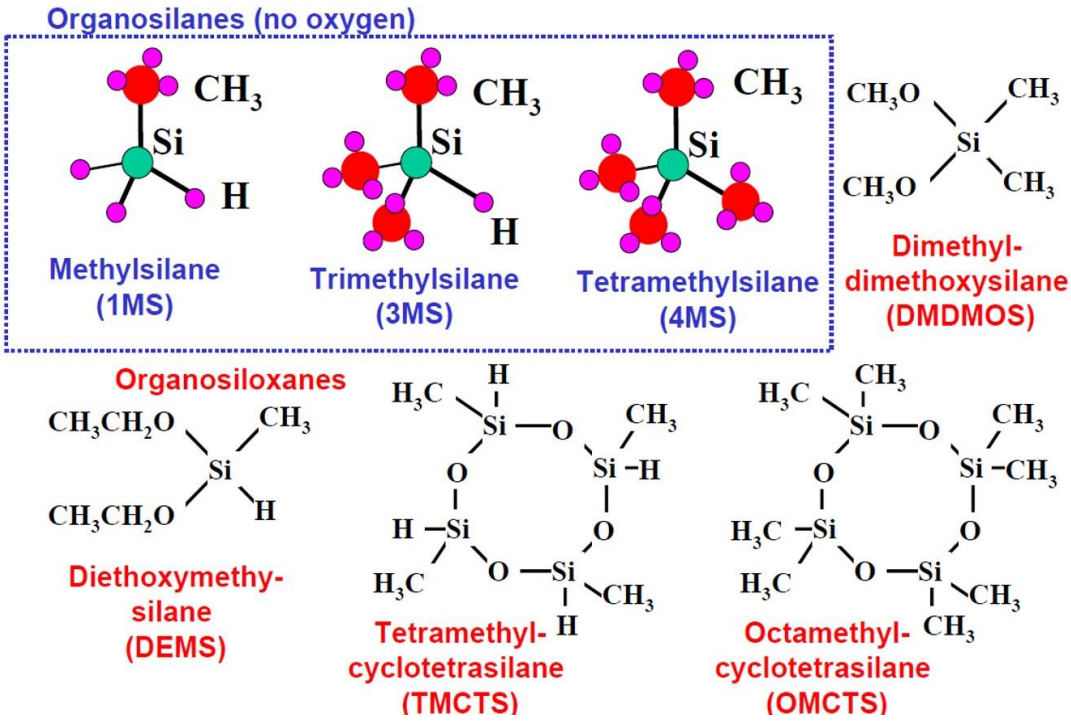

Fig. 1.8 Schematic illustration of precursor structures for CVD OSG [20]

During the deposition of the precursor, a volatile organic species or porogen precursors are mixed with the matrix precursor, creating a dual phase material like SiCOH-CH_X material. The organic species (the labile CH_X fraction) or porogens are removed by either annealing the film for several hours at temperatures below 400ºC or annealing it with energetic species such as electrons (EB cure) or photons (UV cure) at 350-400ºC. By the removal of the porogen during curing process, the decomposed precursor forms a porous low-k film (pSiCOH) with a silicon dioxide skeleton and terminating organic groups, consisting of hydrogen or methyl groups (-CH_3) [9]. Such materials are called porous low-k dielectrics (PLK), and hence make it possible to further reduce dielectric constant of low-k materials by the reduction in film density due to the fact that the methyl group is substituted for oxygen in SiO_2. This is because replacing an oxygen atom by a -CH_3 group introduces a less polar bond and creates additional free volume. It is called constitutive porosity.

Table 1.1 summarizes the recognized dielectric material candidates for ILD integration.

Table 1.1 Candidates for low-k dielectrics [21,22]

Materials	K value	Deposition Methods
SiO_2	3.9 – 4.2	CVD
Fluorosilicate glass (FSG)	3.2 – 4.0	CVD
Diamond-like Carbon (DLC)	2.7 – 3.4	CVD
Fluorinated DLC	2.4 – 2.8	CVD
Black Diamond ™ (SiCOH)	2.7 – 3.3	CVD
Parylene-F	2.4 – 2.5	CVD
Parylene-N	2.7	CVD
Hydrogen silsesquioxane (HSQ)	2.9 – 3.2	Spin-on
Methyl silsesquioxane (MSQ)	2.6 – 2.8	Spin-on
B-staged Polymers (CYCLOTENE and SiLK)	2.6 – 2.7	Spin-on
Fluorinated Polyimides	2.5 – 2.9	Spin-on
Polyimides	3.1 – 3.4	Spin-on
Poly (arylene ether)(PAE)	2.6 – 2.8	Spin-on
PTFE	1.9	Spin-on
Porous HSQ	1.7 – 2.2	Spin-on
Porous SiLK	1.5 – 2.0	Spin-on
Porous MSQ	1.8 – 2.2	Spin-on
Porous PAE	1.8 – 2.2	Spin-on
Aerogels/Xerogels (Porous Silica)	1.1 – 2.2	Spin-on
Air Gaps	1.0	?

1.4 Integration and reliability challenges of Cu/low-k interconnect

The tremendous number of difficulties appearing during the integration of the low-k into copper dual-damascene structures delayed the introduction of these dielectrics as compared with the ITRS roadmap predictions. [23] For dense low-k materials, the poor mechanical and thermal properties were identified as the main showstoppers for their integration. However, in the case of ultralow-k materials the introduction of pores increases the number of integration issues even further. In this section, the integration issues linked with the porosity in ultralow-k dielectrics (as schematically shown in Fig. 1.9) will be discussed in more detail.

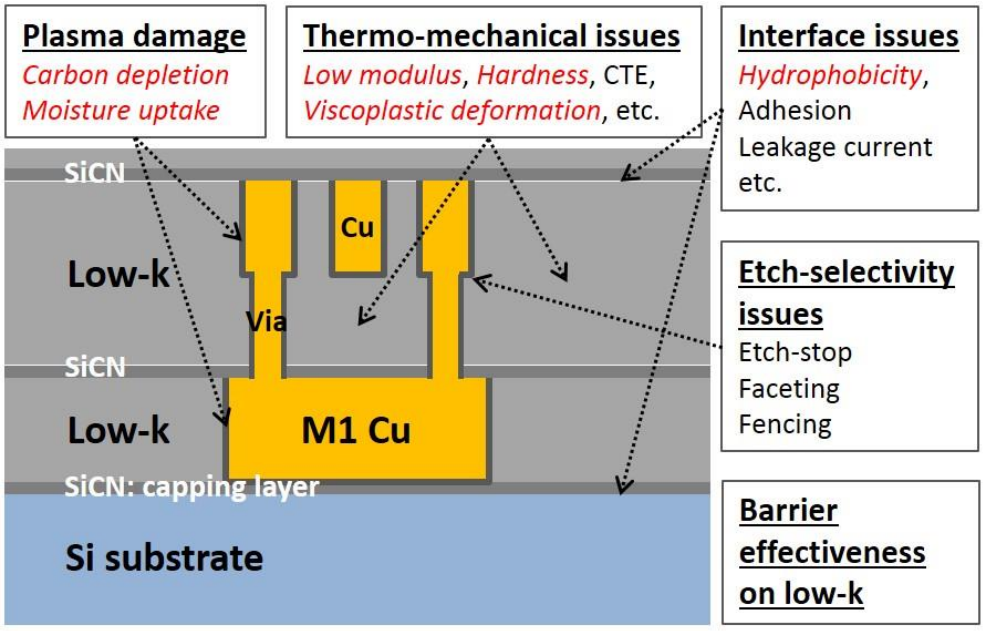

Fig. 1.9 Integration challenges and issues of porous low-k dielectrics

1.4.1 Mechanical reliability

The introduction of porosity into dielectric films leads to inferior mechanical properties as compared to their dense equivalents. Both elastic modulus and hardness are decreasing with increasing porosity in the low-k matrix. [8] While the elastic modulus has been shown to correlate with the ability to survive integration processes, which involve large mechanical force, such as chemical mechanical polishing (CMP) [24], it appears not to be the only parameter for mechanical performance of dielectric materials. The ability to withstand stress without crack propagation (i.e. fracture toughness) is also important. Like the modulus, the fracture toughness degrades with porosity. Modeling of the fracture toughness revealed that the softest of these materials, porous aromatic organic materials, show the most attractive fracture toughness capability. [25]

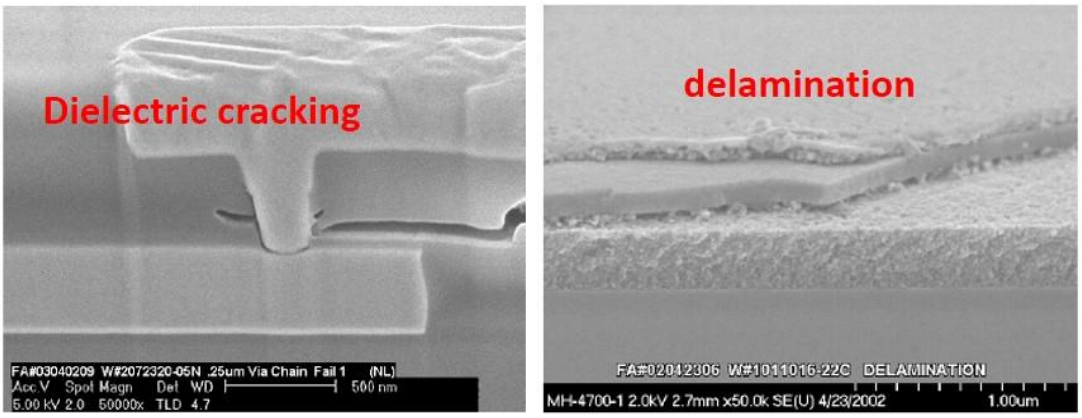

Fig. 1.10 Examples of weak mechanical property issue during integration

In addition to the inferior modulus, the lower adhesion strength of low-k materials can also initiate interfacial crack formation and propagation [26]. Adhesion can be improved by careful interface engineering. It is well known that additional treatments, such as plasmas, can enhance both adhesion and elastic modulus by densification of the surface [27]. Unfortunately, a negative side effect of this densification is the deterioration of the low-k properties, as will be discussed later on in the section ‘plasma damage’. The elastic modulus can also be improved through UV and/or e-beam cure treatments [28-30]. Due to the large penetration depth of these treatments, the low-k material will be altered throughout the entire layer (and not all low-k properties might benefit from that) and the CMOS transistors underneath might even be affected [30].

Although CMP compatibility might be the first manifestation of mechanical failures, the ability to withstand packaging stresses and lifetime testing is essential to successful integration of low-k materials. In addition, more and more metal levels are required in interconnects, due to increasing circuit complexity and density. Consequently, the question arises whether the increasing number of layers will have an impact on the reliability and failure mechanisms of the structures within packages. Extensive thermos-mechanical modeling [26-30] has been used to understand the stresses induced in the die back-end layers due to the package, and to identify the key modulators that impact these stresses.

1.4.2 Thermal conductivity

In general, there are three causes of interconnect temperature rise: Joule heating (i.e. metal resistive heating), heat dissipation from the substrate and heat dissipation from nearby interconnect lines. As increasing temperatures in the interconnect will lead to increasing line resistances and decreasing electromigration lifetimes, the heat flow to a cooled substrate has to be maximized. The thermal conductivity decreases rapidly with the incorporation of porosity, as heat conduction is limited to the solid phase of a porous material. The low thermal conductivity might cause heat dissipation problems. Hence, simulations of the thermal behavior of interconnect systems, using low-k dielectrics and copper, are important. For that, the measurement of the thermal conductivity is a prerequisite. Delan et al. [31] used the 3ω measurement technique (transient hot wire method) to determine the thermal conductivity of a variety of low-k materials. All of them were found to be in the range 0.11-0.19 W/mK, which is a factor of 13 - 7 smaller than thermally grown SiO_2.

In advanced technology nodes, the poor thermal conductivity of low-k materials does not facilitate the heat transport to the substrate sufficiently. Therefore, more research is needed to investigate the use of the metal as heat carrier, since it provides a low thermal resistance path. Chiang et al. [32] proposed using dummy metal (stacked vias) in advanced interconnect structures to transport the heat to a sink. They have shown that thermal vias would be required approximately every 30 μm in copper-polymer interconnect structures and every 20 μm in copper-air to match the temperature rise of copper-SiO_2. The latter suggests that the issue of thermal conductivity might be solved by optimized mask design.

1.4.3. Chemical stability and moisture absorption

With respect to chemical reliability issues, the pore structure makes the low-k materials prone to the penetration of moisture and other chemicals during the integration process such as

CMP, plasma-based etching and ashing. It has been reported that low-k materials are vulnerable to moisture contamination even though they are usually hydrophobic. [33-40] In order to remove the absorbed moisture in the low-k films, annealing or curing process is usually carried out at high temperatures within the range that the low-k material can tolerate. However, a portion of chemisorbed and/or trapped moisture in low-k materials typically is not removed thoroughly. Moreover, when the low-k samples are exposed to a moisture-rich environmental again, re-adsorption of moisture may occur. [35] The existence of moisture in low-k films can have a negative influence on electrical reliability of interconnect structure and their mechanical integrity. With regard to electrical reliability, the dielectric constant value of water or moisture is as high as 80 due to the polar O-H bonds, so that even a small amount of water intrusion into the low-k films can significantly raise the dielectric constant of porous low-k films.

Water also impacts the leakage current of the dielectrics adversely. From the mechanical point of view, the presence of water deteriorates interface-adhesion properties between dielectrics and cap layers. [41,42] Such a moisture uptake is especially important for porous low-k materials because they have a large surface area per unit volume, where moisture could potentially be adsorbed, resulting in even more severe and problematic reliability issues in Cu/PLK interconnects.

1.4.4. Plasma-induced damage

Plasmas are widely used in the semiconductor industry. Many materials, including most low-k materials, are deposited using CVD-plasmas; plasmas are used to transfer the resist-pattern into the deposited films and nowadays more and more additional plasma treatments are used to improve adhesion and mechanical strength and to seal the porous surfaces. All these plasmas will however differ on chamber design and processing details, such as e.g. reactant concentration, power and duration. These factors determine the performance of the process, as well as the extent of the plasma damage in the low-k films.

A commonly observed consequence is carbon depletion of (non)-porous organosilicate or silsesquioxane films after resist-ashing using an O_2-based plasma. [43-47] Oxygen radicals oxidize the Si-CH_3 and the Si-H groups and convert them into a Si-OH group. Since the Si-OH group is hydrophilic, it easily induces moisture uptake. For higher porosity low-k films, the impact of this damage is expected to increase, since the penetration of the radicals will be deeper as well as the absorption of water. The latter can lead to dramatic k-value increments. The contribution of this damage on the overall electrical performance gains importance as the dielectric spaces between the interconnect lines shrink.

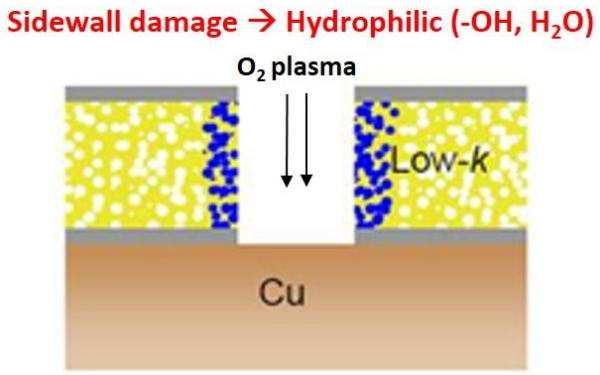

Fig. 1.11 Schematic description of plasma-induced damage

When the technology approaches 45 nm or lower, low-k materials have more methyl groups and pores to further reduce dielectric constant. In such a case, the plasma damaging effect is more pronounced for highly porous low-k materials, causing reliability issues and yield loss in Cu/PLK interconnects.

Since resist ashing is assigned to be the most critical process for low-k materials, most attempts to minimize the plasma damage are focused on new ashing processes and / or new integration schemes. H_2/He ashing seems to be one of the most promising resist removal processes for post-etch wafer cleaning compatible with SiOC films. [47-49] The physical damage caused by these light ions is reduced, however the chemical damage can still be extensive. It

should also be mentioned that this process is quite inefficient in resist-removal and it should therefore be operated at elevated temperatures (to reduce the ash-time and consequently the plasma damage). [48]

Other researchers focus on shifting the resist removal process to an earlier point in the integration flow, consequently the low-k will not be exposed to the ash-plasma. Most of these approaches involve the use of multiple CVD hard masks [50,51] or metal hard masks. [52,53] The resist patterns are transferred into the hard mask layers. After removing the resist, the low-k is patterned using the hard mask. The remainder of the hard masks on the dielectric layer after etch will be removed during the CMP process.

All these hard mask approaches assume that the ash plasma causes the major part of the sidewall damage. However, the damage by the etch-plasma should not be neglected. The carbon-depleted sidewall region has been decorated by a diluted HF-treatment, which selectively etches SiO_2. The plasma damage caused by the oxygen-free via-etch cannot be neglected, since a large part of the sidewall has been etched. In addition, a thin fluorine-containing polymer-layer was found to be present at the sidewalls. In contrast to what was expected, this passivation layer was not able to stop the plasma damage.

The possibility of repairing the plasma damage in organosilicate or silsesquioxane films is being investigated as well. These techniques involve the use of silylating agents, such as trimethylchlorosilane (TMCS) [54] or hexamethyldisilazane (HMDS). [54-56] The hydrophilic Si-OH groups are replaced with hydrophobic Si-O-Si$(CH_3)_3$. The change of hydrophobicity reduces the moisture uptake and consequently restores the k-value to a large extent. However, due to the presence of a densified surface layer, the repair of the low-k materials will occur mainly at the surface.

As at present, it seems extremely challenging to exclude plasma damage during the integration of ultralow-k materials into on-chip interconnects, some authors [57,58] proposed hybrid integration schemes. In these approaches, the SiOC material at trench-level is replaced

with a porous aromatic polymer (i.e. porous SiLK) in order to prevent plasma damage at these levels. Preliminary capacitance measurements [59] suggest however that the porous organic polymers are also prone to plasma damage (accompanied by a significant k-value increase), which would eliminate the advantage of the hybrid integration approaches.

More recently, researchers demonstrated successful integration of ultralow-k materials using a gap fill based integration scheme. [60] In this approach, a reliable metal level is fabricated in a dense organic or inorganic material. Following the metal CMP, the bulk dielectric is selectively etched out between the metal lines. After the etch-back, any desired low-k material can be used for (over) filling the gaps. However, in this scheme it is necessary that the deposited low-k fills the narrow gaps and withstands direct CMP. This expensive approach also shows the desperate need for a breakthrough in the “red brick wall” in the back-end-of-line part of the ITRS roadmap. [1]

1.5. Research motivation

As discussed, continuous scaling down of the multilevel integrated circuits requires replacing interlayer dielectrics to improve device performance by reducing resistance-capacitance coupling delay. The International Technology Roadmap for Semiconductors (ITRS) indicates that permittivity of dielectric constant (k) with below 2.0 will be required for inter-level metal insulators in the future. [1] In accordance with this technology trend, embedding nano-size pores into the carbon-doped oxide dielectrics (SiCOH) has become the leading approach to produce the ultralow-k materials. However, the porosity incorporation into a dielectric material necessarily decreases mechanical properties and increases its active surface area, making it more susceptible to potential damage from the reactive chemicals used in plasma etch and ash during device process. Therefore, lowering of the effective dielectric constant while maintaining the mechanical and electrical reliability of PLK dielectric thin films has been extensively studied as a key factor in Back-End-Of-Line (BEOL) integration. [8,61] Equally important is to find an effective way to restore the physical and chemical changes during the integration processes to

the original structure.

In the BEOL integration of semiconductor devices, one of the major applications of plasma exposure process is the removal of photoresist and polymer residues after dry etching process. [62] Plasma exposure to the dielectrics film causes complex change in the chemistry morphology involved with carbon depletion and the formation of Si-OH (silanol) or Si-H bonds, and film densification. [63-65] Among various plasma sources, exposure of SiCOH films to O_2 plasma induces breaking of Si-CH_3 and thereby, relatively non-polar Si-CH_3 groups are replaced with significantly more polar Si-OH groups and oxidized carbon groups. These changes in surface chemistry upon plasma exposure produced significant increases in the dispersive and polar surface energy components. [66] In addition, Sun et al. and Lee et al. reported that O_2 plasma treatment induced the pore collapse and the densification of low-k dielectrics materials between pores, leading to the non-uniform structure degradation in porous low-k dielectrics. [67,68] A series of these changes result in the loss of hydrophobicity as well as the increase in the dielectric constant due to polarizability of silanol and moisture uptake, making PLK films to instigate various physical and functional reliability failure of the interconnects. It is therefore important to fabricate the robust PLK dielectric matrix that creates less damage to physical and chemical structure of PLK. Equally important is to find an effective and practical way to remove the damage in PLK matrix incurred by integration processes and restore their original stability. Several methods of damage restoration have been proposed in the past, most notably the silylation treatment; however, they offer limited effectiveness, and also, they are not easy to incorporate into the flow of integration processes. For example, $SCCO_2$ based process requires high pressure (~80 bar) to maintain supercritical state of CO_2 and thus pose considerable challenges in its implementation to actual fab environment. Furthermore, the byproduct of silylation reaction may react with CO_2 forming a residue that produces adverse influence on the PLK properties. [69] UV cure has been also reported that it induces Si-O-Si crosslink by condensation reaction. However, UV cure is usually conducted at high temperature of 400^{o}C, which causes thickness shrinkage. It is

potentially problematic source of integration process when it comes to ultra-fine technology node. Besides, producing of H_2O by condensation reaction is definitely undesirable because dielectric constant of water is ~80. Therefore, the present dissertation is basically motivated to find the effective ways to restore the integration-process-induced damage (mainly, plasma-induced damage) based on understanding of the fundamentals behind the intrinsic instability of PLK and suggest the feasible methodology to produce the robust configuration of PLK matrix that causes less damage with respect to integration process.

1.6 Objectives of research

As mentioned so far, plasma-induced damages have presented significant challenges to the integration of Cu/low-k interconnect. This has generated great interests recently in studying plasma-induced damage to low-k dielectric and damage repair by using several methods including silylation process and UV cure. In our previous study, viscoplastic properties of PLK films were traced depending on variation of plasma exposure by using ball indentation creep test with weighted emphasis on the mechanical stability. [70] It was found that PLK films indeed plastically deformed with time, and that PLK stability was significantly influenced by porosity (intrinsic factor) and plasma damage (extrinsic factor). Furthermore, it was revealed that the involved mechanism for viscoplastic deformation in PLK films was chemical evolution in incomplete bond network catalyzed by Si-OH formation from the temperature dependence indentation test. With the previous study and result, degradation in properties of porous SiCOH films induced from plasma process during integration is clearly observed, however, PLK stability and its change with plasma process conditions are determined to be much more complicated than previously thought due to the complexity of low-k plasma surface interactions including both chemical and physical effect. The former arises from chemical reactions of plasma with low-k constituents, while the latter involves physical bombardment, the intensity of which depends on the plasma density and energy. Unknown details in the backbone structure could be the factor to

reveal the correlation between PLK stability and structural evolution. From this point of view, a whole series of characterization in PLK structural change could suggest the outlook of restoring the original structure and repairing the plasma-induced damage in PLK matrix. Interestingly, one of the clues that viscoplastic deformation can be manipulated is found when we do the same indentation test with different PLK specimen containing much more unstable hydrocarbon residue. The indentation test result shows swelling phenomena rather than exhibiting indentation behavior, obviously indicating that the thermo-mechanical instability related to viscoplastic deformation can be improved by modifying chemical bond configuration.

From this perspective, the present dissertation research will show key findings along with the discussion on the techniques for the future work that aims to provide complementary evidences supporting the proposed mechanism of structural change induced by plasma exposure and restoration process. For this, we investigate the correlation between film chemistry and viscoplasticity (measure of structural weakness) by closely tracking chemical changes in the film matrix using FTIR (Fourier Transform Infrared) spectroscopy and XPS (X-ray Photoelectron Spectroscopy) with variation in plasma exposure and recovery processes. Based on our observation, primary mechanism of viscoplasticity is mainly related to the hydrophilic nature of the film after plasma exposure and dielectric constant change is relevantly involved with the cage-like configuration in Si-O-Si backbone structure. FTIR spectra exhibit that such change is involved with the oxidation of hydrophobic Si-$(CH_3)_X$ bond groups and its transformation into more hydrophilic Si-OH bond groups. And also, the reaction with plasma induces silicon suboxide (~1023 cm^{-1}) to increase with an expense of cage structure (~1135 cm^{-1}) in the Si-O-Si backbone. This results in shrinkage of the film with collapse of pores inside of the film. Its structural restoration is found to be possible by treating such damage using silylation agent and soft x-ray radiation with thermal assistance, because all those treatments promote reconfiguration of the bond network around the pore and enhance structural stability. The level of instability driven by plasma exposure in PLK matrix is recovered and desired mechanical and electrical properties are

obtained by enhancing crosslinking with the increase in C content. In addition, we have been searching for an alternative route for damage repair in terms of easy access to IC process flow, leading us to a discovery that a brief exposure to low-energy inert plasma results in the restoration of PLK structure and properties that closely match the undamaged. Peak configuration shift of Si_{2p} in backbone structure revealed by XPS supports that substitution of O with C can be taken place by inert Ar-plasma radiation due to energy transfer. In addition, it is revealed that non-reactive Ar radiation followed by thermal pressure promotes simultaneous reaction of elimination of –OH groups, crosslinking with bridging methane (Si-CH_2-Si), and production of methyl group in the Si-O-Si structure.

Comparably as the study of damage restoration in PLK dielectrics, research on the enhanced mechanical stability of ultralow-k dielectrics with self-organized molecular pores will be highlighted. It proposes an alternative deposition method for robust PLK dielectrics with smaller and uniform porosity by steric hindrance of matrix precursors. Pores fabricated by removal of organic fragments (porogen) in ultralow-k dielectric film produce lower mechanical properties as well as incur electrical degradation during chip integration process because pore surface acts as a reactive path for moisture uptake or Cu diffusion. Furthermore, UV cure used in porogen removal simultaneously breaks the skeleton crosslinks in silica matrix. To overcome this issue, ultralow-k film with self-organized molecular pores due to steric hindrance is deposited by using particular precursors. Dielectric constant of ~2.1 with superior modulus (>13 GPa) is achieved by inducing uniform distribution of porosity and lower polarizability, which modulus is significantly improved compared with that of porous SiCOH film fabricated by subtractive method with same k value. Also, it shows enhanced resistance against plasma-induced damage and thermally-induced film shrinkage. Analysis of the film structure indicates that symmetric linear Si–O molecular chains with –CH_3 terminal bonds are grown and cross-linked to each other in the film, leading to the decrease in dipole moment and improvement in the mechanical properties.

It is believed that all these changes are beneficial for improving PLK stability as will be

detailed in this study. Especially, the academic originality and particular advantage of this research on IC manufacturing process regarding plasma-induced damage repair will be highlighted.

1.7 Description of dissertation thesis

The dissertation is organized into the following chapters.

In chapter 1, the advanced technology of modern Cu/PLK interconnects is briefly introduced and some functional properties of low dielectric constant materials are reviewed. Also, the integration challenges and reliability issues due to the material properties of Cu and PLK are discussed. Among them, thermo-mechanical instability of PLK in relation to reliability concerns is emphasized.

Chapter 2 discusses the experimental details that are extensively used through this dissertation. First, the indentation creep test method developed in our group will be overviewed. This technique particularly suitable to characterization of permanent deformation in PLK film, which will influence the integration failure due to dimensional change. Then, the characterization techniques, such as FTIR, XPS, Ellipsometry, AFM, Nano-indentation, etc., used for sample evaluation will be briefly introduced.

Chapter 3 is devoted to understand the backbone structure in PLK matrix. It is organized as two parts. The first part of this chapter presents the experiment result exhibiting the IC process damage on PLK properties. Influence of every step in IC process on PLK stability will be quantified and studied. Then, the suggestion for the modification of backbone structure which is favorable will be made by investigating various samples that have different chemical configuration.

In chapter 4, it is devoted to the investigation of dielectric recovery method including silylation process and soft x-ray radiation combined with thermal treatment. The silylation process restores the surface carbon and hydrophobicity but recovery is restricted to the surface. Soft x-ray with thermal annealing modifies the backbone structure, but recovery for hydrophobicity is

limited. Finally, recovery with low-energy inert Ar plasma treatment will be highlighted. The result obtained in our study shows that Ar plasma treatment provides the most effective way to restore the damaged mechanical and electrical properties at the same time.

Chapter 5 proposes an alternative deposition method for robust chemical configuration that has higher resistance against IC integration process damage. Ultralow-k film with self-organized molecular pores due to steric hindrance is deposited by using particular precursors and thermo-mechanical properties of ULK film are characterized with respect to IC integration process damage. Dielectric constant of ~2.1 with superior modulus (>13 GPa) is achieved by inducing uniform distribution of porosity and lower polarizability, which modulus is significantly improved compared with that of porous SiCOH film fabricated by subtractive method with same k value.

In chapter 6, the summary of the thesis and future research will be presented.

Chapter 2

EXPERIMENTAL SETUP

2.1 Introduction of indentation test

Most of the indentation tests are applied for the determination of static plastic properties of materials (e.g. hardness, yield stress). For the investigation of the time-dependent properties of materials, termed indentation creep, the indentation tests with various indenters such as spherical ball, pyramidal, conical and cylindrical indenters have been largely used due to the simplicity of operation, involving relatively little demand on the sample preparation and the small volumes related to the deformation during indentation process in comparison with the tensile tests which are generally applied to examine the time dependent mechanical properties of materials (e.g. creep, viscous flow). In our study, among various types of indentation tests the ball indenter is employed to investigate the existence of thermo-mechanical instability of PLK dielectrics. The primary advantage of the ball indenter is that it is less sensitive to alignment between the indenter and material surface, which is essential to obtain precise geometries in hard materials, thereby experiments are easy to perform. Another advantage for use in ball indenters is that indentation contact begins elastically as the load is first applied, but then changes to elastic-plastic at steadily increasing the load, which can theoretically be used to examine yielding and associated phenomena (e.g. strain-hardening behavior) in a single test. [71]

The ball indentation test was performed to determine the viscosity of glasses by Heynes and Rawson in the 60s. [72] The theoretical interpretation of this measurement was suggested by Douglas. [73]

2.2 Fundamentals of indentation creep test for a ball indenter

In the case of crystalline materials at temperatures above 0.5 T_m, the time-dependent deformation mechanism is typically described by

$$\dot{\varepsilon} = A\sigma^n \tag{2.1}$$

Where ε is the strain rate in a uniaxial test, σ is the applied stress, A is a constant for a given material and temperature, and n is the stress exponent of power-law creep. For pure metals or glasses, it is reasonable to assume that the threshold stress (σ_0) is zero within an acceptable error. As shown in Fig. 2.1, an incompressible ball indenter is pressed onto the surface of sample and the pressure distribution varies along the contact radius (a) during the indentation performed under a constant load (F). Under this loading, the indenter sinks into the material to a depth (h) with time (t).

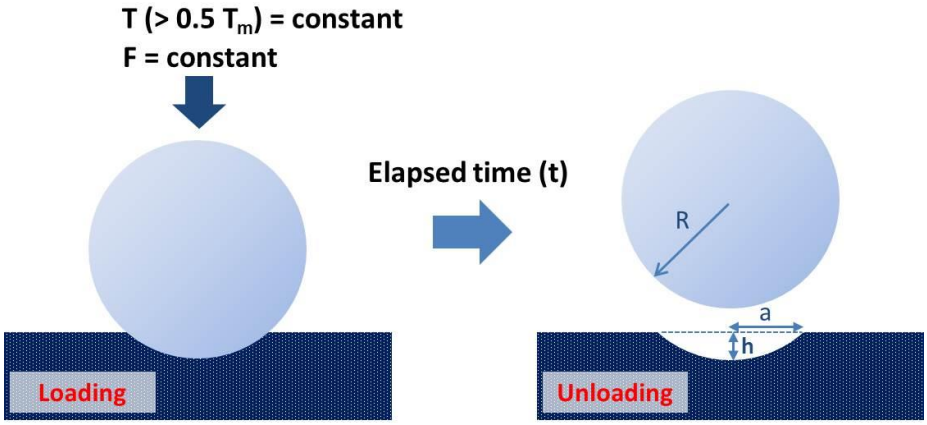

Fig. 2.1 Scheme of the indentation creep under constant load (F) with a ball indenter

During indentation creep test the pressure, p_s, under the ball indenter, can be expressed as a function of the indentation depth

$$p_s = \frac{F}{\pi a^2} = \frac{F}{\pi h(D-h)} \tag{2.2}$$

Assuming that D >> h, where D (=2R) is the diameter of the ball indenter, equation (2.2) can be expressed in the following form

$$p_s = \frac{F}{\pi h D} \tag{2.3}$$

In this case, the strain rate can be defined as the ratio of the indentation rate and the radius of the contact at the given indentation depth. Applying the same approach as in equation (2.3)

$$\dot{\varepsilon} = \frac{1}{2a}\frac{dh}{dt} = \frac{1}{2\sqrt{h(D-h)}}\frac{dh}{dt} \approx \frac{1}{2\sqrt{hD}}\frac{dh}{dt} \tag{2.4}$$

Accordingly, the strain rate during indentation test will be determined by the shape of indenter and indentation rate. Therefore, it is reasonable to conclude that the residual indentation depth (h) after unloading in time (t) represents plastic deformation at given conditions of temperature and load, and is related to the pressure stress through the stress-strain rate response equation (2.1) [refer to Appendix 1]. From the measurement of indentation depths with time using a ball indentation test we introduced, the thermo-mechanical instability of PLK dielectrics can be effectively verified, leading to understanding the related viscoplastic deformation mechanism in PLK dielectrics.

2.3 FTIR (Fourier transform infrared spectroscopy)

Fourier transform infrared spectroscopy (FTIR) is commonly applied to characterize the bonding configuration or molecular structure of dielectric materials. FTIR is based on the IR absorption arising from the dipole-photon interaction. [74] In the infrared (IR) range, atoms in solid material have various types of vibrations, including asymmetrical stretching, symmetrical stretching, in-plane bending (scissoring or rocking) and out-of-plane bending (wagging or twisting). Once the IR photon energy matches the characteristic energy difference between two energy levels of specific vibration modes, IR absorption occurs. According to the Beer-Lambert's law, the absorbance (*A*) is proportional to the molar absorptivity (*α*), bond concentration (*c*) and film thickness (*t*) and can be expressed as

$$A = -\log\left(\frac{I_1}{I_0}\right) = \alpha \cdot c \cdot t \tag{2.5}$$

where I_0 is the incoming light intensity and I_1 the outgoing light intensity. In this study, a Nicolet™ 6700 Spectrometer was applied in the transmission mode for FTIR measurement, under the

condition of the wavenumber resolution ~ 4 cm^{-1}, the number of scan ~ 256, and the wavenumber range ~ 4000 cm^{-1} – 520 cm^{-1}. During measurement, the FTIR chamber was purged with N_2 gas to remove vapor moisture and carbon dioxide. Instead of using tons of discrete monochromatic lights, FTIR uses a broadband IR source. IR photons with wavenumber from 4000 cm^{-1} to 520 cm^{-1} pass through the sample at the same time.

The FTIR detection is based on the principle of the Michelson Interferometer. [75] As shown in Fig. 2.2, by using the collimating mirror, the IR light is directed to the beam splitter. Then, the beam is split into two directions, one toward the fixed mirror and the other toward the moving mirror. By adjusting the displacement (x) of the moving mirror, the optical path difference between the two beams can be varied. After bouncing back from the fixed mirror and the moving mirror, the two beams recombine at the beam splitter with a certain phase difference and are directed toward the sample. Then, the intensity of the light transmitted through the sample is measured by a detector. By setting up a proper interference condition by adjusting the optical path difference between the two beams, the resultant light intensity can be computed. The procedure to collect the FTIR spectrum consisted of two steps. First, the transmission spectrum of a bare Si substrate was collected and saved as a background spectrum. Second, the transmission spectrum of low-k dielectrics on Si substrate was measured. By subtracting the background from the transmission spectrum of low-k dielectrics on Si substrate, the FTIR spectrum of low-k dielectrics was obtained.

A typical FTIR absorbance spectrum for the porous SiCOH dielectrics is described in Fig. 2.3. The spectrum shows several broad absorption bands representing the diversified film structures that result from the plasma polymerization process.

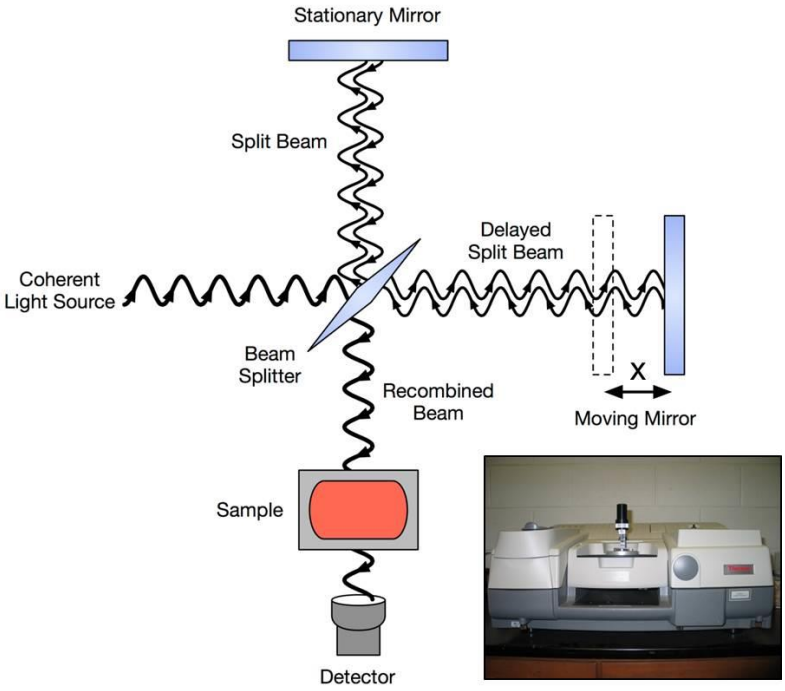

Fig. 2.2 Schematic illustration of FTIR

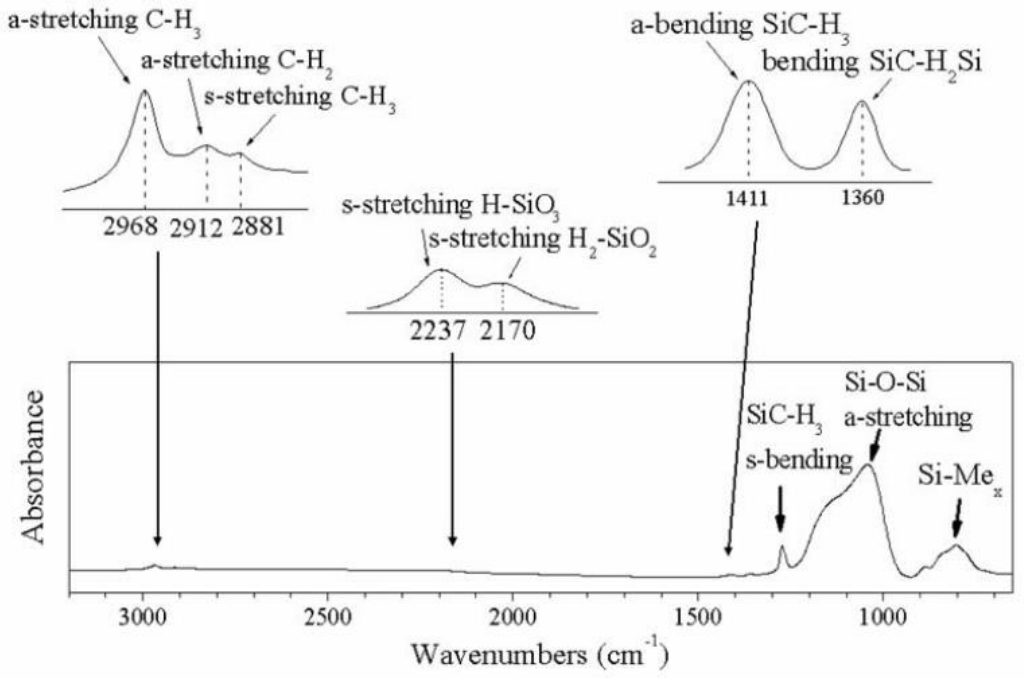

Fig. 2.3 Representative FTIR spectrum of p-SiCOH dielectrics with major absorption bands

Detailed peak assignments are listed in Table 2.1. The broad absorption band from 1200 to 950 cm^{-1} belongs to the Si-O-Si asymmetric stretching mode, typical for a siloxane network. This backbone structure of organosilicate glass low-k dielectrics is the cross-linked SiO_2-like tetrahedral structure. The Si-O-Si bonding configuration can be separated into three peaks, including the cage (1135 cm^{-1}, Si-O-Si~150º), the network (1063 cm^{-1}, Si-O-Si~140º), and the suboxide (1023 $cm^{-1,}$ Si-O-Si<140º) peaks. [76] The relationship between the wavenumber and Si-O-Si bridging angle can be interpreted by the central force model proposed by Sen. et al. [77]:

$$\omega^2 = \frac{\alpha}{m_0}(1 - \cos\theta) + \frac{4\alpha}{3m_{Si}} \tag{2.6}$$

where ω is the angular frequency, α is the Si-O bond-stretching constant, θ is the Si-O-Si bridging angle, m_0 is the oxygen atomic mass, and m_{Si} is the silicon atomic mass. Because wavenumber is proportional to angular frequency, Equation (2.5) shows that the wavenumber increases with the Si-O-Si bridging angle. Due to the large Si-O-Si bridging angle, the cage structure contributes primarily to the formation of pores [78] and the reductions of film density and dielectric constant. Usually, with increasing concentration of cage structure, the porosity increases and the film density decreases, resulting in a lower dielectric constant.

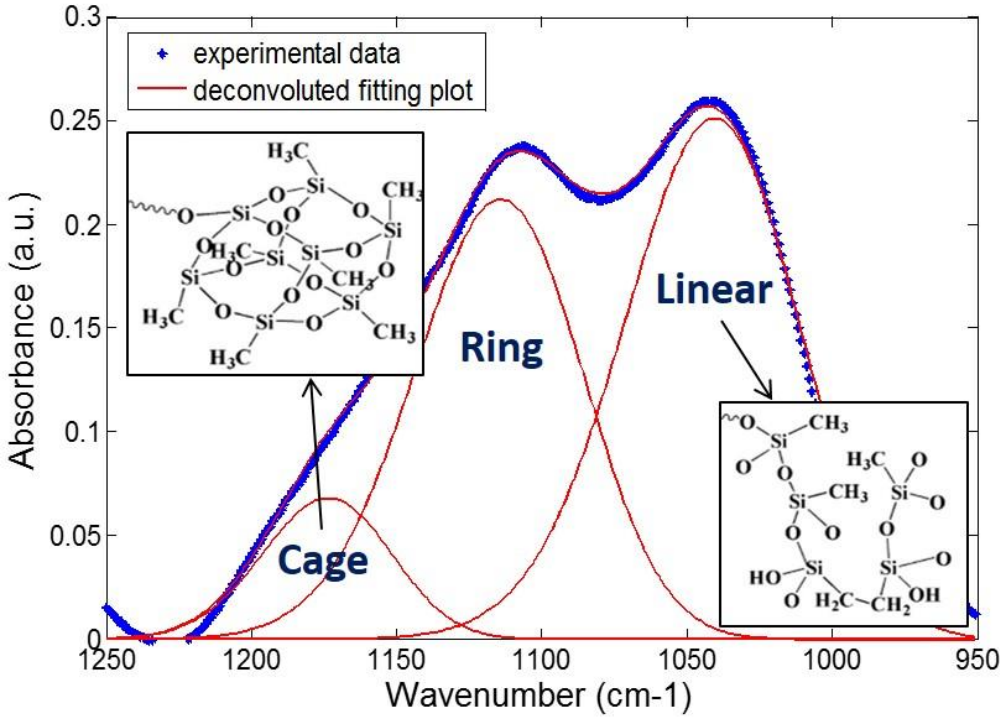

Fig. 2.4 Deconvolution of the Si-O-Si asymmetric band

Table 2.1 FTIR peak assignments of SiCOH low-k Dielectrics

TMCTS	$k=2.8$	$k=2.05$	Mode	Comment
2968	2969	2968	ν^a C–H_3	sp^3 CH_3
2906			ν^s C–H_3	sp^3 CH_3
	2916	2932	ν^a C–H_2	sp^3 CH_2
	2880	2875	ν^s C–H_2	sp^3 CH_2
	2232		ν^s Si–H	H–SiO_3
	2178		ν^s Si–H	H–SiO_2Si
2165			ν^s Si–H	H–SiOSi
		1740, 1714	ν C=O	As deposited only
		1461	δ C–H_2	CH_2 isolated from Si
1405	1412	1412	δ^a C–H_3	$SiMe_x$
	1358	1379	δ C–H_2	Si–CH_2–Si
1259	1273	1274	δ^s C–H_3	$SiMe_x$
	1135	1140	ν^a Si–O–Si	Cage Si–O–Si angle ~150°
			ν C–O	Si–O–C
1063	1063	1065	ν^a Si–O–Si	Network (network) Si–O–Si angle ~144°
	1023	1035	ν^a Si–O–Si	Silicon suboxide, Si–O–Si angle <144° D_{3h} ring structure
	890		δ H–Si–O	H–SiO_3
			ν Si–C, ρ^s CH_3	$SiMe_2$
865			δ H–Si–O	H–SiO_2Si
	848	843	δ H–Si–O	Network smaller angle
			ν Si–C, ρ^a CH_3	$SiMe_3$
	802	800	ν Si–C, ρ^a CH_3	$SiMe_2$
754			ν Si–C, ρ Si–CH_3	$SiMe_1$
	773	779	ν Si–C, ρ CH_3	$SiMe_1$
			ν Si–C, ρ^s CH_3	$SiMe_3$
710	730	720	ν^s Si–O–Si	
	440	440	δ of O–Si–O	Network and ring opening vibrations

2.4 Spectroscopic ellipsometer (SE)

Because measurements by the spectroscopic ellipsometer (SE) are nondestructive and easy and fast to operate, the SE technique has been widely employed to determine film thickness,

refractive index, and extinction coefficient in the semiconductor industry. This technique is based on the change of light polarization induced by the reflection and transmission at the film interface. As shown in Fig. 2.5, the SE system consists of a light source, polarizer, rotating analyzer, and photomultiplier. By using a polarizer, the unpolarized light given out by the light source becomes linearly polarized. After reflection and transmission at the film interface, the linearly polarized light becomes elliptically polarized. By using rotating analyzer and photomultiplier, the change of light polarization is measured.

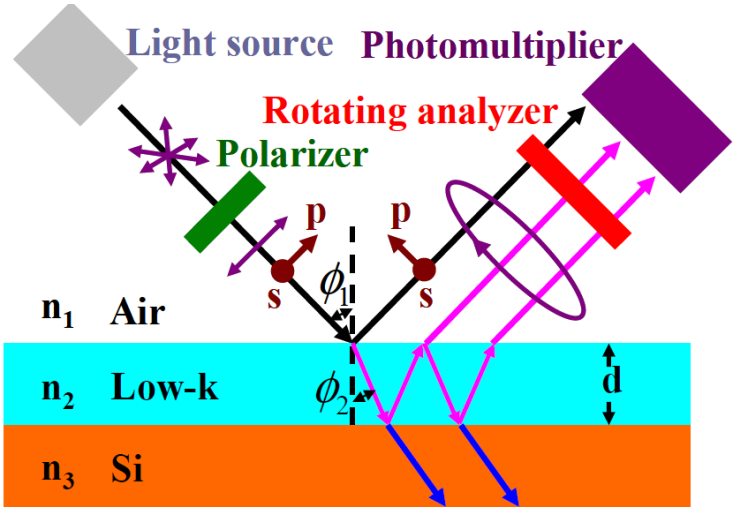

Fig. 2.5 Description of spectroscopic ellipsometer

2.5 Optic surface profilometer

In order to determine the indentation depth of PLK films after the indentation creep testing, the measurements of the depth of indentation were conducted under a WYKO® optical profiler NT9100™. The WYKO® NT9100™ optical profiler combines non-contact interferometry with advanced automation for highly accurate, 3D surface topography measurements. The working principle of the WYKO® optical profiler is shown in Figure 2.6. Light from the illuminator travels through the IMOA (Integrated Modular Optics Assembly) and downs to the objective (2.5X Michelson, etc.). A beamsplitter inside objective splits the light into two beams. One beam, called

reference beam, reflects from a super smooth reference mirror inside the objective. The other beam, called the test beam, reflects from the sample and back to the objective. When these two lights recombine, an interference pattern is received by the camera, and the signal is transferred to the computer, where it is processed by Vision software. Vision then computes and produces a graphical representation of the sample surface.

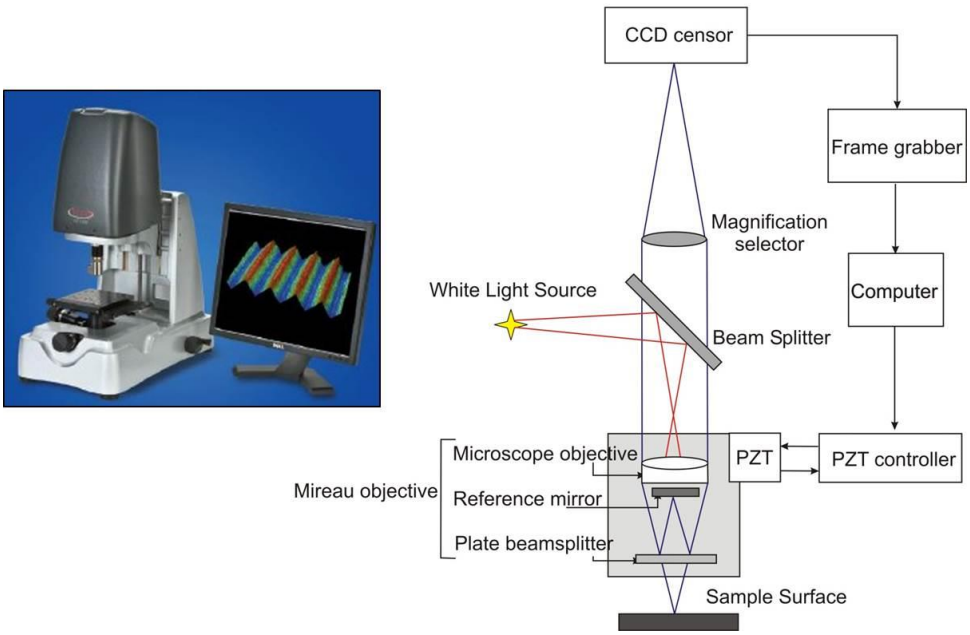

Fig. 2.6 Schematic diagram of optic surface profilometer

In our study, VSI (Vertical scanning-interferometry) mode was used to measure indentation depth and surface roughness. Vertical scanning-interferometry is a newer technique than phase-shifting interferometry. The basic interferometric principles are similar in both techniques: light reflected from a reference mirror combines with light reflected from a sample to produce interference fringes, where the best-contrast fringe occurs at best focus. However, in VSI mode, the white-light source is not filtered, and the system measures the degree of fringe modulation, or coherence, instead of the phase of the interference fringes. In vertical-scanning interferometry, a white-light beam passes through a microscope objective to the sample surface.

A beam splitter reflects half of the incident beam to the reference surface. The beams reflected from the sample and the reference surfaces recombine at the beam splitter to form interference fringes. During the measurement, the objective moves vertically to scan the surface at varying heights. A stepper motor precisely controls the motion. Because white light has a short coherence length, interference fringes are present only over a very shallow depth for each focus position. Fringe contrast at a single sample point reaches a peak as the sample is translated through focus.

The system scans through the focus (starting above focus) at evenly-spaced intervals as the camera captures frames of interference data. As the system scans downward, an interference signal for each point on the surface is recorded. The system uses a series of advanced computer algorithms to demodulate the envelope of the fringe signal. Finally the vertical position corresponding to the peak of the interference signal is extracted for each point on the surface.

2.6 XPS (X-ray photoelectron spectroscopy)

Due to the penetration of the IR source, the intensity of the FTIR detects the bulk change of the bonding characteristics in low-k films. Thus surface bonding changes in less than 30 nm are difficult to differentiate by FTIR due since it is not a particularly surface sensitive technique. X-ray photoelectron spectroscopy (XPS), on the other hand, are sensitive to the surface chemical composition and bonding configuration. The schematic setup for XPS measured is shown in Fig. 2.7. On the surface, the electrons of the material absorb the X-ray photon energy and escape from the atom to vacuum and detected by a spectrometer. The kinetic energy of this photoelectron is measured by an electron energy analyzer. Because the energy of the X-ray is known, the binding energy of each emitted electron can be determined by the following equation,

$$E_B = h\nu - E_K - e\varphi \qquad (2.7)$$

where E_B is the binding energy of core level electron, $h\nu$ is the characteristic energy of X-ray photon, E_K is the kinetic energy of ejected photoelectrons and $e\varphi$ is the work function of the

detector. [79] Since the electrons are easy to be block by the material, the detection depth is generally limited to less than 10nm depending on the escaping path.

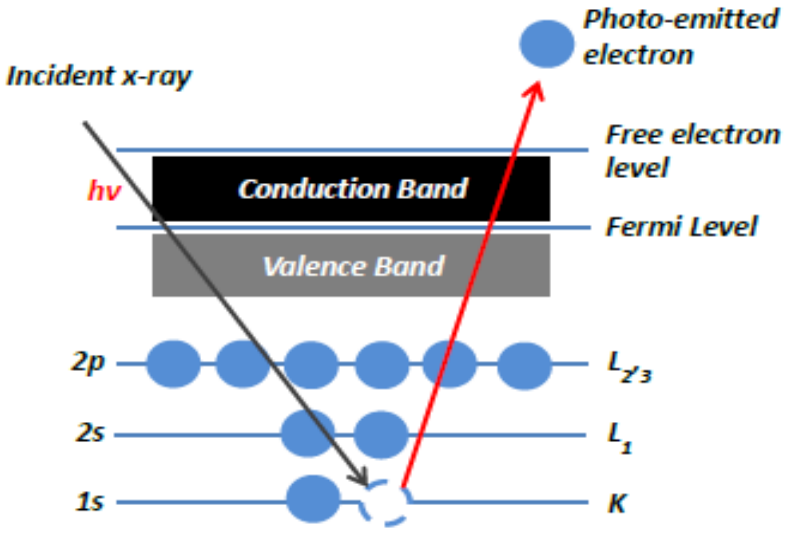

Fig. 2.7 Schematic principle of x-ray photoelectron spectroscopy

The binding energy, which is the energy required to release an electron from its atomic or molecular orbital, is a characteristic value of atoms or molecules. Therefore, it can be used to identify elements inside a material. Typical binding energy values used in this study include C_{1s} (~285 eV), and Si_{2p} (~103 eV).

XPS results in this study were obtained by a Perkin-Elmer Phi 560 XPS/Auger System. The X-ray source was a monochromatic 1486.7 eV Kα Al source with 0.16 eV energy width. Due to the pass-energy setting of electron energy analyzer and the peak-width of X-ray source, the ultimate energy resolution of the spectrum is usually 0.4-0.6 eV.

2.7 Contact angle measurement

Measurement of the contact angle for low-k dielectrics was done with Ramé-Hart Model 250 Standard Goniometer. As shown in Fig. 2.8 (a), the goniometer consists of fiber optic illuminator, sample stage, microsyringe, straight needle, and a CCD camera. By measuring the

shape of water droplet on low-k dielectrics, the water contact angle can be determined. Because the contact angle measurement depends on several parameters including the surface roughness and the surface chemical and physical homogeneity [80], contact angles of low-k films in this study were measured at various post processes and their average was reported.

As shown in Fig. 2.8 (b), the contact angle (θ) is the angle formed by the intersection of three phases including solid (low-k dielectric), liquid (water), and vapor (air). γ_{sv} is the surface free energy of solid, γ_{lv} is the surface free energy of liquid, and γ_{sl} is the solid-liquid interfacial energy. Based on the force balance or energy minimization, Young's equation can be derived [81]

$$\gamma_{sv} = \gamma_{sl} + \gamma_{lv} \cdot \cos\theta \tag{2.8}$$

By dividing the surface energy (γ) into dispersive (γd) and polar (γp) components,

$$\gamma \approx \gamma^d + \gamma^p \tag{2.9}$$

Owens et al. derived the following equation [82]

$$\frac{\gamma_l(1+cos\theta)}{2\sqrt{\gamma_l^d}} = \sqrt{\gamma_s^p}\left[\sqrt{\frac{\gamma_l^p}{\gamma_l^d}}\right] + \sqrt{\gamma_s^d} \tag{2.10}$$

where γ means the surface free energy, θ the contact angle, subscript *l* the liquid, *s* the solid, *p* the polar component, and *d* the dispersive component. [83] By using a series of liquids with known surface free energy (γ_l) as well as known dispersive (γ_l^d) and polar (γ_l^p) components and measuring the contact angles (θ), the dispersive (γ_s^d) and polar (γ_s^p) surface free energies of solid can be calculated on the basis of equation (2.9). In addition, for specific liquid, with the reduction of contact angle from 90° to 0°, the surface free energy of solid increases.

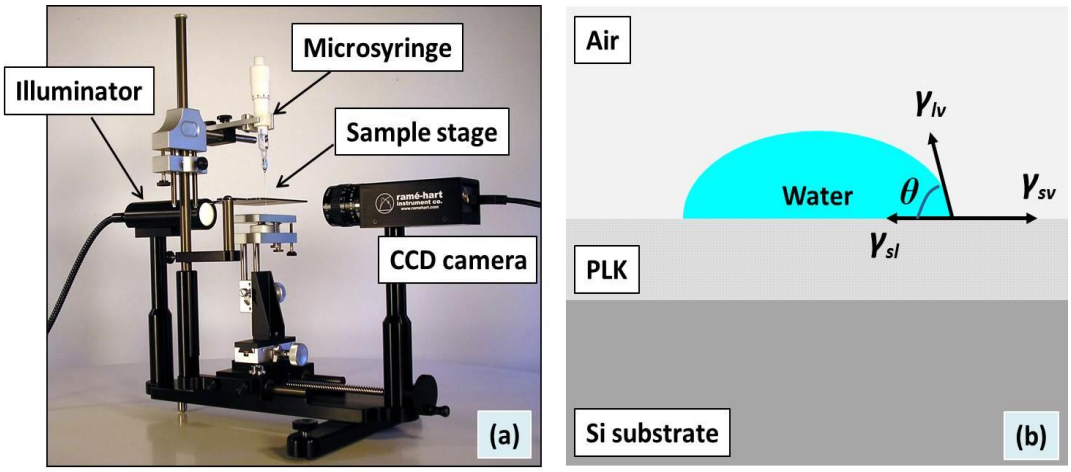

Fig. 2.8 Schematic drawing of (a) contact angle goniometer and (b) contact angle of PLK

2.8 Nano-indentation

The nano-indentation measurements consist of forcing a pyramidal shaped diamond indenter into the sample. The measured force as a function of depth during loading is characteristic of the resistance of the material to deformation, including in general both elastic and plastic responses. During unloading of the indenter, the decrease of force with depth is controlled by the elastic response of the material. The initial rate of change with depth of decrease in force (i.e. the slope) is defined as the sample stiffness. For a bulk sample, analytical methods have been developed to deduce hardness and elastic modulus from the data obtained from the depth sensing indentation technique. Oliver and Pharr method, one of the most advanced techniques in evaluating the modulus by taking the initial unload portion of the load displacement curve is the one used in the nano-indenter.

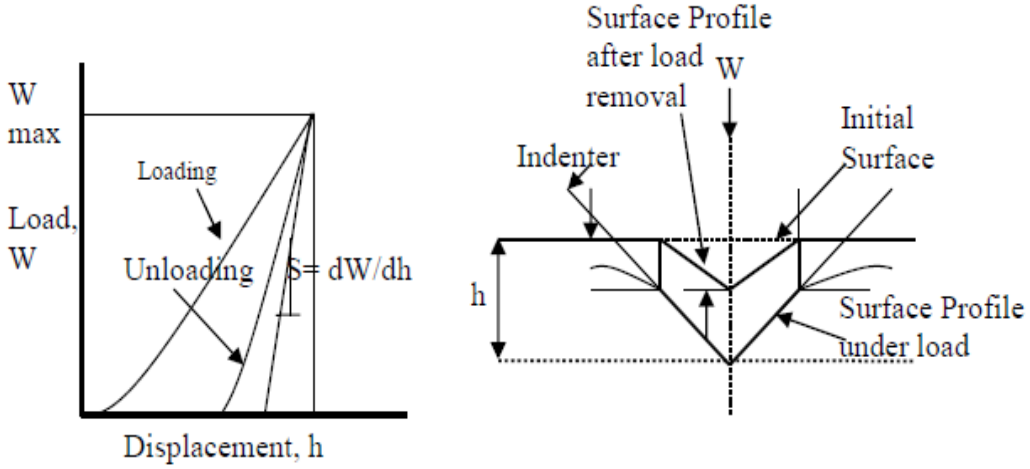

Fig. 2.9 Load-displacement curve showing stiffness calculation from initial unload (left) and surface profile under load and after load removal (right)

There are three important quantities measured from P-h curves: they are maximum load P_{max}, the maximum displacement, h_{max}, and elastic unloading stiffness, S=dP/dh (the slope of the upper portion of the unloading curve during the initial stages of unloading, also called as contact stiffness). The accuracy of the measurements depends inherently on how well these parameters can be measured. Hardness (H) and modulus of elasticity (E) are the two major mechanical properties measured by nano-indentation techniques. When indenter is forced into the sample both elastic and plastic deformation occurs. When the indenter is removed, elastic portion of the displacement regimes its original position. As shown in the figure, 'h_{max}' is the maximum displacement at peak load 'P_{max}'. 'h_c' is the contact depth and is defined as the depth of the indenter in contact with the sample under load. 'h_f' is the final depth after completing unloading and 'S' is the slope of the unloading curve called contact stiffness from which modulus of elasticity of the material can be calculated. The unloading curves are distinctly curved and usually approximated by the power law relation given by

$$P = B(h - h_f)^m \tag{2.11}$$

where '*B*' and '*m*' are the power law fitting constants. Oliver and Pharr approach is the basic approach to calculate hardness and modulus of elasticity. [84] Nano-indentation hardness is defined as the indentation load divided by projected contact area.

$$H = \frac{P_{max}}{A} \tag{2.12}$$

Where *H* is the hardness, P_{max} is the maximum load and *A* is the projected contact area. Elastic modulus can be obtained from initial unloading contact stiffness which is given as dP/dh and can be obtained by differentiation of the equation.

$$\frac{1}{E_\gamma} = \frac{(1-\nu^2)}{E} + \frac{(1-\nu_i^2)}{E_i} \tag{2.13}$$

Correction factor was added by Jenny Hay et al., [85] and is added to the Sneddon's equation [86] for accuracy in measuring mechanical properties shown in equation

$$S = \frac{dP}{dh} = \beta \frac{2}{\sqrt{\pi}} E_\gamma \sqrt{A} \tag{2.14}$$

'E_r' is the reduced elastic modulus, 'β' depends on the geometry of the indenter [87] and for spherical 1.0, triangular 1.034, and for square 1.012. The above relation is independent of indenter geometry. Therefore modulus of elasticity and contact area can be calculated from the initial unloading slope of load-displacement data.

2.9 Force amplitude microscopy by AFM (Atomic Force Microscopy)

Force Modulation Microscopy (FMM) is an extension of AFM imaging that operates in contact atomic force microscopy (C-AFM) mode and is used to detect variations in the mechanical properties of the sample surface such as surface elasticity, adhesion, and friction. In FMM mode, the AFM tip is scanned in contact with the sample surface, and the Z feedback loop maintains a constant cantilever deflection as in constant-force mode AFM. In addition, a periodic signal known as the 'driving signal' is applied to the bimorph piezo and vibrates either the tip or the sample. The resulting tip motion is converted to an electrical signal. This electrical signal is separated into AC and DC components for analysis. The DC signal represents tip deflection as in contact AFM.

The Z feedback loop uses this signal to maintain a constant force between the tip and the sample to generate a topographic image. The AC signal contains the tip response due to oscillation. The amplitude of the AC signal (called 'FMM Amplitude') is sensitive to the elastic properties of the sample surface. A hard surface will deflect the oscillation, resulting in a large amplitude response. On the other hand, a soft surface will absorb the oscillation, resulting in a small amplitude response. The FMM image, which is a measure of the sample's elastic properties, is generated from variations in the FMM amplitude. Schematic description of AFM operation and an example of the Amplitude Response using FMM are shown in Fig. 2.10 and 2.11, respectively.

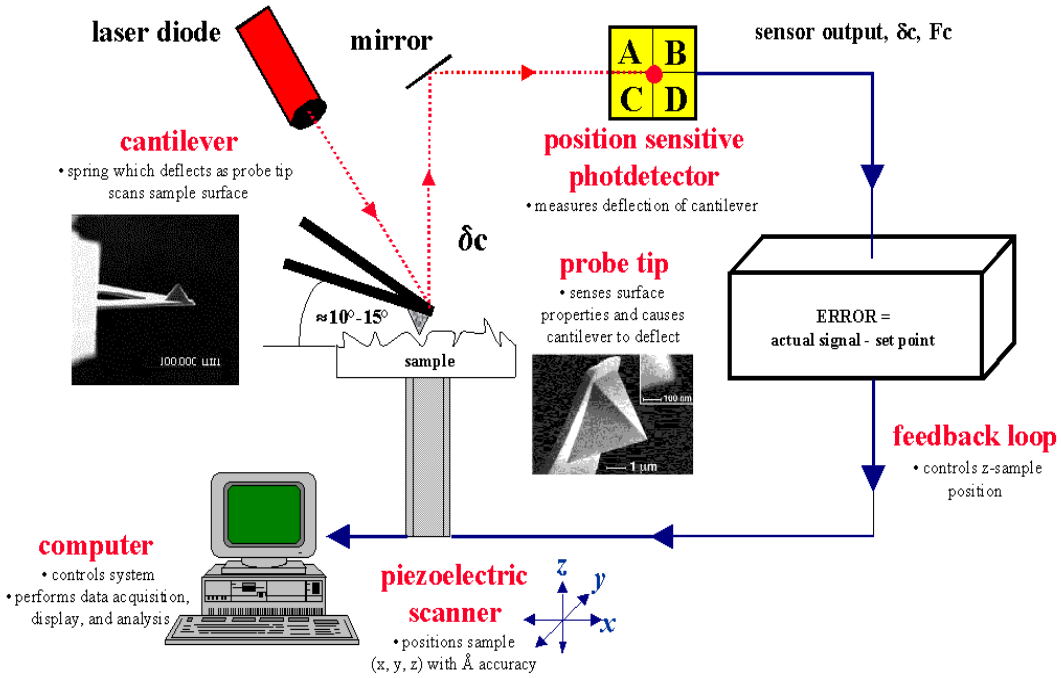

Fig. 2.10 Schematic description of AFM operation

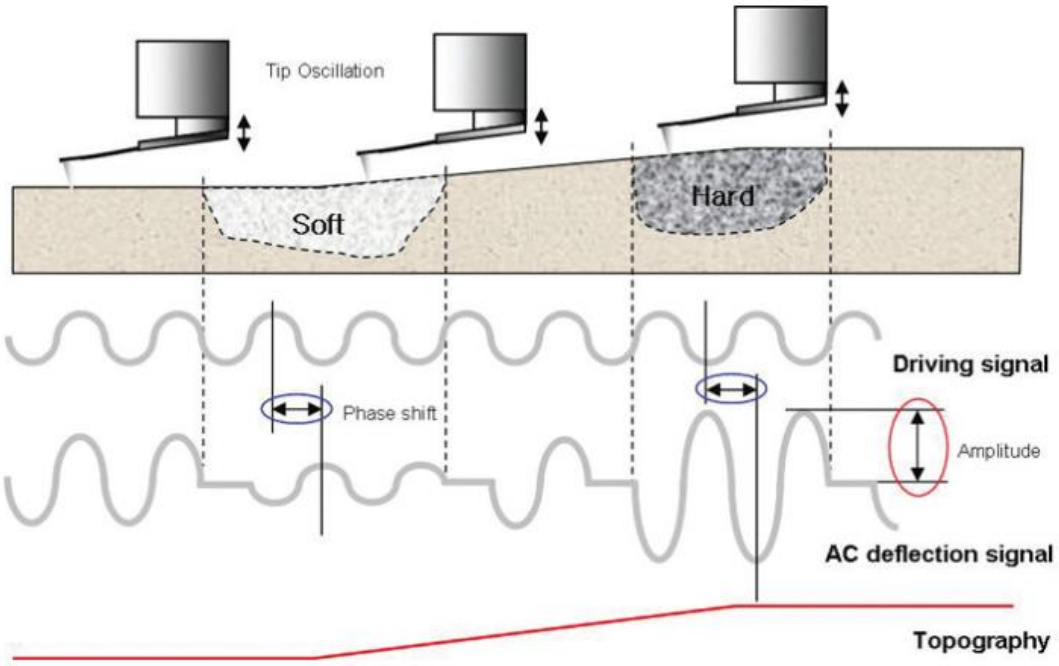

Fig. 2.11 An example of the Amplitude Response using FMM

2.10 Preparation of PLK films and classification

The porous SiOCH films deposited by subtractive method in this study were synthesized from an alkoxysilane matrix precursor and an organic porogen (BCHB; bicylcoheptadiene) by plasma-enhanced chemical vapor deposition. In case of the constitutive p-SiCOH film, particular matrix precursor was used without organic porogen. The methyl ($-CH_3$) groups included in the precursor as a $Si-(CH_3)_X$ lower the film's density, polarizability and make the film hydrophobic, resulting in the decrease of the dielectric constant (k) of the film. Capping layer of SiCN, which usually acts as diffusion barrier in interconnects, was not deposited in the present research in order to characterize SiCOH material itself. The films had a nominal thickness of 400 nm, a porosity of 25~35%, and a dielectric constant of approximately 2.0~2.4. Porosity was created by incorporating an organic porogen into the film that was later removed by thermal and electron beam to form porous SiCOH dielectrics. The films would have some residual levels of F in them since it is a background contamination in the CVD chamber. Chamber cleaning was done with

NF_3. As shown in Fig. 2.12, the structure of PLK film fabricated by PECVD is highly complicated by a variety of different crosslinked networks. [76] For comparison of the effect from the different plasma exposure, the PLK films were processed with O_2 and CO_2 plasma source, respectively. The pressure and flow rate under plasma exposure were kept constant.

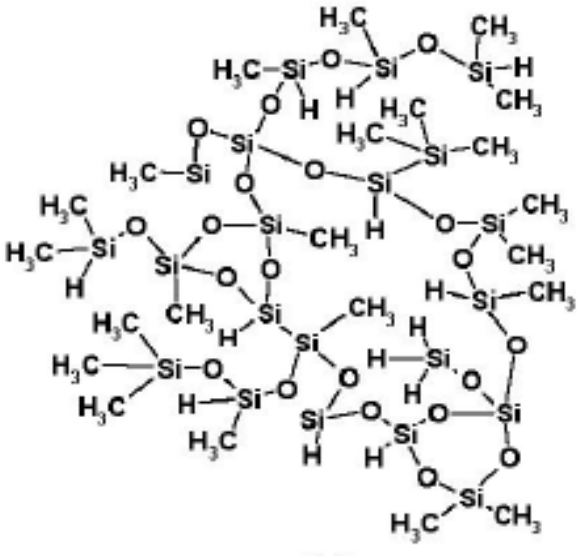

Fig. 2.12 Diagram of networked structure of PLK film deposited from a matrix precursor

Basically, specimens are prepared for identifying for the effect of chemical bond configuration and its plasma exposure on the thermo-mechanical instability of PLK. Details in specimen history are exhibited in Table 2.2 and TEM image with the dimension measured and the diffraction pattern indicating the PLK film matrix is amorphous are displayed in Fig. 2.13. The PLK blanket film is deposited onto the Si substrate with the thickness of 400 nm.

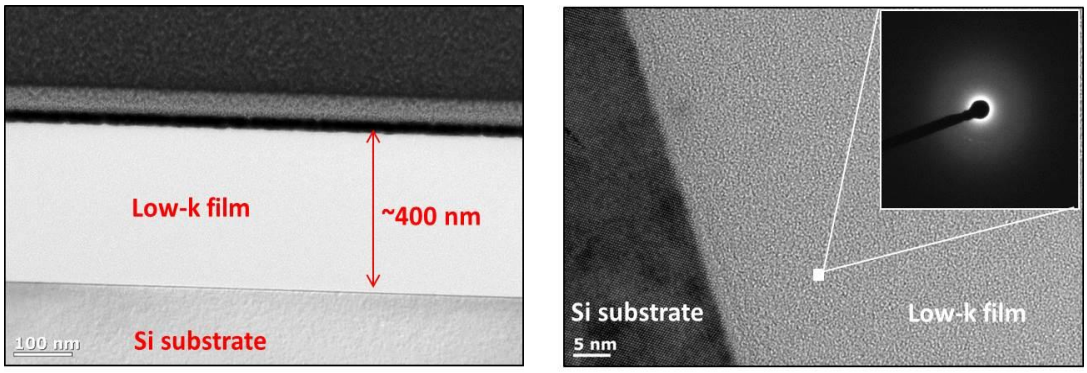

Fig. 2.13 TEM images displaying cross-section and diffraction pattern

Table 2.2 Classification of PLK specimens used in the study

Specimen	Dielectric constant (k)	Porosity (%)	Plasma exposure	Remark
As-prepared (1)	2.1	30~35	n/a	
Plasma-exposed sample (1)	2.1	30~35	O_2 & CO_2 gas	Plasma by supplier
Moisture-exposed sample (1)	2.1	30~35	n/a	
As-prepared (2)	2.1	30~35	n/a	More C residue
Plasma-exposed sample (2)	2.1	30~35	O_2 & CO_2 gas	Plasma by supplier
Plasma-exposed + recovery sample (2)	2.1	30~35	O_2 & CO_2 gas	Plasma and recovery by supplier
As-prepared (3)	2.4	25~30	n/a	Same as as-prepared (1) except k value
As-prepared (4)	2.1	30~35	n/a	Structural fabrication Free volume

Chapter 3

EFFECT OF OXIDIZING PLASMA EXPOSURE ON THERMO-MECHANICAL RELIABILITY

3.1 Introduction

Reduction of the effective dielectric constant while maintaining the thermo-mechanical and chemical stability of PLK dielectric materials for interlayer dielectric applications is considered to a key challenge in BEOL integration. It is known to be particularly challenging for ultralow-k dielectrics with k-value of 2.0~2.4 because their chemical configuration with porosity in backbone bonds is more prone to be spoiled by exposure to chip integration processes such as CMP (chemical mechanical polish), plasma etch/ash, and annealing, and so on.

In this chapter, firstly, the influence of integration process steps on thermo-mechanical instability of PLK is investigated in terms of viscoplastic deformation. While it is evident that lowering the density and mechanical strength by the introduction of porosity into the existing low-k film, it is still unclear that how much integration damage is induced by each process step and little is known if the integration damage is cumulative with individual process. Therefore, it is important examine the impact of each integration process step to PLK stability so as to develop effective PLK process methods to minimize the damages in PLK resulting from integration processes and find a proper way to make PLK to be stable by restoring its original stability. Our previous studies find that viscoplastic deformation, measured by our ball indentation technique, [70] correctly reflects the change in the chemical back-bone of PLK films and therefore can be used for tracking damage in PLK bond structure in variations with the integration process steps.

Secondly, plasma-induced damage in p-SiCOH film is examined in terms of thermo-mechanical and electrical properties degradation. Time-dependent deformation (it was shown as permanent deformation) with high temperature was already evidenced and its possible mechanism was suggested in the previous study. [70] However, the electrical instability and its structural evolution in low-k dielectric material should be correlated to suggest the outlook for

timely implementation of PLK into the chip integration. In standard integration processes, different plasma chemistries are employed to cap layers, etch patterns and ash photoresist. Plasma treatment processes result in complex combinations of chemical reactions between the surface species and the radicals formed in a discharge volume, and the physical impact or sputtering by ion bombardment. [88] A number of factors including the plasma composition, temperature and treatment time influence this process and determine etching rate, uniformity and selectivity as well as the extent of damage to the dielectric film. Interaction of reactive plasmas with SiOCH materials causes carbon depletion that induces silanol formation, film densification and dangling bonds defects, concomitantly, increasing the film dielectric constant. [88] Degradation of porous SiOCH films due to plasma processing under integration is evident, but because of the complexity of low-k plasma surface interactions, several phenomena continue to remain unclear. Therefore, further investigation of porous low-k films becomes necessary to better understand their response to various plasma processes used in the fabrication of integrated circuits. This chapter will detail such findings by presenting experimental evidence.

3.2 Experimental procedures

The porous SiCOH films were synthesized by plasma-enhanced chemical vapor deposition. The films have a nominal thickness of ~400 nm, a porosity of ~32 %, and a dielectric constant of approximately 2.0 measured by spectroscopic elliposometer. For comparison purpose, the PLK films were exposed to O_2 and less oxidizing plasma source, respectively. The pressure and flow rate under plasma exposure were kept constant.

As a way of quantifying the PLK mechanical instability, especially viscoplasticity, ball indentation technique was introduced. In our test equipment, 20 mm diameter Alumina ball with static weight was placed on top of PLK films. The weight was chosen to produce 100~150 MPa pressure stress to the film in order to simulate the stress that PLK would experience during PLK/Cu integration process. The whole test assembly, the ball with static weight and PLK film on

Si substrate, was in a chamber where temperature and environmental conditions can be controlled. The test sequence was consisted of removal of trapped moisture in PLK films, degassing the chamber, heating stage, applying load. Removal of water and degassing was achieved with vacuum and N_2 gas purge cycle at room temperature without making contact between the ball and PLK films. Test temperature was set as 400 ˚C, which is typically used in the integration process. Ball indentation was done by bringing the ball into contact with the PLK films after target temperature was reached without holding time. The indentation surfaces were observed using an optical microscope and quantified using a Wyko model NT9100 optical profilometer equipped with Vision software. Characterization for whole series of changes due to plasma damage was done by ellipsometry, contact angle measurement, FTIR, XPS, and so on.

3.3 Results and discussion

3.3.1 Effect of integration processes on viscoplastic deformation

Although the mechanism behind the property degradation of PLK films is reasonably well understood, it is still unclear how much damage is created by each process step in back end integration. Equally unknown is if the damage is cumulative with individual process. These are important questions to answer because proper and effective resolution to PLK instability problem can only be well understood when the most critical process is identified. Nevertheless, this is not an easy task and therefore hasn't been attempted yet. The difficulty is related to the lack of methods in quantifying the PLK stability, especially the status of the bond network. In this regard, the ball indentation technique that is developed and introduced in our previous study can offer an effective solution. This technique was originally developed to study the viscoplastic properties of PLK films. The discovery of direct correlation between the viscosity of PLK, measured from the indentation, and the chemistry of PLK backbone enables us to track the level of PLK damage with the process steps. Also possible is the quantitative and sensitive measurement of damage repair resulted by processes like UV cure or silylating treatment.

Fig. 3.1 shows the change in indentation depth with process steps represented by interpolated table in the plot. The films used for this experimental has a dielectric constant of 2.3 and covered with 10 nm thick SiCN capping layer. It can be seen that damage to the PLK film by each process step is cumulative. Note that fact that the indentation depth increases from ~7 nm to 28 nm, meaning that damage level is really substantial by the time when PLK integration processes are all done. Interestingly, the result shows that UV cure does not add any meaningful help for the stability of PLK. This is somewhat contradicting result from the conventional idea because UV cure is believed to make the bond network to be more complete by removing unsaturated bonds. The reason why UV is not effective may be related to the fact that the ball indentation is more sensitive to the bond chemistry than the presence of unsaturated bond. Furthermore, the heat created by UV radiation may increase the possibility of unintended chemical reaction, such as the formation of –OH from H2O present in the film. This, formation of –OH bond, may nullify the benefits gained from the removal of unsaturated bonds. Regardless of the mechanism, our result suggests that UV is not effective in terms of repairing process damage and that development of new repair method is necessary.

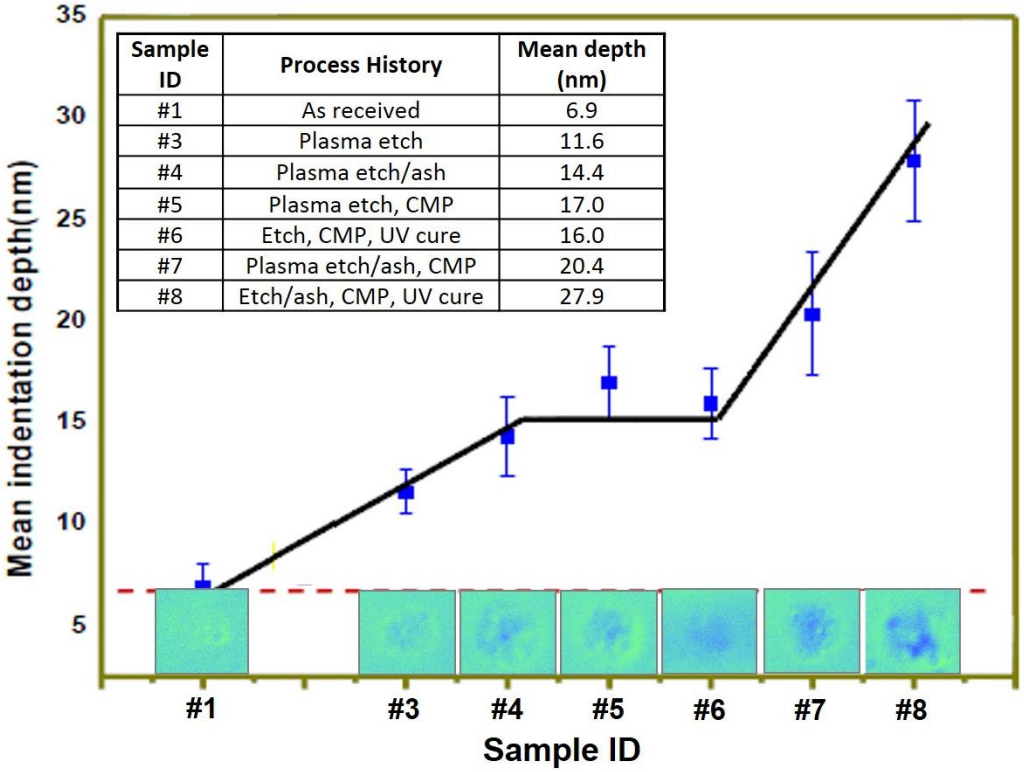

Fig. 3.1 Effect of back end integration process steps on viscoplasticity

In this regard, the result that damaging process to PLK stability is the plasma etching and ashing process deserves a special attention. They are essential part of PLK integration process yet produces most vexing damage to PLK backbone chemistry. In order for proper control of PLK stability, it is necessary either to modify the plasma process or to treat PLK films after each plasma exposure. As a part of attempt to develop the repair process, PLK films (k=2.2) with two different plasma level exposures were created; 1) CO_2 ash processed PLK, and 2) O_2 ash processed PLK. The important difference between these two is the concentration of oxygen level. The variation in the plasma source may result in different type of bond damage in addition to the amount of damage. It is therefore possible that these two PLK films react differently to the repair treatment, providing further insights to the type of chemical damage present in PLK films.

3.3.2 Viscoplastic behavior of PLK films

In order to evaluate the potential effect of plasma exposure on the mechanical response of porous SiCOH films, a first series of ball indentation tests were performed on the specimens with different plasma conditions, which results were compared with the series of indentation data taken from moisture-exposed samples. A series of surface profile images shown in Fig. 3.2 presented the comparison of deformation behavior and indentation depth in PLK films and its sensitive dependence on plasma process conditions and the existence of H_2O ambient. The results clearly showed that the degree of deformation by indentation, visible as the dark contrast, increased with test time. It was noteworthy that gradual increase in the indentation depth with time was clearly evidencing the occurrence of viscoplastic deformation in PLK films. It was observed that indentation area and depth of plasma exposure film was more pronounced than those of non-plasma exposure films. It was also known that O_2 plasma exposure induced more alternation than CO_2 plasma in terms of change in indentation depth, indicating that plasma surface interactions of p-SiCOH dielectrics are even more complex with process conditions than previously discussed.

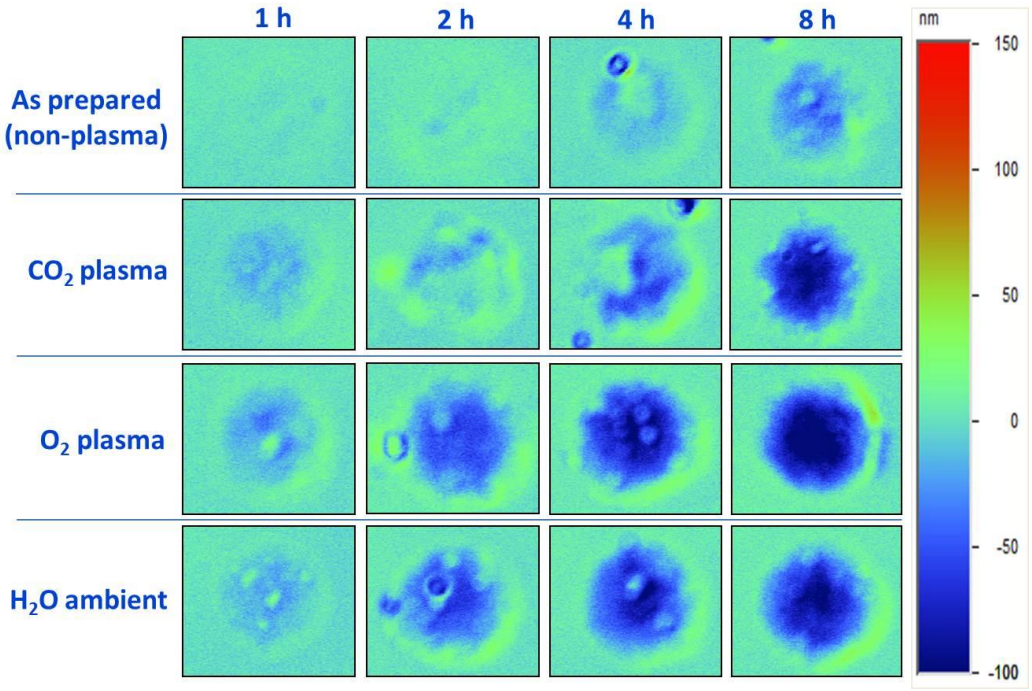

Fig. 3.2 Topographic images of residual indentation depth with different plasma exposures and existence of moisture

Generally, decarbonization of p-SiCOH dielectrics by plasma exposure is well-known phenomenon. Si-CH_3 bonds are broken, creating dangling bonds that can react with moisture to form Si-OH (silanol) or with hydrogen to form Si-H (silane). [90,91] Silanol groups make the film surface hydrophilic, and the polarization of silanol and moisture uptake not only increase in dielectric constant but reconfigure chemical bond network. Fig. 3.3 evidences the decarbonization and hydrophilic transformation by variation of contact angle in PLK surface with respect to the plasma exposure source, which results from –OH group increase. In case of as-prepared film, contact angle was 100.87^o, but it was sharply decreased to 44.54^o and 56.68^o after O_2 plasma and CO_2 plasma exposure, respectively. Due to reactive oxygen species, PLK film surface was altered into hydrophilic from hydrophobic.

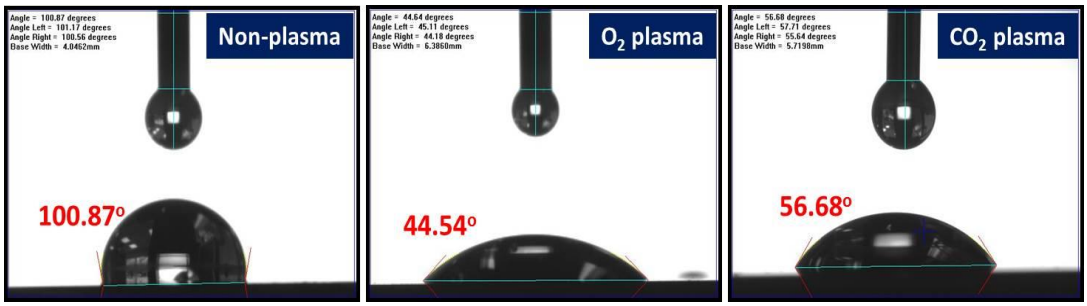

Fig. 3.3 Variation of contact angle depending on plasma exposure

It is believed that the mechanism of viscoplastic behavior of p-SiCOH films is due to chemically assisted viscous flow linked to the formation of silanol and silane even though p-SiCOH materials are regarded as brittle linear elastic materials. [70] It was also obvious that the mass of pile up region around indented area defended the viscoplasticity of p-SiCOH film by viscous flow among several mechanisms.

Along with the investigation of viscoplastic deformation induced plasma exposure on PLK films, moisture effect on viscoplastic behavior of PLK films was also studied. Since O_2-plasma induces hydrophilic nature in the PLK matrix by forming Si-OH group and subsequently H_2O as mentioned, it was expected that tracking of thermo-mechanical instability for H_2O ambient PLK film and its comparison with those of plasma-exposed film could provide the clue upon the restoration of plasma-induced damage in PLK matrix. As seen in Fig. 3.2, it is clearly observed that the degree of deformation in H_2O exposed film was increased, indicating that absorption of moisture has a significant negative influence on the stability of PLK film, which is in the similar manner with those of plasma exposed film.

It is our belief that the viscoplasticity seen in our investigation is fundamentally driven by the viscous flow but chemical reaction may act as a catalyst for making the PLK films to be viscous. The viscous flow of Newtonian solid (amorphous solid) occurs by body translation of entire solid under stress. In case of PLK films under test conditions used in our test, body translation may be difficult to achieve because silicate backbone provides a reasonable strong

resistance against it. In order for the backbone molecule to move, it requires momentary breakage of the bond and re-bond, which is known to require activation energy over 4 eV. However, when there exists a chain of weak links in the bond network, the resistance against body translation may be reduced because the colony that is encompassed by the weak link may act as one moving solid (like the grain boundary in crystalline solid as shown Fig. 3.4).

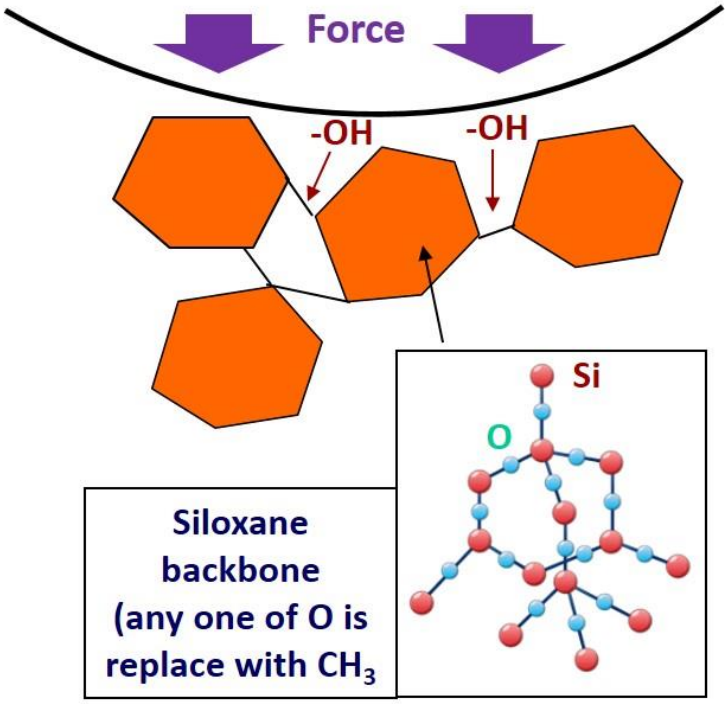

Fig. 3.4 Schematic illustration of a chain of weak links in the backbone network

In this case, all the principle behaviors of viscoplastic deformation appear to follow the viscous flow yet activation energy can be significantly lower because colony motion does not require breakage of high energy bond. We believe Si-OH or Si-H that may serve as the defective bond and exist in PLK films due to 1) trapped defects during deposition, 2) damage to CH_3-Si-O bond due to plasma damage, and 3) reaction with trapped moisture. This explains the low activation energy seen in all PLK films and also keen dependence of indentation kinetics on PLK film condition. The PLK films with plasma damage or moisture update would show faster

deformation rate because the colony size is much smaller than the others. However, since the principle deformation mechanism is controlled by the colony motion itself, the activation energy would not be a keen function of the film condition. This mechanism, chemically assisted viscous flow, appears to explain all observations seen in our investigation.

3.3.3 Effect of plasma exposure on structural evolution in PLK film

The effective dielectric constant at the wavelength of 500 nm was measured by spectroscopic ellipsometry. Fig 3.5 plots the dielectric constant change depending upon the types of plasma source and plasma exposure time. In both cases, dielectric constant was increased in the parabolic manner with plasma exposure time. After 5 min plasma exposure, the effective dielectric constant increased about 10 % and O_2 plasma induced slightly more increase in k value compared with CO_2 plasma exposure. This is related to the reactive oxygen radical concentration. In case of CO_2 plasma source, it is supplied with more thermodynamically stable phase due to strong bonding between C and O, the concentration of oxygen radicals that participate in the surface reaction in PLK matrix is lower than that of O_2 plasma source. Basically, oxidative plasma causes decarbonization of p-SiCOH dielectrics by breaking Si-CH_3, and subsequently creates dangling bonds that can react with moisture to form Si-OH (silanol) or with hydrogen to form Si-H (silane). [90,91] Silanol groups modify the film surface hydrophilic, and the polarization of silanol and moisture uptake contribute to the increase in dielectric constant. During these series of transformation, the densification of low-k dielectrics materials between pores is also involved. As will be shown in the following sections, the bonding configuration changes and film densification contributed to this increase.

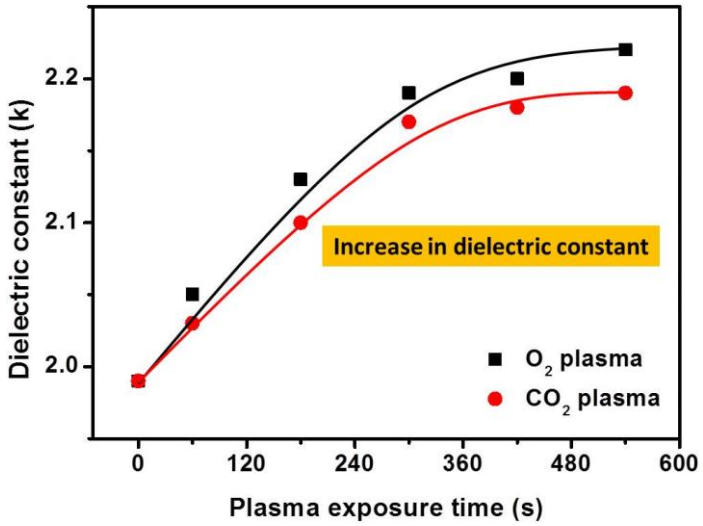

Fig. 3.5 Dielectric constant change upon the types of plasma source and exposure time

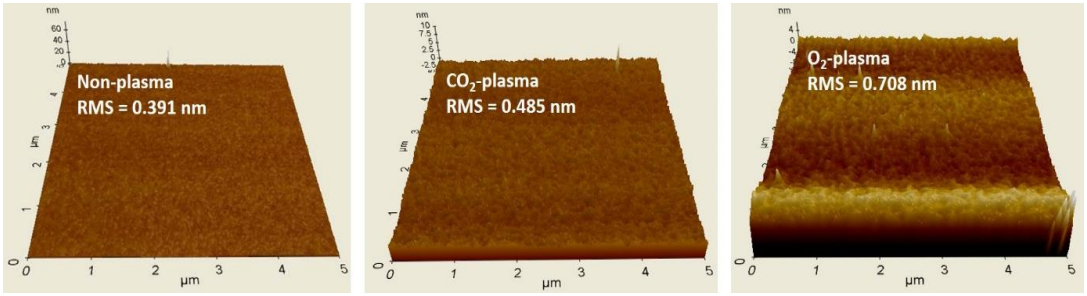

Fig. 3.6 Variation of root mean square (RMS) with respect to plasma exposure

Three-dimensional AFM images of p-SiOCH films treated by different gas plasmas are presented in Fig. 3.6. A fine network of structures forming a smooth surface (R_{rms} = 0.391 nm) was observed for the non-plasma exposed sample (right image). The O_2 and CO_2 plasma treated films showed a dense arrangement of very fine surface topographies (middle and left image, respectively). From the results of the change in dielectric constant and RMS value, as similarly as viscoplastic deformation result, O_2 plasma exposure has more impact on the alternation of PLK film matrix compared with that of CO_2 plasma exposure.

In order to characterize the bonding configuration changes, differential FTIR spectra

were obtained by subtracting the spectrum of as-prepared film from that after plasma exposure. A typical result over the wavenumber range of 750 ~ 4000 cm^{-1} is shown in Fig. 3.7 and each peak absorbance under magnification is displayed in Fig. 3.8 and 3.9. The spectral data indicate that the bond intensities of Si-(CH_3)x (1280~1250, 870~760 cm^{-1}), cage-like structure (1135 cm^{-1}) and CHx (~2960, 2925, 2865 cm^{-1}) were reduced while those of –OH/H_2O (3100~3500 cm^{-1}), and Si-O-Si network (~1063 cm^{-1}) structures increased. These FTIR spectra results are closely matched with prevailing chemical transition induced by plasma exposure.

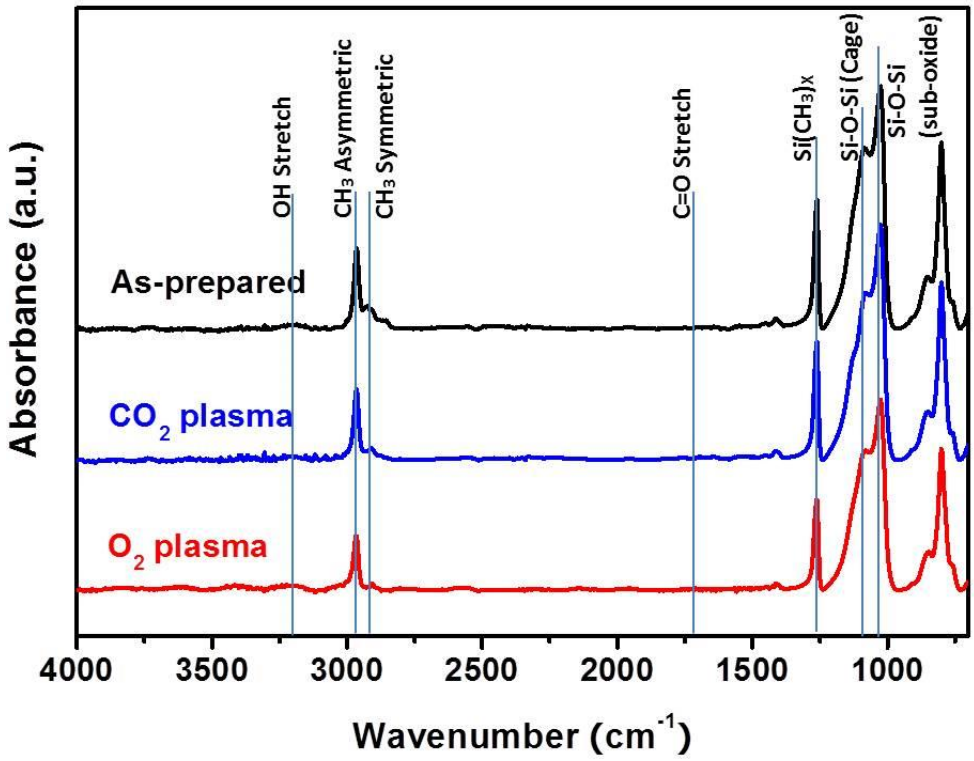

Fig. 3.7 Differential FTIR spectra evolution after plasma exposure

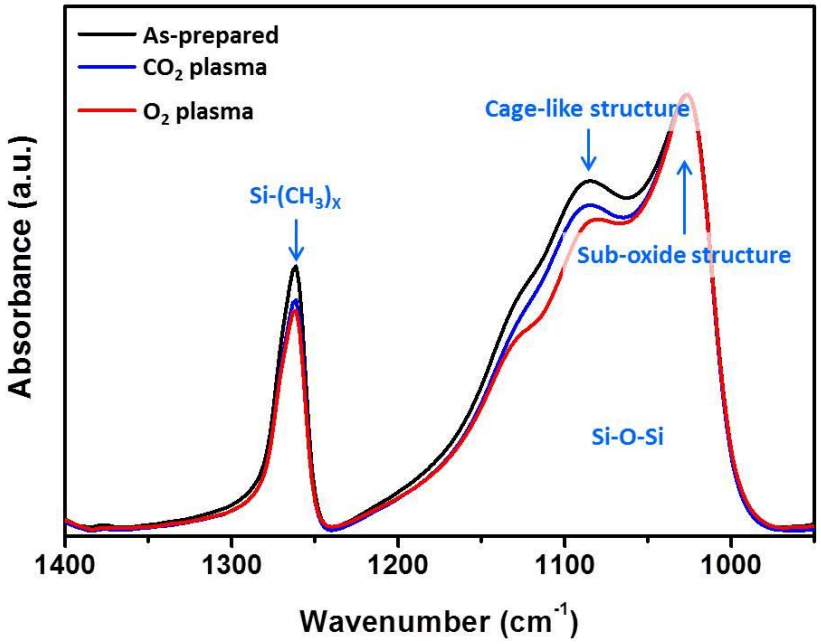

Fig. 3.8 FTIR spectra of as-prepared PLK and plasma-exposed PLKs

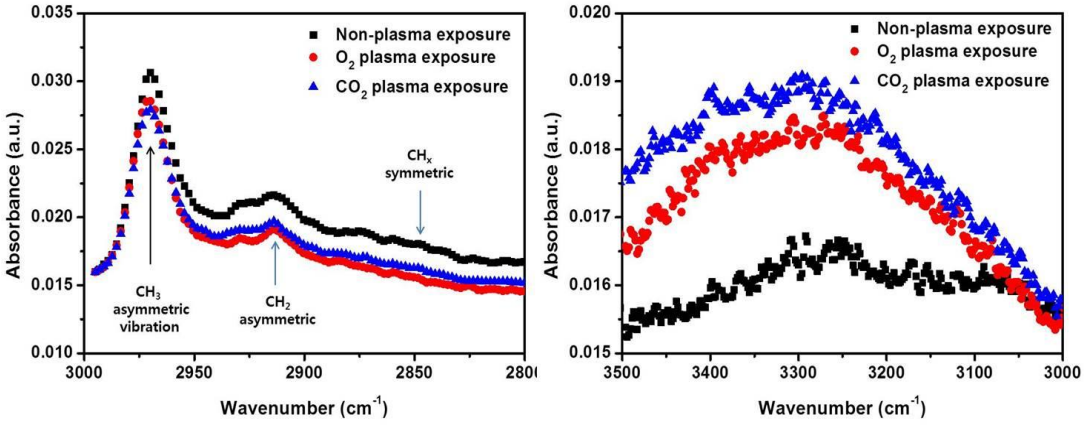

Fig. 3.9 FTIR spectra evolution for methyl and hydroxyl group after plasma exposure

It is well-known fact that the intensity change in shoulder of Si-O-Si peak is due to the ratio change of cage-like structure in backbone, however, deconvolution of the peak into three components was conducted in order to analyze the ratio change quantitatively as shown in Fig. 3.10. Deconvoluted fitting was done by using MatLab and it was assumed that all peaks to be

perfectly Gaussian and to have the same FWHM (Full width at half maximum). As discussed previously, according to the area ratio of the fitted subpeaks, the relative concentrations of all the components were calculated.

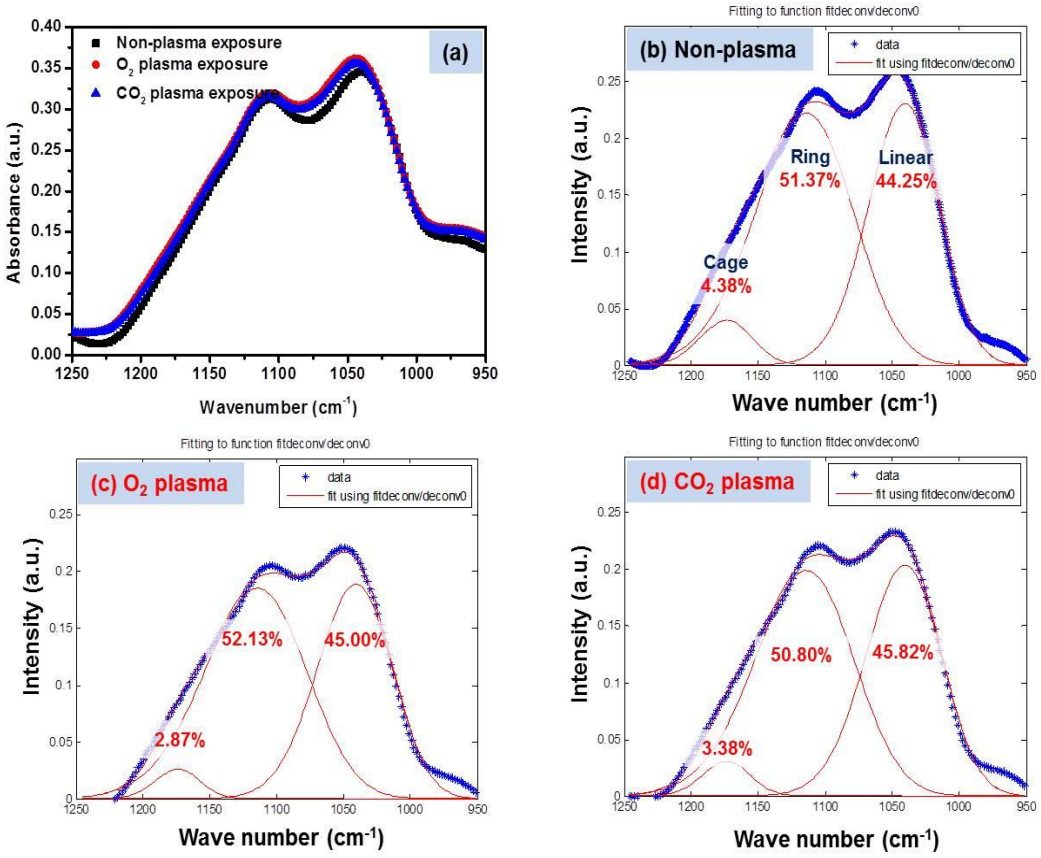

Fig. 3.10 FTIR spectra evolution with plasma exposure: (a) before deconvolution, and deconvoluted fitting of Si-O-Si peak for (b) non-plasma exposure, (c) O_2 plasma exposure, and (d) CO_2 plasma exposure

The comparison of structural morphology evolution supported that plasma exposure reduced the cage structure, which indicated that free volume in the film matrix was reduced, leading to pore collapse and densification. In addition, O_2 plasma treatment was more effective to reduce the cage structure than CO_2 plasma, which was considerably matched with the results as discussed above. These evolutions are believed to be caused mainly by backbone breakage.

Fig. 3.11 shows schematic description of backbone breakage induced by extrinsic factors such as plasma, moisture, and thermal exposure. Extrinsic stress breaks the Si-O bonds and CH_3 groups which are terminally bonded to the backbone structure, leading to the Si-OH group formation and smaller size of backbone cluster. As a result, it was seen that overall peak intensity of siloxane was slightly dropped after plasma exposure.

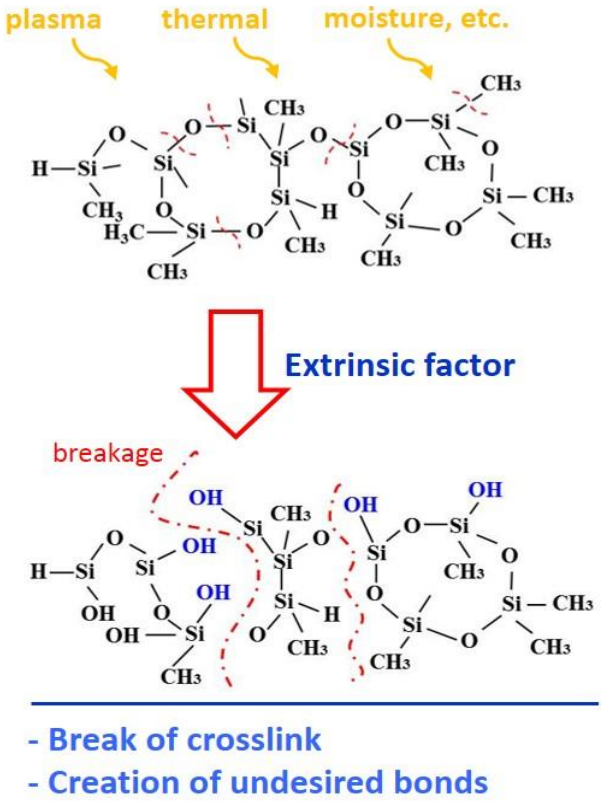

Fig. 3.11 Schematic description of backbone breakage induced by extrinsic factors such as plasma, moisture, and thermal exposure

3.3.4 Indentation swelling phenomena of PLK films

In order to reduce the dielectric constant in p-SiCOH, the industry has extensively been developing various precursors containing different configuration of non-polar species such as methyl group for reducing dielectric constant. By replacing oxygen or hydrogen species with

methyl species, PLK film matrix transforms into a less polar structure and has lower density due to creation of additional free volume. With an aim to enhance the properties of PLK film, different precursors and organic fragments were used for deposition of low-k dielectric film. Interestingly, the indentation results showed that all films were swelled instead of indented although all test conditions were identical. Fig. 3.12 displayed surface profile images with swelling height and contact angle change with respect to the specimen history. Swelled height was drastically increased with plasma exposure, which was totally different behavior from the other case we discussed. PLK film with more C content incorporated showed more swelling compared to as-prepared. Even though all other plasma parameters, such as total flow through reactor, pressure in reactor, and RF power applied to sustain the plasma, influence the deposition process and film properties, swelling phenomena and its comparison with indentation behavior strongly indicated that PLK instability involved with viscoplastic deformation could be recovered by modifying chemical bond configuration.

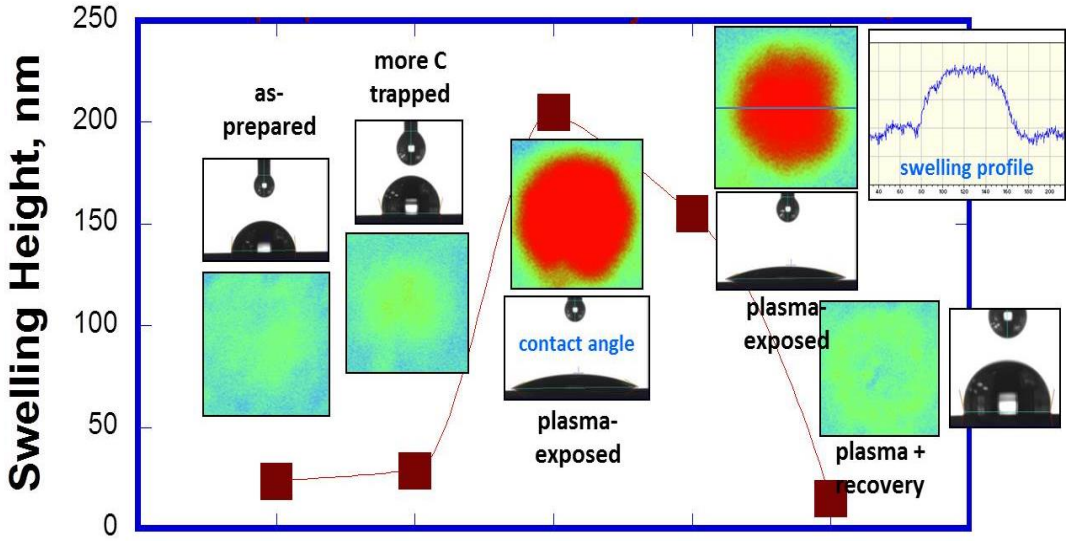

Fig. 3.12 Surface profile images with swelling height and contact angle change with respect to the specimen history

In order to verify why the indentation behavior is totally different between two types of

PLK film, comparison of FTIR spectra over the range of 950~3400 cm^{-1} was conducted and peak area ratio upon Si-O-Si peak was summarized in the plot as shown in Fig. 3.13. Major contrasting aspect was that the films showing swelling phenomena had much more carbon residue involved with unstable organic fragments than those showing indented behaviors. From the intensities of Si-(CH_3)x (1280~1250 cm^{-1}) peak, it is informed that the swelled films contain smaller free volume, and also comparison of siloxane peak configuration indicates that swelled film matrix has less crosslinking backbone structure. Noticeable is the fact from FTIR study between indented and swelled PLK film that degraded properties of PLK induced by plasma exposure can be recovered and enhanced by modifying chemical bond configuration. Possible scenario is to generate the more C contents from porogen residue or unstable -C bond and then induce them to be crosslinked to the backbone structure.

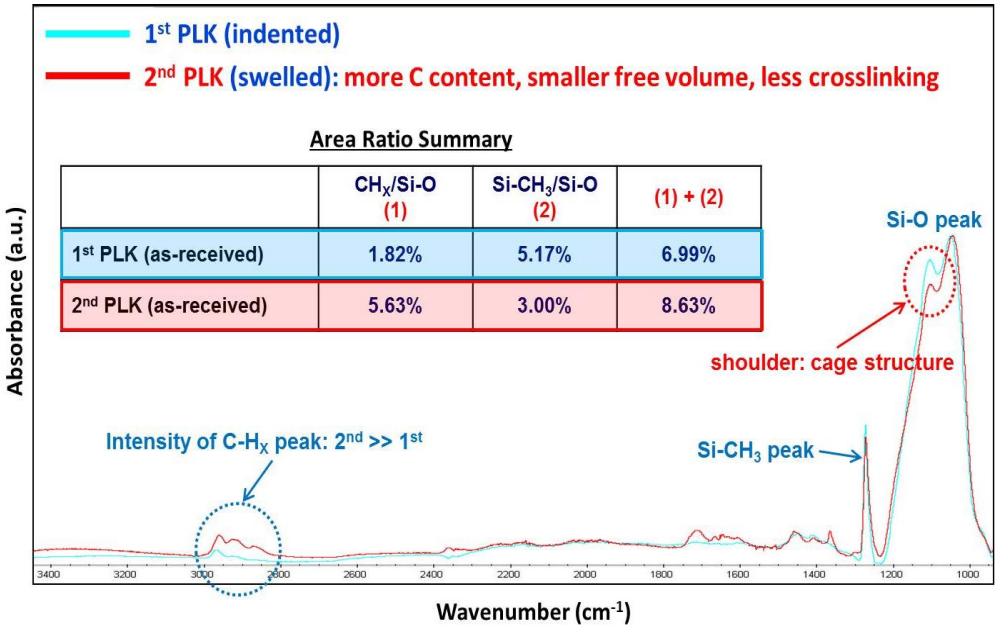

Fig. 3.13 Comparison of bond configuration between indented and swelled film

3.4 Summary

In this chapter, first, the investigation attempts to quantify the damage in PLK backbone network as a function of integration process steps by the use of viscoplastic property as a tracing

method of chemistry change. Our investigation reveals that the damage to the PLK backbone by integration processes is cumulative and also that any process that exposes the film to oxidative plasma is the most vexing among BEOL integration process steps. Hence, thermo-mechanical instability of PLK with respect to the different plasma source is studied in order to find the effective way of restoring plasma-induced damage. Primarily, it is found that formation of –OH bond is found to be prevailing, which causes the decrease in –C group content and the breakage of backbone crosslink. The observations made from viscoplasticity and FTIR characterization of PLK films with plasma exposure suggest that the main plasma damage appears in two ways. The first damage is the loss of carbon in the terminal bond ($SiC\text{-}H_3$) and in the crosslink (C-H) bond. The breakage of the terminal bond makes the free volume (pore) to decrease while the breakage of crosslink decreases mechanical strength of the backbone structure. The second damage is the formation of unstable bonds such as Si-OH and Si-H bonds. These bonds must form as terminal bonds and break the long range cross-linking of the backbone structure, substantially decreasing PLK's resistance against thermal and mechanical instability. In particular, we believe that such bonds are responsible for viscoplastic deformation. Collation of such bonds can result in the formation of small cluster that is chemically isolated from surroundings due to terminal Si-OH or Si-H bonds. Due to the lack of long-range crosslink, the cluster can slide along the cluster boundaries, resulting in viscoplastic deformation by viscous flow. Their formation is also responsible for the increase in the dielectric constant because they carry considerable dipole moment (polar). Our results produce multiple insights that are helpful in understanding the nature of the damage and developing repair process.

Chapter 4

REPAIR OF PLASMA-INDUCED DAMAGE IN POROUS LOW-K DIELECTRICS

4.1 Introduction

Plasma etch and ash processes induce the depletion of methyl species and the increase of moisture uptake in porous low-k films, leading to degradation of dielectric constant and their sensitivity to thermo-mechanical instability. [64,92] Our previous study clearly shows that PLK thin films exhibit a significant level of viscoplasticity with a rate sensitive to the degree of oxidative plasma damage and moisture exposure when tested using a ball indenter at relevant conditions to interconnect applications. [70] These changes in PLK properties and physical stability have been persisting challenges for next-generation interconnects because they are the causes of failure in interconnect integration as well as functional and physical breakdown appearing later in the chip manufacturing.

Several methods of damage restoration have been proposed in the past, most notably the silylation treatment. However, it offers limited effectiveness, and also, they are not easy to incorporate into the flow of integration processes because of the requirement for supercritical CO_2 and hazardous reaction byproduct. [93] In order to maximize the efficiency of damage repair by silylation treatment in terms of both property restoration and process simplicity, we adopted simple immersion into silylating agent and optimized the silylation treatment by combining mild annealing under inert ambient. From the result, it is clear that damage repair is possible, but it is found that restoration of the electrical property and thermo-mechanical reliability is somewhat compromised.

Also, as another way of enhancing the properties of PLK films, UV cure has been employed by the industry to correct the limitations of the silylation process. However, UV cure is mostly conducted at temperatures of ~400^{o}C for durations of minutes, indicating that although it yields PLK films with superior mechanical properties, it can lead to integration failure due to dimensional change induced by high temperature anneal. Zenasni et al. reported that thickness

reduction of PLK films occurred ~ 17 % after 15 min UV cure. [94] Furthermore, since UV cure is performed by use of broadband UV lamp, penetration depth is not enough to stimulate entire PLK film matrix. From these perspectives, low-energy inert plasma radiation, what is called soft x-ray treatment, was also investigated. Soft x-ray radiation could induce gentle reconfiguration of chemical bond by controlling the energy level, and consequently desired properties of PLK dielectrics were obtained. Even though it showed the improvement in property restoration, effectiveness was not favorable yet.

It is therefore important to find an effective and easy-to-implement way to reverse the plasma induced damages in PLK. Our approach is based on the idea that damage repair can be achieved by providing energetic stimulation to chemical bonds already existing in PLK films and forcing them to reconfigure to a beneficial structure. Various radiation treatments have been tried in our exploration, and this search leads us to a conclusion that low energy Ar plasma treatment holds the most promising potential as it is found to result in the restoration of PLK structure and properties that closely match with the original state PLK before exposure of oxidative plasma process.

This chapter presents the mechanism responsible for the repair of the bond structure and recovery of mechanical stability and dielectric property in PLK films.

4.2 Experimental procedures

The porous SiCOH films used in this study were plasma-damaged by O_2 source. The films have a nominal thickness of ~361 nm, and a dielectric constant of approximately 2.05 measured by spectroscopic elliposometer. Initially, film thickness was ~400 nm and dielectric constant was 2.0, however, they were degraded due to plasma-induced damage. The other characterization techniques are identical as described in chapter 3.

For silylation process, the one reported here was done using an immersion of PLK films to pure HMDS solution followed by an annealing at 120^{o}C for 30 min under flowing N_2 environment.

For soft x-ray radiation as a way of damaged property repair, Perkin-Elmer Phi 560 XPS/Auger System was used. Mg Kα (1.25 keV) source was applied to stimulate the film matrix. Soft x-ray radiation was performed with operating pressure ~1 x 10^{-9} Torr. Exposure time to x-ray radiation was 10 sec. A series of PLK films were annealed for 30 min after soft x-ray radiation to enhance the chemical bond rearrangement.

Treatment of plasma damaged PLKs films with low energy Ar plasma is conducted using an inductively coupled RF reactor. A plasma power is varied from 15 ~ 100 W (total chamber power) and exposure time was 30 ~ 300 seconds. Since the substrate is biased under -200 V, the Ar plasma ion is likely to carry 200eV kinetic energy toward PLK films. This energy is far lower than the soft X-ray but is much higher than the deep UV (~6 eV) used for UV cure. After Ar plasma treatment, the films are annealed at 400^{o}C for 30 min to assist the reconfiguration reaction of PLK backbone.

4.3 Results and discussion

4.3.1 Properties restoration by silylation process

Based on the structural morphology evolutions induced from plasma process conditions as mentioned in this study, repair treatment on the plasma exposed SiCOH films was carried out by restoring the original chemical structure. Alternatively, treatment with silylating agent followed by annealing was proposed as a way to modify plasma-induced damage in PLK films. Among several silylating agents, HMDS ($(CH_3)_3$-Si-NH-Si-$(CH_3)_3$) was chosen for the present study because it is the solvent with low vapor pressure at room temperature. Silylating reaction can substitute the hydrophilic –OH group with hydrophobic methyl species, thereby it is expected to be restored the original structural morphologies before plasma exposed as shown in Fig. 4.1.

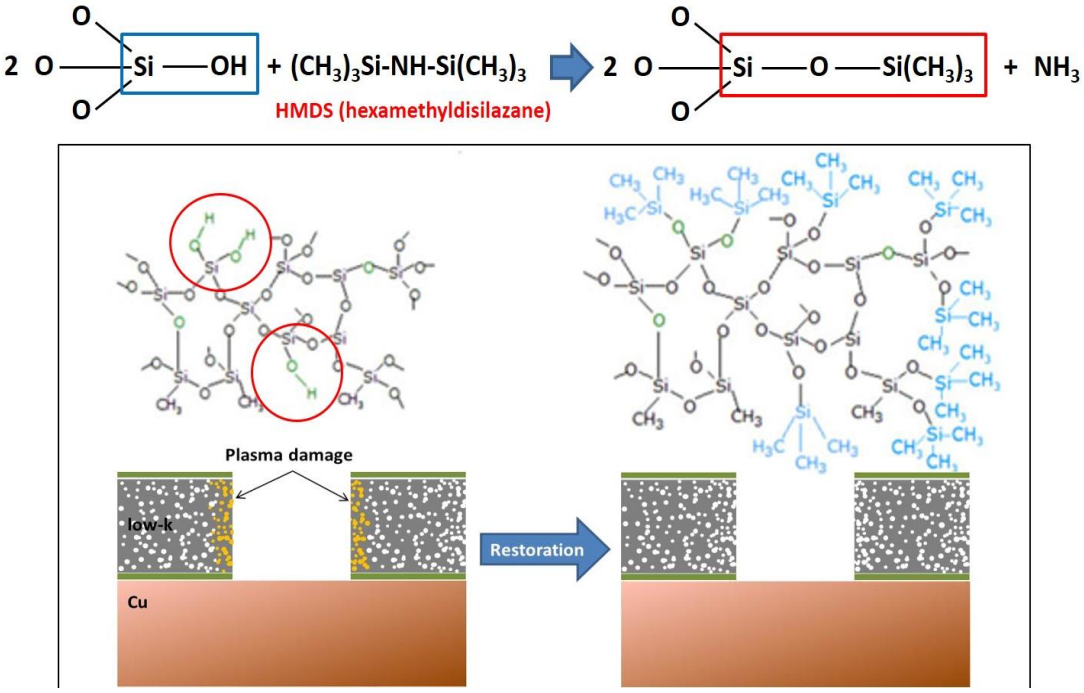

Fig. 4.1 Schematic illustration of silylation treatment with HMDS agent

Fig. 4.2 showed the change in the indentation depth and contact angle for plasma exposed specimens after 4 h indentation test at 400°C. The results presented that hydrophilic surface was transformed to hydrophobic by incorporating methyl groups, which lead to the strengthening of the films as well. The contact angle for O_2 plasma exposed was measured as 44.54°, and 56.68° for CO_2 plasma exposed. The alternation in surface chemistry induced from plasma exposure produced significant increases in the dispersive and polar surface energy components. However, the contact angle was restored up to 83.92° and 84.42°, respectively by controlling the annealing temperature and time. For a reference, contact angle for non-plasma specimen was 100.87°. In addition, it was proven that chemical treatment followed by annealing at elevated temperature made dielectric constant to be recovered about 65 % and viscoplastic deformation to be deceased without any further densification.

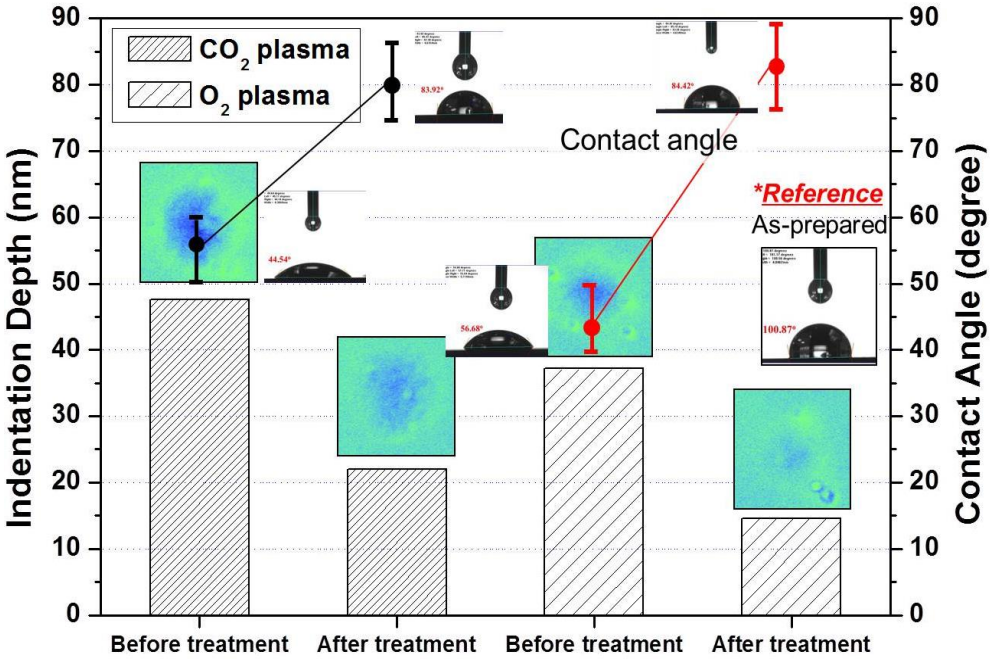

Fig. 4.2 Effect of chemical treatment on the change of indentation depth and contact angle

Structural evolutions by silylation process were investigated in order to understand the way of restoring quantitatively as exhibited in Fig. 4.3. From the comparison of deconvoluted Si-O-Si fitting, diminished cage-like structure by O_2-plasma exposure and linear structure were increased at the expense of network structure after silylation reaction. In fact, the network structure is the transition structure from linear structure to cage-like crosslinking structure, which appears to be a relatively unstable and weak bond configuration. Symmetric linear Si-O chain reduced dielectric constant by decreasing dipole moment of molecule in film and its networking into cage-like structure showed excellent properties in terms of resistance to damage from acid or alkali solution and oxygen plasma. [95]

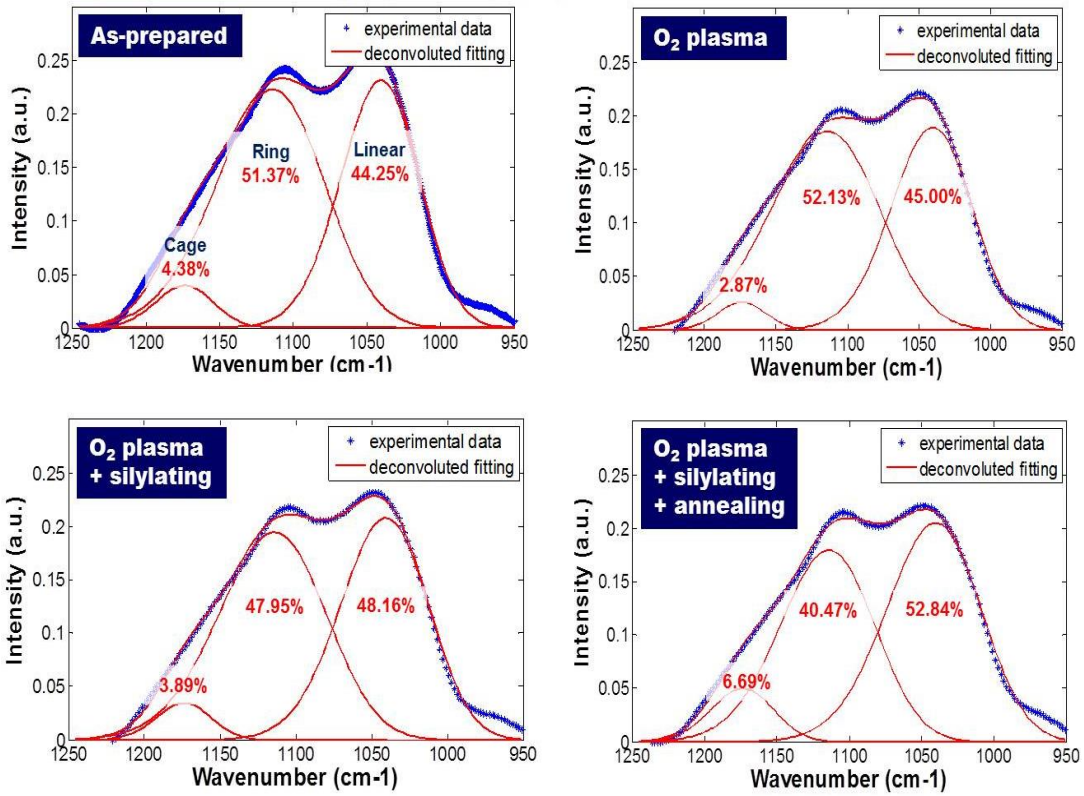

Fig. 4.3 Structural evolutions induced by silylation process

It was also noticeable that structural evolution by chemical reaction was more activated with thermal assistance. Cage-like structure and linear structure were increased ~53 % and ~20 % compared with those of as-prepared films, respectively when silylation process was combined with thermal annealing. It is possible that the silylating reaction at room temperature produces an intermediate bond state that is not fully incorporated into the bond network but exists near to the reacted area. With thermal annealing given, those intermediate bonds are activated to bond completely with the damaged site.

4.3.2 Properties restoration by soft x-ray

As another approach to resolve the problem from UV cure and improve PLK properties, soft x-ray (target: Mg Kα) radiation was also investigated. The originality of this research is on

that it is not only effective to manipulate the bond configuration but also easy to incorporate into the flow of integration processes. This method has not been reported yet it was found that it could induce gentle reconfiguration of chemical bond and by controlling the energy level, and consequently desired properties of PLK dielectrics were obtained. Firstly, in case of x-ray radiation, it has wavelength of 10^{-10} m which is smaller than that of UV by 10^{-2} order (Fig. 4.4), stimulation depth should be deeper compared with UV cure. Another advantage is that treatment time can be achieved within 5 sec with thermal assistance and it does not cause any serious thickness reduction since the applied temperature is below ~300°C from our experiment. However, it was revealed that x-ray radiation with Cu Kα target induced high level of energy and removed some skeleton bonds such as Si-CH_3, Si-O, leading to the acceleration in viscoplastic deformation. Therefore, it is required to optimize the x-ray radiation conditions for the desired chemical bond configuration.

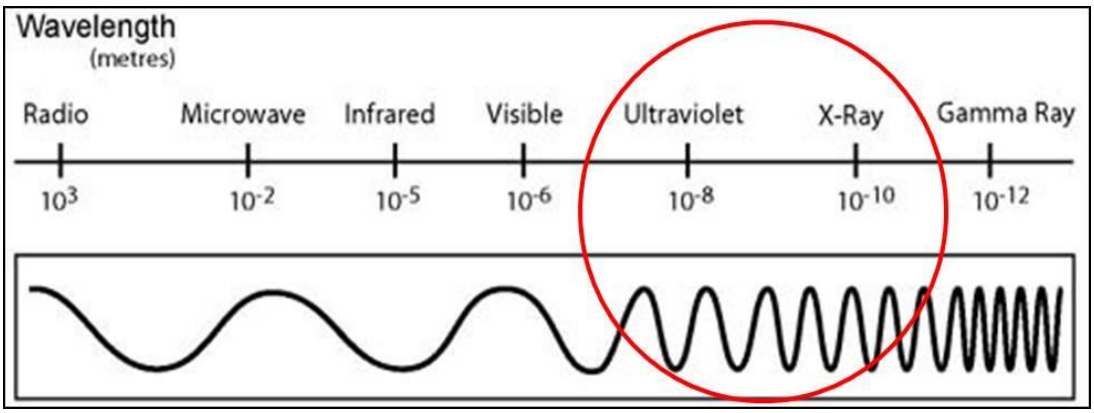

Fig. 4.4 Electromagnetic spectrum [*www.viewzone2.com]

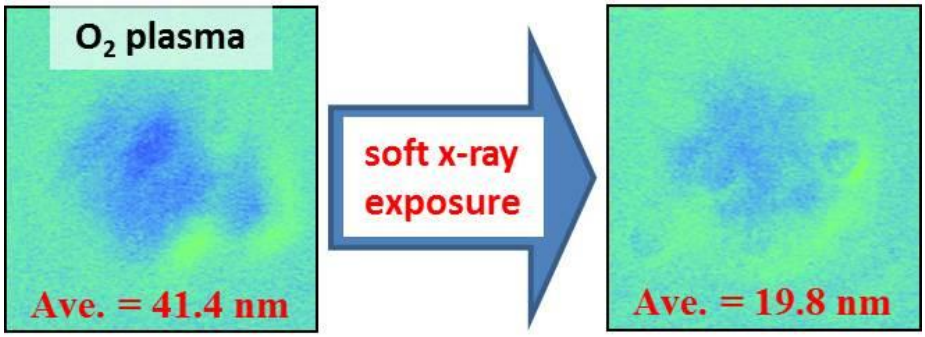

Fig. 4.5 Indentation depth profile change after soft x-ray radiation

Fig. 4.5 shows the indentation depth profile change after soft x-ray radiation. It was clearly observed that indentation deformation depth was increased and also, it was found that reduction in dielectric constant occurred simultaneously while film thickness remained the same. (Fig. 4.6) This result is very interesting in terms that plasma-induced damage can be repaired without any sacrificial properties of dielectrics. Conventionally, it has been considered that the enhancement of thermo-mechanical property and lower dielectric constant in PLK was offset by Si-CH_3/Si-O concentration ratio, thus, it should be optimized for proper tradeoff. [96-99]

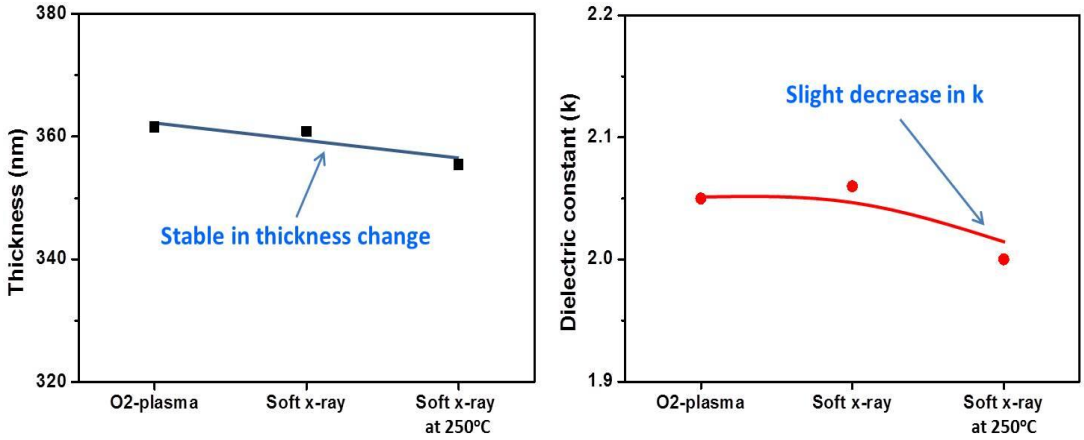

Fig. 4.6 Effect of soft x-ray on thickness and k variation

4.3.3 Low-energy Ar plasma treatment for repair of plasma-induced damage

Furthermore, we have been searching for an alternative route for damage repair which is the most convenient to incorporate into the flow of integration processes, leading us to a discovery that a brief exposure to low-energy inert plasma results in the restoration of PLK structure and properties that closely match the undamaged. Abell et al. applied He plasma treatment to seal the surface of low-k dielectrics by forming an ultra-thin SiO_2-like layer and found that it induced the increase of porosity (or reduction of k value) by sealing the low-k surface efficiently. [100]

Our approach of using inert plasma as a way for damage repair is motivated by our realization that plasma damage appears in two major areas. The first is the loss of –C from PLK matrix, and the second is the increase in Si-H and Si-OH terminal bonds as a byproduct. The first change causes the dielectric constant to increase because of increased density and/or loss of free volume. The second causes PLK to lose thermal and mechanical stability because Si-H and Si-OH act as catalysts for reactions that break the cross-linked backbone. Clearly, both changes in PLK chemistry and bond structure must be addressed in order for any repair method to be successful. Silylating treatment works because it replenishes –C while removing –H and –OH bonds; however, the silylating agent cannot penetrate deep into PLK matrix with its low permeability, making it difficult implement. Alternatively, it is possible to find a source of –C in the PLK matrix because a good portion of -C is in the cross-link (CHx) chain network. When the CHx is broken from the cross-link and forced to react with –H or –OH, then the reconstruction of PLK backbone can be realized.

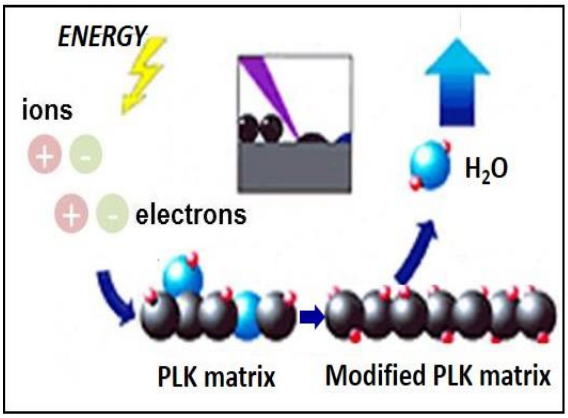

Bond	Bond energy (eV)[3]
Si-O	8.3
C-O	11.2
O-H	< 4.4
C-H	3.5
Si-H	< 3.1

Fig. 4.7 Schematic illustration of Ar plasma radiation and bond energy found in p-SiCOH film matrix

For this very reason, we utilize the inert Ar plasma because the kinetic energy transfer from Ar ions can effectively break CHx bonds, and also, Ar ions can promote a dehydration reaction during repolymerization. Schematic illustration of Ar plasma radiation and bond energy found in p-SiCOH film matrix are shown in Fig. 4.7. Our trial with various Ar plasma conditions reveals that such reactions are indeed occurring, as evidenced by the recovery of dielectric constant, increase in film thickness, and improved resistance against thermal instability as well as viscoplastic deformation. An even greater and more interesting discovery is the fact that such reactions become more intense when the repolymerization is induced under hydrostatic pressure. Fig. 4.8 exhibits the evidence that altered PLK film matrix by inert Ar plasma radiation experiences chemical reaction with hydrophobic groups. This is because usually indented area during ball indentation creep test is transformed into hydrophilic as marked in conventional behavior in Fig. 4.8, however, the indented area was become hydrophobic after the test in case of Ar plasma radiated film. It indicates that matrix chain is obviously reconstructing under thermal pressure and desired property can be obtained.

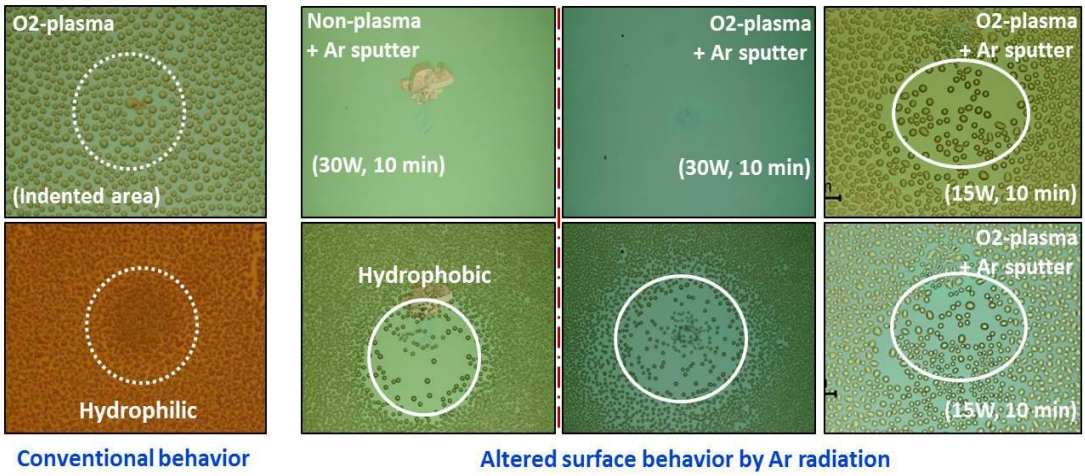

Fig. 4.8 Effect of Ar plasma radiation on surface morphology

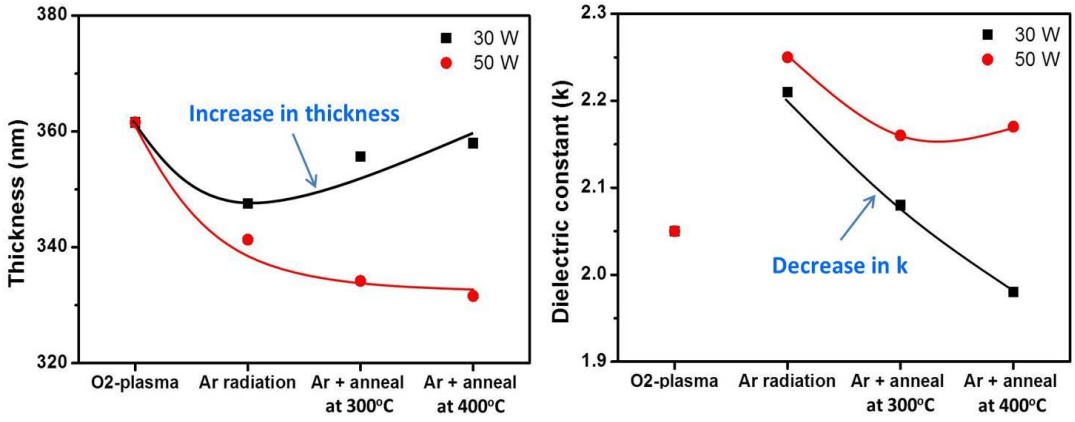

Fig. 4.9 Effect of Ar plasma radiation on film thickness and k change

In order to support the idea that repolymerization occurred in PLK matrix, the variation of film thickness and dielectric constant was examined shown in Fig. 4.9. The results convinced that it did occur. Interestingly, film thickness was increased ~ 2.5 % in case of Ar plasma radiated film followed by thermal annealing. Simultaneously, it was evidently seen that dielectric constant was reduced.

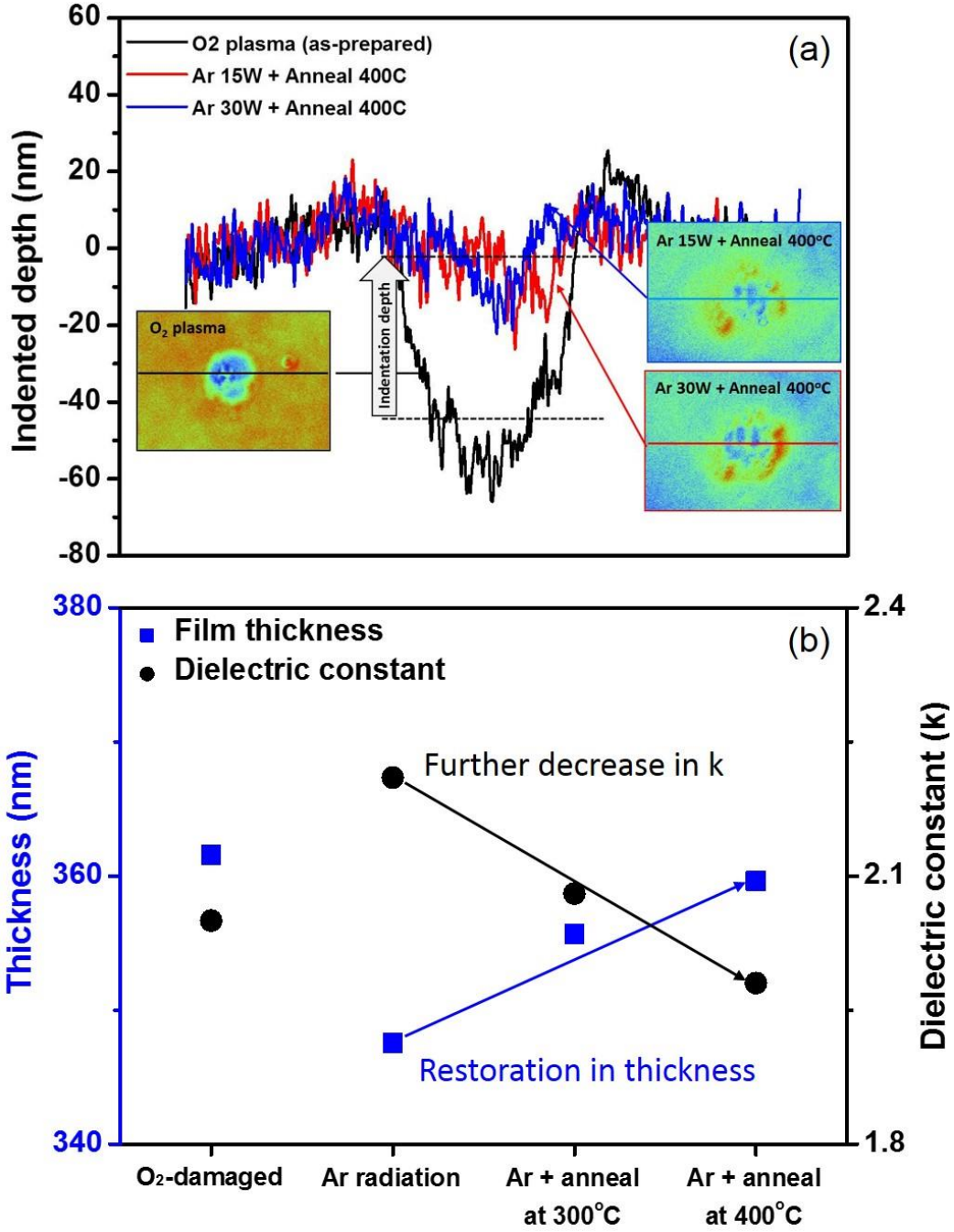

Fig. 4.10 Variations in (a) indentation depth, and (b) thickness and dielectric constant with proposed recovery processes

Fig. 4.10(a) compares the indentation depth of PLKs films with variation in PLK

treatments. Notice that indentation depth of Ar treated films shows a substantial reduction from the plasma damage condition and becomes the same as the as-prepared PLK films. Fig. 4.10(b), where film thickness and dielectric constant are shown as a function of treatment condition, clearly evidences the effectiveness of Ar treatment in restoring film thickness and dielectric constant. Interestingly, the hydrophobization of PLK surface is found be more pronounced in indented area. It is found that ~85 % recovery in contact angle (hydrophobization) is achieved in the indented area. This result indicates that the chemical reaction for hydrophobicity is more favored under pressure. The exact nature of reaction preferred under pressurized condition is currently unknown. It is our speculation that incorporation of C in the $–CH_3$ terminal bond is favored reaction under hydrostatic pressure based on the analysis of C_{1s} XPS binding energy shift, which will be discussed later in Fig. 4.13.

Fig. 4.11 shows the effect of Ar treatment on the change in dielectric film thickness, indicating that Ar treatment plays a critical role to reconfigure the bond network in the film matrix. The plot compares the different behaviors in film thickness change with respect to the Ar treat presence. Initially, film thickness damaged by O_2 plasma is 361 nm and it is further decreased up to 349 nm after Ar treat since Ar plasma treat acts as sputtering process as well. However, remarkable fact to observe is that the PLK film without Ar treat shows continuous decrease in thickness during the post annealing process. As mentioned in Fig. 4.10(b), annealing process on the Ar treated film increases the film thickness. From the comparison of two contrasting behavior, it is assumed that Ar treat stimulates the chemical bond ready to re-polymerize in the film matrix and post annealing assists such reaction to happen. However, without Ar treat, annealing probably contributes to removal of organic fragment or porogen residue in the film matrix, leading to densification and the decrease in film thickness. In other words, chemical bond in the film matrix is not activated to rearrange without Ar treat.

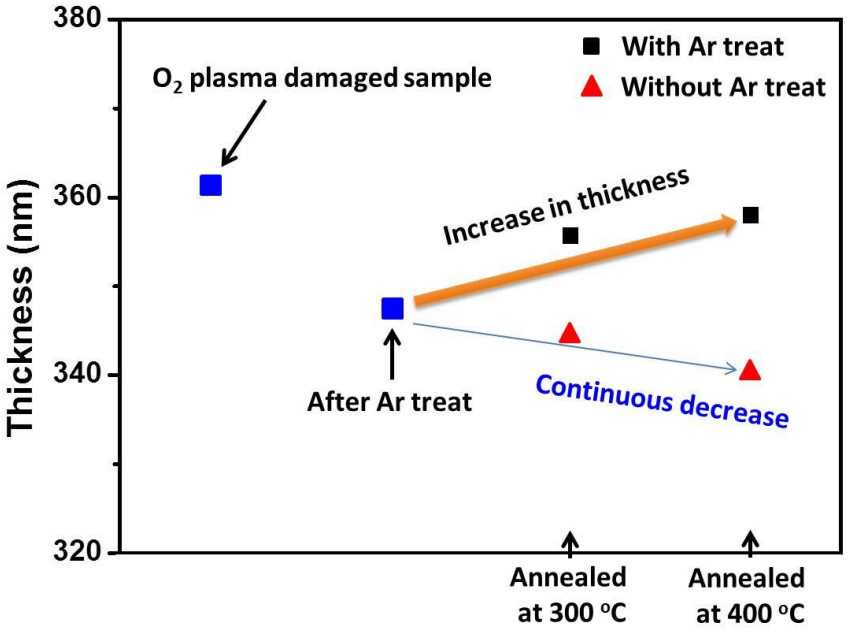

Fig. 4.11 Effect of Ar treatment on the change in dielectric film thickness

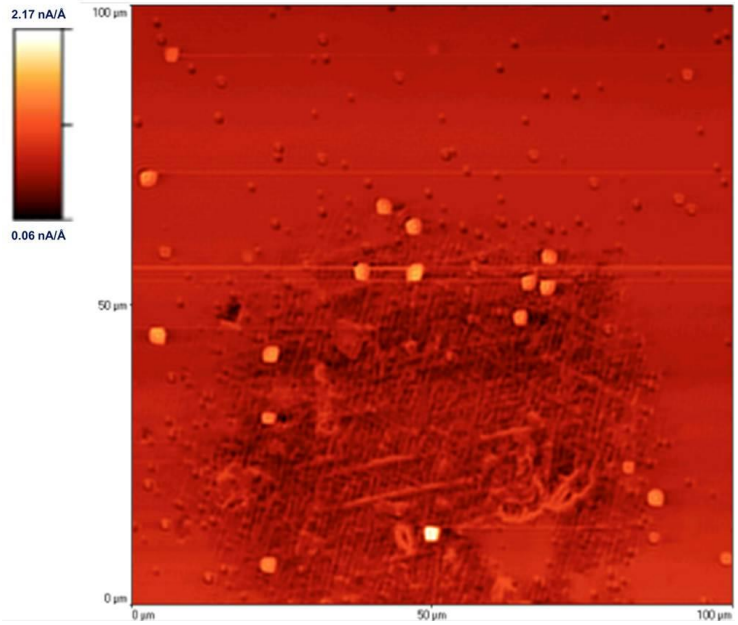

Fig. 4.12 FMM image of ball indented area for PLK film treated by Ar plasma

Fig. 4.12 shows the FMM (Force Modulated Microscopy) image of Ar treated film produced by AFM in our lab. The area with dark contrast indicates the indented area, which becomes harder compared with non-indented area since dark contrast means that it needs more current to penetrate the same depth. As the contact area between indentation ball and film surface create the pressure with high temperature, this result evidences thermal pressure facilitates the reaction of hydrophobization (refer to Fig. 4.8) and mechanical hardening simultaneously in case of Ar treat film.

In order to understand the restoration mechanism of PLK properties by Ar plasma treatment, the change in backbone structure is analyzed by using Si-O-Si absorption band as shown in Fig. 4.13. In our analysis, the Si-O-Si FTIR peak is deconvoluted with an assumption that all sub-peaks follow the Gaussian function and have the same FWHM as mentioned. The relative concentrations of three sub-peaks, namely cage-like, ring, and sub-oxide structure, are computed using the peak area. It can be seen that the O_2 plasma reduces the case-like and sub-oxide structures (Fig. 4.13(a) vs. (b)). Ar plasma treatment followed by thermal annealing restores the cage-like and sub-oxide component (Fig. 4.13(c-d)) with an expense of the ring structure. It is commonly believed that the cage structure is responsible for the pore formation (free volume) and the sub-oxide structure is associated with the PLK strength as it enables long-range crosslink. Based on this analysis, it can be concluded that damage restoration (increase in stability and reduction in dielectric constant) is a result of increase in the cross-linking of the backbone that is facilitated by the sub-oxide, and the cage structure that lowers dielectric constant.

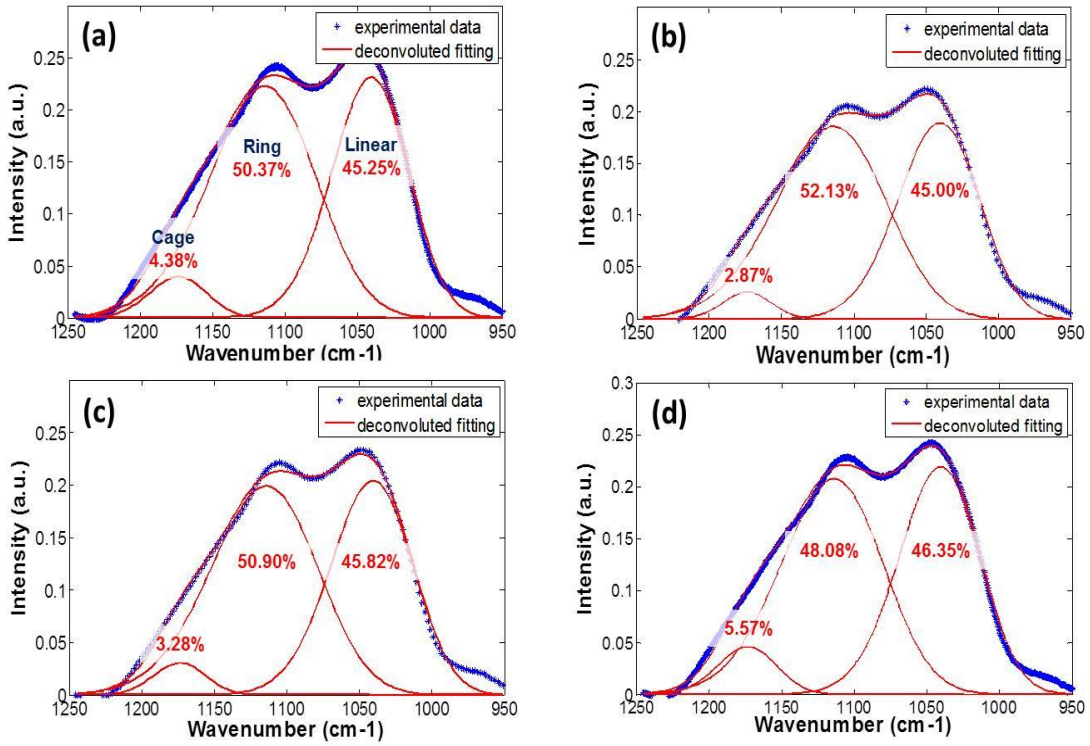

Fig. 4.13 Evolution of the absorption bands of Si-O-Si with deconvoluted peak information; (a) as-received, (b) O_2 plasma exposed, (c) Ar plasma + thermal anneal treated, and (d) Ar plasma + thermally pressured anneal

To further verify the mechanism, Si bonding status is investigated by XPS (X-ray Photoelectron Spectroscopy) and each spectral region is deconvoluted into individual peaks as shown in Fig. 4.14. It is clearly observed that binding energy peak exhibiting the highest intensity is shifted from 103.2 eV to 105.2 eV after Ar plasma treatment, which describes the shift to SiO_4 from SiO_2-C_2. This result obviously implicates that Ar plasma treatment reconfigures the chemical bonds to be mechanically strengthened, and it is drawn that oxygen content is related to strengthening of the film matrix due to the enhancement of the Si-O structure. In other words, energy source from Ar plasma breaks the Si-H or Si-O-H links and induces –H radicals to react with Si-CH_2 in the backbone or porogen residue, which produces Si-CH_3 and Si-O-Si crosslinking

by involving -O into the O-Si- structure. This is in good agreement with the increase of Si-O_4 configuration in the backbone structure.

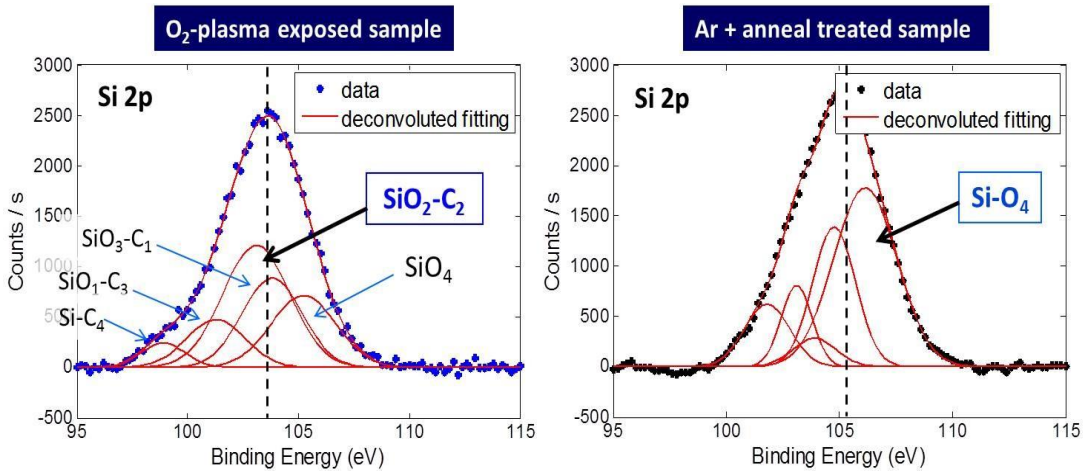

Fig. 4.14 XPS binding energy profile shift of Si_{2p} after Ar plasma process

The exposure of the PLK films to the Ar plasma beam is sufficient to break chemical bonds (C-H, O-H, Si-H), leaving free radicals at near the surface. These radicals can react only with other surface radicals or by chain transfer reactions. In case of porous film matrix treatment under Ar plasma condition, plasma ions are accelerated towards the pore surface where crosslink is less stable or –OH / –H are terminally bonded to silicate backbone cluster and lead to an increased reactivity of the respective surface. As response of the molecular structure in SiCOH films, one of the following events proceeds; branching, chain scission or recombination. [101] In addition, the inert plasma eliminates low molecular weight species or substitutes them with high molecular weight species by crosslinking. In summation, it is assumed that kinetic energy from Ar ion scissions undesired bonds and effectively reconfigures them towards superior properties on the carbon depletion region in PLK films. While silylation process brings –C species into the damaged PLK films, alternatively, it is possible to find a source of –C in the PLK matrix and trapped aliphatic hydrocarbon chains induced by porogen precursors, which are generally used for the creation of porosity, because a good portion of –C is in the polymer chain network.

Accordingly, it is suggested that the immediate event of an Ar plasma beam radiation is to deposit energy from the plasma species (ions, electrons) and this energy input produces the excited state species because Ar cannot chemically react with the film matrix. As a consequence, the radical sites are generated at the less stable area such as colony boundary or pore surface with the decay of the excited species, leading to the production of free radicals by an energy transfer to the bonds which are to be broken. Then, the activated sites experience chemical bond rearrangement by chain-scission, branching, or cross-linking. In our case, crosslink with C is involved with silylmethylene (Si-$(CH_2)_x$-Si) groups and possibly porogen residues and it is turned out that some of these groups are converted to methyl groups terminally bonded to siloxane backbone structure under 300~400^oC by reaction with –OH, and simultaneously creating a new Si-O-Si crosslink as shown in Fig. 4.15. [102] However, solid low-k films do not work with this suggested mechanism. This is due to the fact that the plasma action is a strong function of the morphology and relative stability of the surface, thus, it tends to concentrate on the preexisting defects on the matrix.

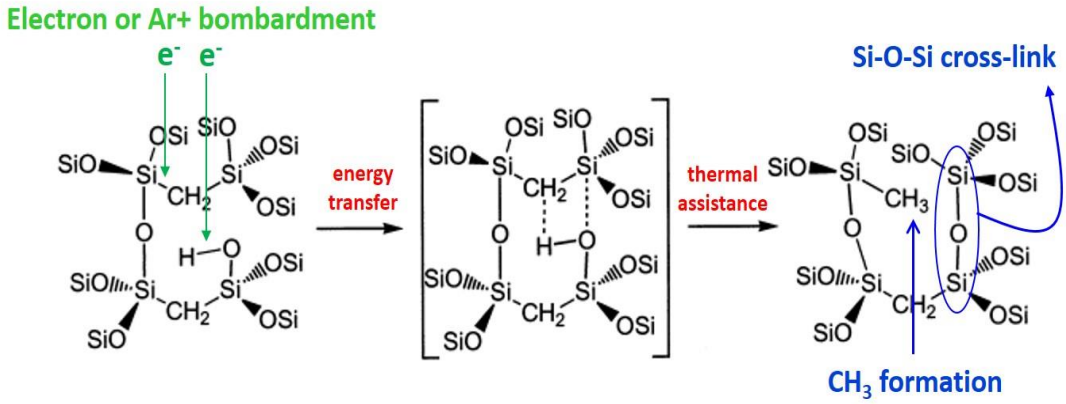

Fig. 4.15 Proposed mechanism of chemical bond restoration

The simplicity of the Ar plasma treatment yet its excellent ability of damage repair has a profound practical implication. It can be simple to implement without altering much of current processes used in industry. For example, Ar treatment can be done immediately after processes

involving oxidizing plasma processes. This can be done even in the same process chamber by changing the process gas. By doing this, the structural damage created during plasma process can be immediately repaired. Nevertheless, since our understanding on the restoration mechanism is still at infant state, it may demand more investigation before its implementation. It is our view that Ar plasma works because Ar plasma is inert but carries considerable kinetic energies sufficient to disturb unstable bonds in PLK backbone. Energy transfer from Ar beam to unstable bonds in PLK backbone (such as colony boundary), pore surface or in porogen residue activates them to be susceptible for chemical bond rearrangement by chain-scission, branching, or cross-linking.

4.4. Summary

This study finds that low energy Ar plasma radiation is extremely effective in restoring the mechanical stability and dielectric constant of plasma-damaged PLK film by oxidative plasma. The damage repair appears to work because kinetic energy from Ar ion beam stimulates the unstable bonds in PLK backbone and force them to form C-bridged crosslinking. This reaction also promotes the removal of Si-OH bonds, which increases the thermal and mechanical stability of PLK films.

Chapter 5

ENHANCED MECHANICAL STABILITY OF ULTRALOW-K DIELECTRICS WITH SELF-ORGANIZED MOLECULAR PORES

5.1 Introduction

Implementation of ultralow-k (ULK) interlayer dielectric materials for on-chip interconnects has been extensively studied to achieve ultra-large-scale integrated (ULSI) devices in terms of multi-functionality and high performance. Development of a porous carbon-doped silicon oxide (p-SiCOH) dielectrics has been a leading solution to realize ULSI electronics by reducing RC coupled delay in Cu/low-k interconnect wiring. Microelectronics industry mostly adopts the subtractive approach to produce porous low-k (PLK) dielectric film since it is much more flexible to reduce dielectric constant. In the subtractive method, a SiCOH matrix precursor mixed with an organic precursor is introduced in PECVD chamber. The deposited film is essentially a dual-phase SiCOH-CH_x material that is subsequently cured to remove the chemically unstable organic fragment and to convert the film into a porous SiCOH. [18] However, p-SiCOH material is easily damaged during the plasma-induced and thermally-induced processing in back-end-of-line (BEOL) integration due to the pores which surface area are more susceptible to the reactive chemicals used in plasma etch and ash process. Especially, plasma-induced damage is more pronounced when the pores are randomly distributed in the p-SiCOH matrix and their size is bigger. The damage results in the accumulation of trapped charges and an increase in defect-state concentrations. This leads to large leakage currents and exposes to the electrical reliability of devices. [103] In addition, mechanical/chemical damages take place that result in undesirable deviations from the expected physical properties of the dielectric film. [104] Our previous study clearly indicates that oxidizing plasma-exposed p-SiCOH film results in the loss of hydrophobicity as well as thermo-mechanical stability due to formation of silanol and moisture uptake, making PLK films to be prone to the viscoplastic deformation. [70] Also, film shrinkage is easily observed, causing the overall dimensional variation in the chip interconnect system. Given that plasma-

induced damage is difficult to prevent, the alternative is to repair this damage. In accordance with this viewpoint, several methods have been extensively proposed for damage restoration in the past such as silylation process, UV cure. [105,106] Silylation process utilizes reactive silyating agents to convert hydrophilic Si-OH groups into hydrophobic derivatives. However, it is revealed that they offer limited effectiveness or work only on the surface of PLK films since the molecule of silylation agents is generally enormous to penetrate. Also, Zenasni et al. reports the inefficiency of UV cure in that it causes further shrinkage in PLK film and the penetration depth is not enough to stimulate entire PLK film matrix. [94] From these perspectives, a lot of researchers have recently worked on the improvement of mechanical robustness of p-SiCOH matrix by structural modification or rearrangement. [95,107-108] Urbanowicz demonstrates that SiCOH glasses with improved mechanical properties and ultralow dielectric constant can be obtained by controlled decomposition of the porogen molecules prior to the UV hardening step. [107] Iacopi shows that the combination of thermal activation and UV radiation promotes a selective bonding rearrangement of the organosilicate glass matrix, which induces an improvement of about 40% in elastic modulus and hardness value. [108] More interestingly, Yoshiyuki et al. reports that large-radius neutral-beam-enhanced chemical vapor deposition process is developed to precisely control the film structure so as to produce non-porous ultralow-k SiCOH with sufficient modulus (>10 GPa). Since pores are not formed in this film, it shows that this particular film does not incur any damage from acid or alkali solution or oxygen plasma. [95]

In this chapter, we deposit two types of p-SiCOH dielectric films by using subtractive method and porogenless structural (or constitutive) method respectively in order to compare the thermo-mechanical reliability and the resistance for plasma-induced damage. In the structural method, the porosity in the film is obtained by choosing special precursors that contain molecular pores and by adjusting the plasma conditions to minimize the dissociation of the precursors in the plasma and to promote polymerization of the precursor molecules. [109] Since the deposited film is eventually single-phase material, precursor molecules and pores can be uniformly distributed

by controlling the deposition condition. Also, cure process becomes unnecessary by using porogenless structural deposition so that it induces robust structural configuration because normally UV cure can remove not only porogen but the crosslinks silica matrix. Elastic modulus and hardness are investigated for each case and resistance properties of integration damage are also evaluated to show that most integration damage is closely involved with the pore size and distribution. Our experimental data clearly show the feasibility that mechanical stability of ultralow-k dielectric film can be drastically enhanced by producing smaller pore size and uniform pore distribution without porogen fragments.

5.2 Experimental Procedure

The porous SiOCH films deposited with subtractive method in this study were synthesized from an alkoxysilane matrix precursor and an organic porogen (BCHB; bicylcoheptadiene) by using plasma-enhanced chemical vapor deposition. In case of the film deposited by structural method, the matrix precursor is confidential and PECVD condition is skewed from the industry standard. The films had a nominal thickness of 400 nm, a porosity of ~30%, and a dielectric constant of approximately 2.1. Porosity in the subtractive film was created by incorporating an organic porogen into the film that was later removed by thermal and electron beam to form porous SiCOH layer. The mechanical properties with respect to different deposition method were measured at room temperature and compared using Nano-indention test. Conical tip was found to be more suitable for our thin films. Measurements were carried out with a surface approach velocity of 10 nm/s. Ten points on each film were analyzed and the average and standard deviation were calculated. The first 10% of the film thickness was taken as indentation depth range to determine elastic modulus and hardness. Dielectric constant and film thickness were measured by spectroscopic ellipsometer. Three different angles from 65 to 75 degree were used to calculate the change of light polarization induced by the reflection and transmission at the film interface.

5.3 Results and Discussion

5.3.1 Elastic modulus and hardness

In order to evaluate the change in elastic modulus and hardness of p-SiCOH films, a first series of nano-indentation test were conducted on the specimens with respect to the different deposition method. The values of elastic modulus and hardness from specimens were obtained by penetration depth controlled mode and the penetration depth was set as 40 nm to exclude the Si substrate effect. The result exhibited significant difference between two samples. As shown in Fig. 5.1, it was found that the p-SiCOH dielectric film deposited by structural method had excellent mechanical properties, although dielectric constant remained very low (k ~2.1). Measured value of the elastic modulus was 13 GPa. It is considerably superior value among previously reported p-SiCOH thin films with similar dielectric constants. [110-114] In case of the film by subtractive deposition, however, elastic modulus reached 6 GPa with the identical dielectric constant. Correlatively, hardness follows the same trend as elastic modulus in all cases. The measured hardness of the structural film was 2.3 GPa and that of subtractive film was 1.2 GPa. Similar tendency was observed in creep indentation test developed by our research group.

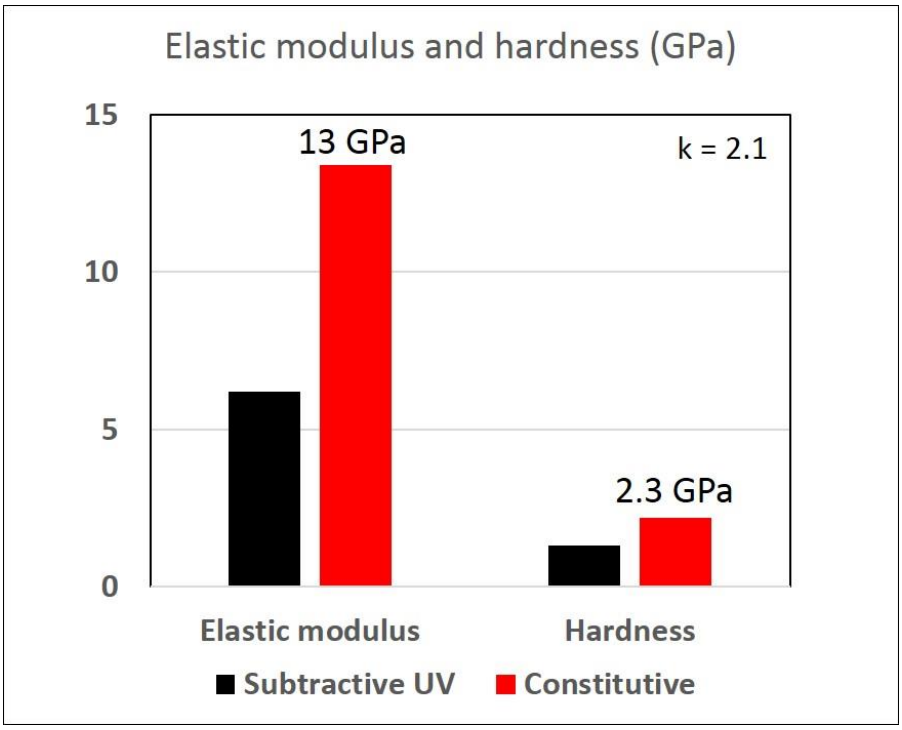

Fig. 5.1 Comparison of elastic modulus and hardness between subtractive and constitutive PLK films

5.3.2 Viscoplastic deformation

Previously, we reported the viscosplastic behavior of p-SiCOH thin film with a rate sensitive to the porosity at relevant conditions to integrated circuit fabrication. [70] This particular property, namely viscoplasticity, has not been considered to be critical for the interconnect system a decade ago. However, as the technology node is shrunken dimensional change induced by viscoplastic deformation plays an important role to achieve reliable chip interconnect system.

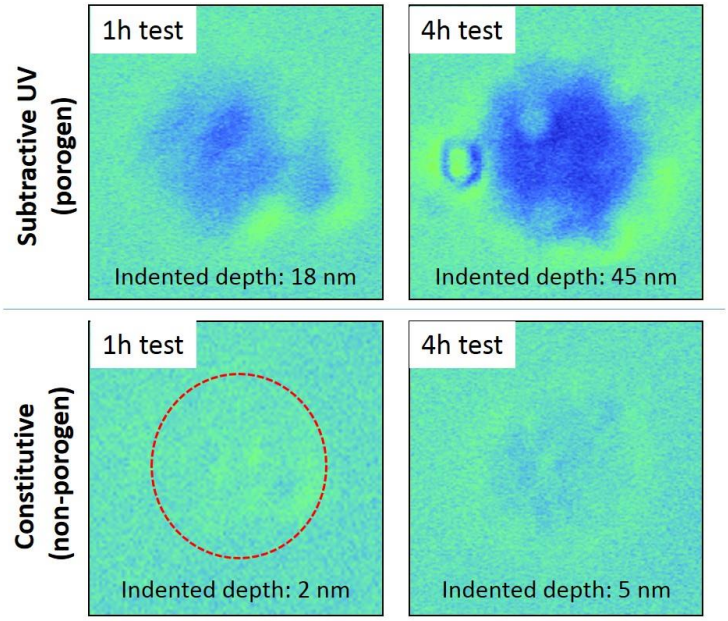

Fig. 5.2 Comparison of viscoplastic deformation between subtractive and constitutive p-SiCOH films

A series of surface profile images shown in Fig. 5.2 presented the comparison of deformation behavior and indentation depth in p-SiCOH films and its sensitive dependence on fabrication methods. The results clearly showed that the degree of deformation by indentation, visible as the dark contrast, increased with test time. It was noteworthy that gradual increase in the indentation depth with time was clearly evidencing the occurrence of viscoplastic deformation in subtractive film. However, important result to notice carefully is the fact that the viscoplastic behavior of structural film displayed the irrelevance with permanent deformation with the identical thermo-mechanical stress. Our previous study on the viscoplastic deformation rate for the subtractive films revealed that even the film with dielectric constant of ~2.7 (porosity: ~20 %) exhibited some level of viscoplasticity. However, even though the structural film had ~30 % porosity and far lower dielectric constant, it had much higher resistance against thermo-mechanical stress, which can lead to timely implementation of ultralow-k dielectrics into the interconnect system.

5.3.3 Thermo-mechanical resistance

Fig. 5.3 showed the comparison of the change in film thickness and dielectric constant with respect to thermal anneal process and oxidative plasma exposure between subtractive and structural p-SiCOH films. It is to examine the thermal stability and its correlation to electrical reliability. Additionally, plasma-induced shrinkage and dielectric constant change were indicated in the same plots because oxidizing plasma exposure induces the porous film to be densified and hydrophilic, leading to the increase in dielectric constant.

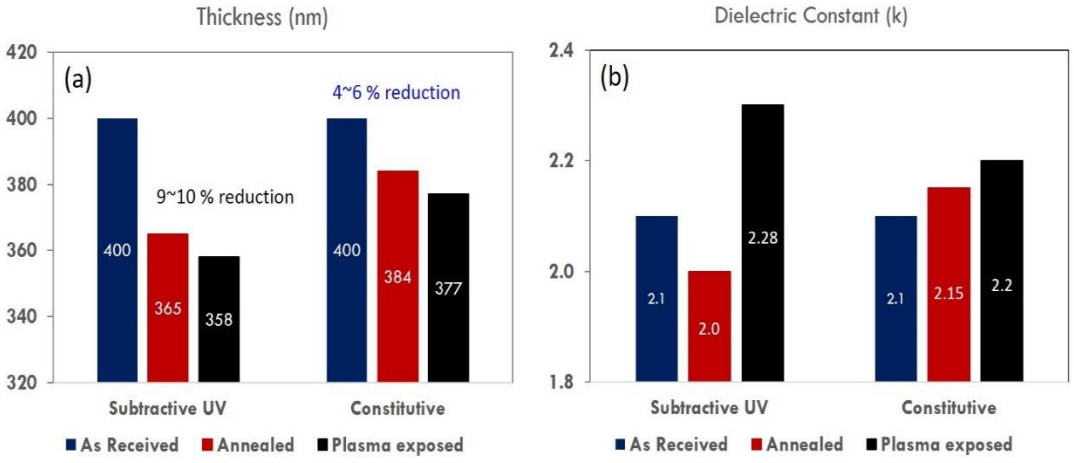

Fig. 5.3 Comparison of the change in dielectric constant and thickness with respect to anneal and plasma exposure between subtractive and constitutive PLK films

This is one of major concerns in the integration process. Annealing temperature and time were 400°C and 1 h, respectively. Plasma source and power used in this study were O_2/Ar and 50 W, respectively and plasma exposure time was 20 min. As shown in Fig. 5.3(a), the thickness reduction of subtractive film after thermal annealing was about 10 % and that of structural film was 4 %. Basically, 4 % thickness reduction is superior to that of previously reported p-SiCOH films. [111,112] Also, this trend in thickness reduction was consistent with the result of plasma

exposed films, indicating that damage formation caused by thermo-mechanical stress was diminished in the structural film. It is assumed that possible scenarios responsible for the acceleration of thermal reduction are related to the pore size, distribution, and interconnectivity of pores. Generally, the porosity incorporation into a dielectric material increases its active surface area, rendering it more susceptible to the extrinsic damage from thermal stress and reactive chemicals used in plasma etch and ash during the BEOL (Back End of Line) process. Thus, its possibility to be damaged becomes more remarkable when the pore size is bigger and pores are interconnected, not sealed. Due to high interconnectivity and bigger size of pores, thermal energy or oxygen radicals and ions from plasma source easily strike the pore surface and penetrate deep into the film matrix. These energy sources consume Si-$(CH_3)_X$ group on the pore surfaces, which induced pore collapse, causing the film shrinkage. However, in case of structural p-SiCOH film, it has much smaller pore size and closed pore distribution by steric hindrance, thermally-induced stress or plasma modification is merely restricted to the surface. Hence, damage formation is limited and thermal reduction appears to be decreased. This indicates that dielectric film fabricated by structural method has a better thermo-mechanical properties and is able to withstand the thermally and mechanically-induced stress during the integration process. Dielectric constant change with respect to the thermal stress and annealing and plasma exposure, meanwhile, was investigated as shown in Fig. 5.3(b). Initial dielectric constant of both films was 2.1. Comparison of the change in dielectric constant clearly demonstrated that subtractive film was more prone to be damaged by plasma exposure in terms of increase of dielectric constant. This is because decarbonization of p-SiCOH dielectrics by plasma exposure occurs. Si-CH_3 bonds are broken, creating dangling bonds that can react with moisture to form Si-OH (silanol) or with hydrogen to form Si-H (silane). Silanol groups make the film surface hydrophilic, and the polarization of silanol and moisture uptake not only increase in dielectric constant but reconfigure chemical bond network. However, dielectric constant change by thermal annealing process displayed a countertrend. This is assumed that labile porogen residue (; trapped porogen)

remained in the backbone crosslinks is removed during thermal annealing, which contributes the decrease in dielectric constant.

5.3.4 Study of structural configuration

To understand the fundamentals of structural difference between subtractive and structural films, FTIR measurements were carried out as illustrated in Fig. 5.4. Si-O peak at 1030 cm^{-1} was observed in dielectric films, which indicates backbone structure of p-SiCOH dielectrics. And the CH_x (x = 1-3) stretching peaks, which indicate aliphatic chains, were detected at 2930 and 2970 cm^{-1}. It could be related to the porogen fragments which were unstable and labile. Peak at 1380 cm^{-1} arises from Si-free CH_2. In case of subtractive film, it represents the trapped porogen whereas in case of structural film, it exhibits the unreacted precursor. From comparison of these two peaks, subtractive film appeared to contain more porogen residue, supporting the fact that dielectric constant decreased after annealing process because the trapped porogen was removed. The absorption peaks at 754, 1260 cm^{-1} represented of $(Si\text{-}CH_3)_X$ vibrations. More terminal –C bonds in these peaks mean more nano-pores in the film matrix. Based on the table interpolated in the FTIR plot, which showed the terminal –C bond proportion calculated from the peak area ratio against backbone Si-O peak, the value of structural film was higher than that of subtractive film. It suggested that the structural film had smaller size of pores since structural film had more nano-pores while the porosity of two different films was identical. At this point, the uniformity of pore distribution was not clear, however, we could draw a conclusion that the variation of thermal and mechanical properties between the films used in the present study was primarily related to the difference of pore size and configuration.

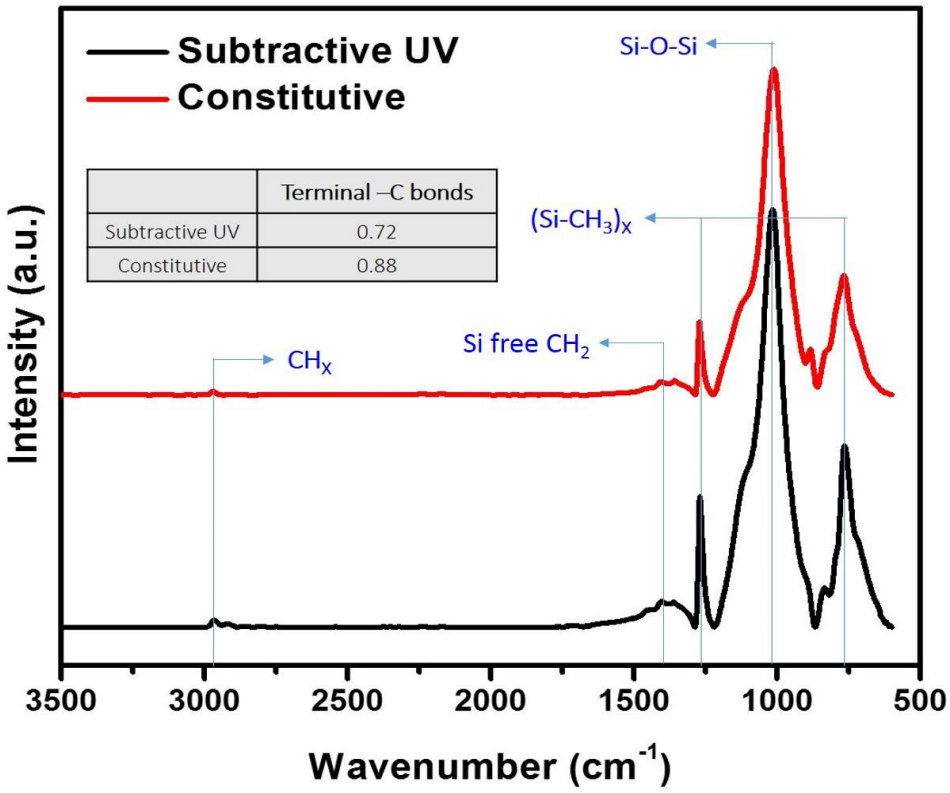

Fig. 5.4 FTIR spectra between subtractive and constitutive PLK films

Fig. 5.5 showed the evolution of the absorption bands of Si-O-Si with deconvoluted peak information based on the assumption that all peaks perfectly follow the Gaussian function and have the same FWHM. The Si-O-Si bonding configuration can be separated into three peaks, including the cage (1135 cm^{-1}, Si-O-Si~150º), the network (1063 cm^{-1}, Si-O-Si~140º), and the linear or sub-oxide (1023 $cm^{-1,}$ Si-O-Si<140º) peaks. [76] According to the area ratio of the fitted sub-peaks, the relative concentrations of all the components are computed. The comparison of structural morphology evolution demonstrated that cage-like structure in structural film appeared to be stronger than subtractive film, which is the indicative of the increase in free volume of the film matrix or the decrease in dielectric constant. Due to the large Si-O-Si bridging angle, the increase in cage-like structure contributes primarily to the formation of pores and the reductions of dielectric constant. [90] And linear structure is involved in the mechanical strength depending on the symmetrical arrangement and crosslinking. [95] Thus, it can be suggested that the

increased linear structure in structural film correlates to the enhancement of mechanical properties based on the FTIR study.

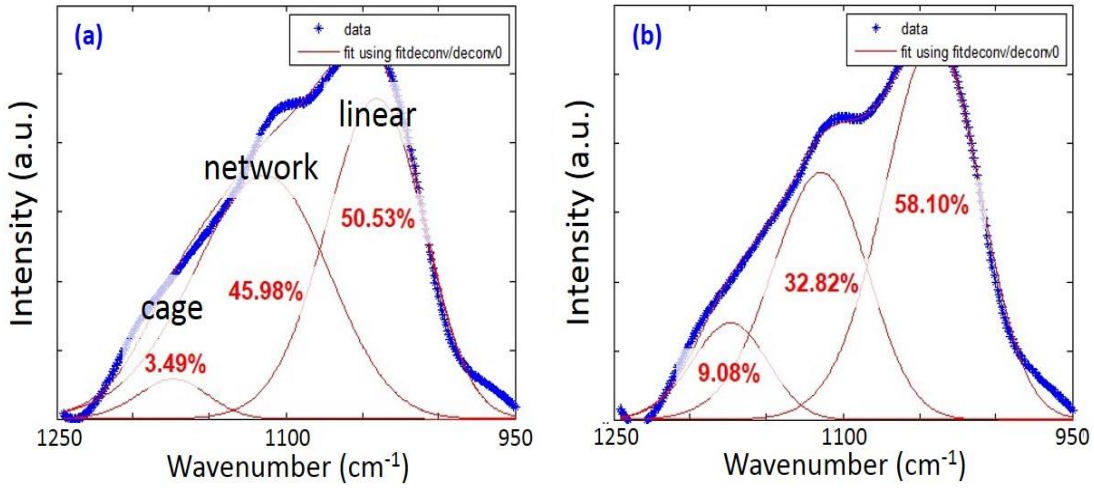

Fig. 5.5 Deconvolution of Si-O-Si backbone peak in FTIR spectra; (a) subtractive film, and (b) structural film

Different aspect of thermos-mechanical robustness in the structural film matrix was evidenced in Fig. 5.6-7. Fig. 5.6 showed the integrated peak area change of Si-O-Si (950 ~ 1250 cm^{-1}) and CH_X absorption (2950 ~ 3000 cm^{-1}) in FTIR after thermal annealing and plasma exposure. First, from the Si-O-Si backbone peak area change shown in Fig. 5.6(a), peak area of structural film remained almost the same against the thermal annealing and plasma exposure whereas that of subtractive film exhibited a sharp drop. This is resulted from the breakage of backbone structure or damage formation induced by external stress. As similarly, CH_X peak area of subtractive film had a faster rate of decrease with respect to thermal annealing process and plasma exposure compared with that of structural film. As exhibited, this is an obvious indication that subtractive film is more sensitive to the process-induced damage and structural film has a solid morphology in terms of pore distribution. It can be assumed that structural film produces not only smaller size of pores in the film matrix but also closed pore distribution with little

interconnectivity, leading to higher resistance to be spoiled by any kinds of stress during BEOL processes.

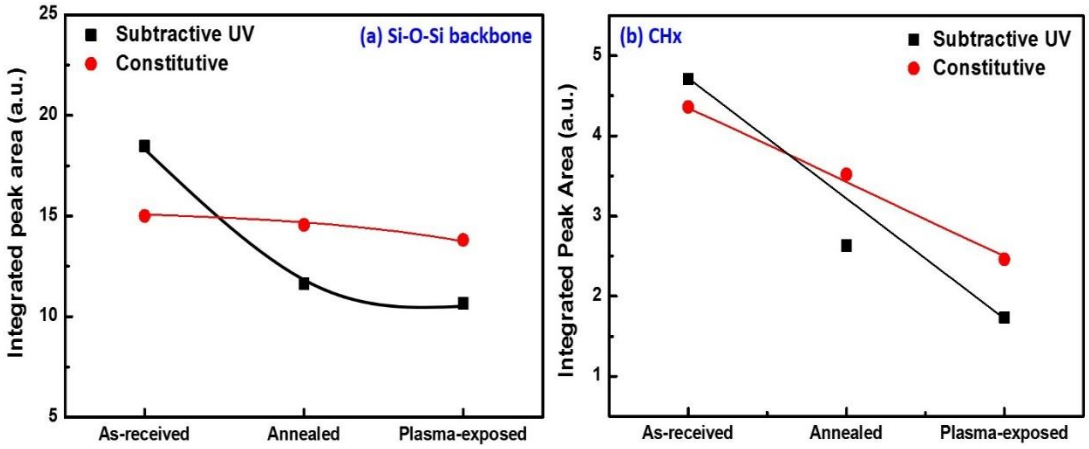

Fig. 5.6 Peak area variations of (a) Si-O-Si, and (b) CHx after anneal and plasma exposure

Depth profiling of Si atom in vertical direction to the film by using XPS was also evaluated to evidence the robustness of structural film matrix as shown in Fig. 5.7. XPS measurements were collected by means of a monochromatic Al Kα radiation and film surface sputtering with Ar ion was applied in order to examine the depth profile of Si. Since the SiCOH film was deposited on top of Si substrate with the same thickness, time-dependent scanning normal to the Si substrate provided the time to reach the substrate. If the film matrix has the strong configuration, it will take longer to strike the Si substrate. Theoretically, the Si 2p spectra consists of five components: SiO_4 (104.9 eV), SiO_3 (103.7 eV), SiO_2 (102.6 eV), SiO_1 (101.7 eV), and SiO_0 (100.6 eV). [115] And the peak at 98.5 eV is ascribed to the Si signature from the substrate. Important result to note from Fig. 5.7 is the fact that Si signal from the substrate along the z direction comes out first in case of subtractive film. It was detected after 10 min sputtering in subtractive film while structural film exhibited the identical signal after 16 min sputtering. Also, equally noticeable was the fact that overall peak intensity of Si 2p was much higher in structural film.

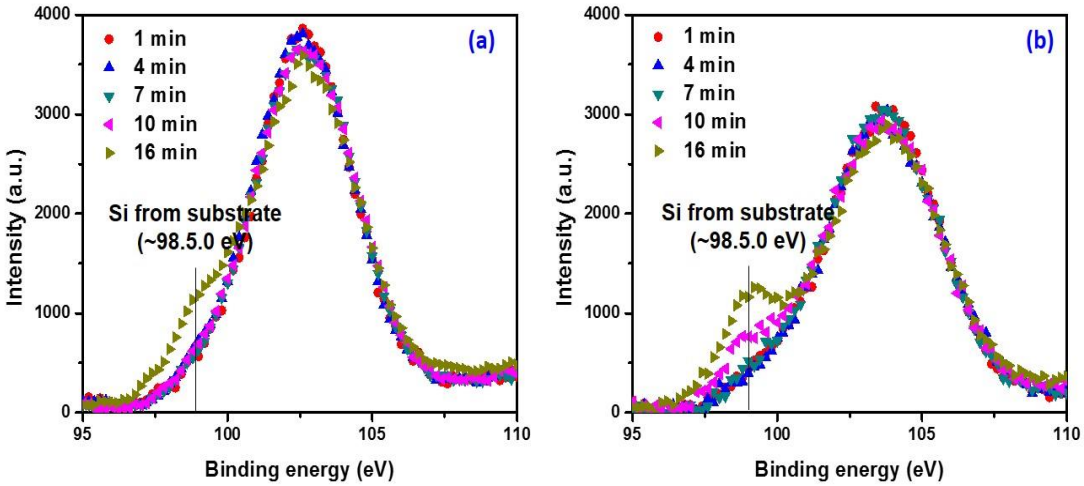

Fig. 5.7 Depth profile of Si atom in vertical direction to the films; (a) structural film, and (b) subtractive film

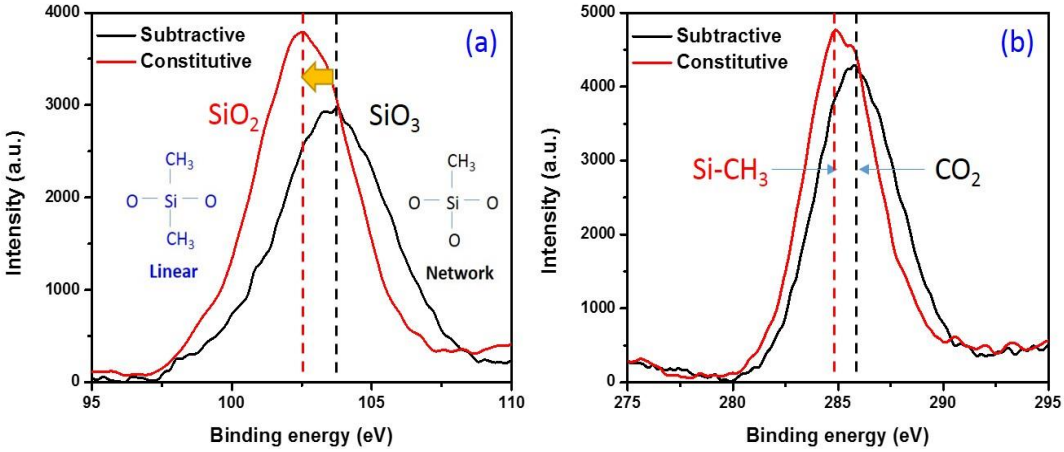

Fig. 5.8 Peak shift of (a) Si 2p, and (b) C 1s

Details of peak shift and intensity change in Si 2p peak information was described in Fig. 5.8(a). In terms of peak intensity, structural film had increased value although binding energy was shifted toward lower value. This result revealed the probability that the dielectric film fabricated

by structural method had high film density, contributing to the mechanical stability. Although binding energy was slightly decreased, however, it was considered that higher density cancelled out the decrease of binding energy. In addition, the occurrence of peak shift with the deposition method showed that the majority of Si component was SiO_3 in subtractive film, but it transformed into SiO_2 in structural film. In this case, it is assumed that the linear Si-O configuration is connected to methyl groups fully and a chain-like structure is formed in structural film. [95] Thus, symmetric bonding configuration of oxygen and methyl group to the Si reduces the polarity and also, more population of methyl groups in the unit backbone structure creates more porosity. This is the feasible explanation that structural film has superior mechanical properties while keeping a lower dielectric constant at the same time. The C 1s spectra were studied to support our mechanism as shown in Fig. 5.8(b). Basically, the C 1s peak is divided into four components: CSi_n (283.5 eV), $Si–CH_3$ (284.5 eV), CO_1 (285.3 eV), and CO_2 (286.3 eV). [115] From the peak assignment, the majority of the C moiety was $Si\text{-}CH_3$ in structural film, which was in good agreement with the peak area ratio of terminal –C bonds as discussed in Fig. 5.4.

Enhancement of these properties, which refer to elastic modulus, hardness, and thermally-induced shrinkage, is essential to increase the reliability and performance of electronic devices. As it turns out, structural deposition approach is feasible for the introduction of smaller nano-pores with little or no interconnectivity. Due to the closed pore system, thermally-induced stress and plasma-induced damage is restricted merely to the surface of the dielectric film. This is attributed to the stable siloxane (Si-O-Si) backbone and the terminally bonded methyl group attached to silicon ($Si\text{-}CH_3$), inducing steric hindrance that lowers the density of the films. The low dielectric constant and mechanical stability are closely involved with the formation of the Si-O-Si cage-like structure and an appropriate combination of stable Si-O-Si, $Si\text{-}CH_3$ groups. Based on the FTIR and XPS spectra, it was concluded that the formation of the Si-O-Si cage-like structure was enhanced by structural method.

5.4 Summary

Robustness of p-SiCOH dielectric materials to withstand thermo-mechanical stress during device integration process is the key to increase the reliability and performance in microelectronics. The present study clearly indicated that thermo-mechanical properties and resistance against the process damage significantly improved by using structural deposition method. Elastic modulus was enhanced up to 13 GPa while lowering the dielectric constant to be ~2.1. In addition, film thickness reduction from thermal stress and plasma exposure was remarkably increased, which leads to the minimization of BEOL damage during the process. This implies p-SiCOH film deposited by structural method can be used without sustaining integration damage in the BEOL integration process.

Chapter 6

CONCLUSION AND FUTURE WORK

6.1 Conclusion

Plasma-induced damage in etching and ashing process poses a great challenge for integration of the porous low-k material into the on-chip interconnects. Particularly, viscoplastic deformation is discovered in porous low-k films at the relevant temperature to BEOL integration process and it is found that plasma-induced damage accelerates the deformation rate. The troublesome feature of the viscoplasticity is the fact that it is slowly progressing that its occurrence becomes difficult to identify. Further, the failure in PLK/Cu integration due to the viscoplastic deformation in PLK layer appears much later stages of processing or in use condition. Therefore, such factors must be removed before PLK proceeds to next process.

The objective of this dissertation is to study the mechanism of plasma-induced damage to porous low-k dielectrics and to develop method/process to restore the loss of properties as dielectrics for enhancing stability of the dielectrics in advanced microelectronics. The studies conducted in this dissertation follow three approaches.

One approach is to investigate the mechanism of the plasma-induced interaction on porous low-k materials with the aim to find the effective way to repair plasma-induced damage. (Chapter 3) Based on the result that the viscoplasticity is due to combination of chemical reaction and the viscous flow, the resistance against viscoplasticity can be achieved by eliminating or reducing the Si-OH or Si-H bond. With reduction in Si-OH or Si-H bond, the colony size increases and so does the PLK's resistance against the viscous flow.

The other approach is to develop process to recover the low-k dielectric properties of plasma-damaged PLK in order to improve the stability of porous low-k dielectrics for integration into interconnect structure. (Chapter 4) There appears to be several routes to restore the degraded properties of dielectrics, including a use of low-energy radiation and thermo-chemical treatment with silylating agent to remove Si-OH or Si-H and restore the cross-linked chemical

bond configuration. Silylation treatment, however, they offer limited effectiveness, and also, they are not easy to incorporate into the flow of integration processes. Soft x-ray radiation is found to be effective in terms of the increase in crosslinking and resistance against viscoplastic deformation, yet hydrophilic surface induced by oxidizing plasma damage is not improved remarkably. From these points of view, inert Ar plasma treatment is employed in order to correct the limitations of silylation process and x-ray cure. It is suggested that the immediate event of an Ar plasma beam radiation is to deposit energy from the plasma species (ions, electrons) and this energy input produces the excited state species because Ar cannot chemically react with the film matrix. As a consequence, the radical sites are generated at the less stable area such as colony boundary or pore surface with the decay of the excited species, leading to the production of free radicals by an energy transfer to the bonds which are to be broken. Then, the activated sites experience chemical bond rearrangement by chain-scission, branching, or cross-linking. In our case, it is proposed that crosslink with C is involved with silylmethylene (Si-$(CH_2)_x$-Si) groups and it is turned out that some of these groups are converted to methyl groups terminally bonded to siloxane backbone structure under 300~400^oC by reaction with –OH, and simultaneously creating a new Si-O-Si crosslink. Property restoration is fundamentally able to be achieved by removing Si-OH groups and inducing cross-linking with –C simultaneously.

Finally, investigation of robust chemical structure that is less damaged during BEOL integration process including plasma-induced damage is performed and the enhancement of dielectric properties is evaluated. (Chapter 5) Pores fabricated by removal of organic fragments (porogen) in ultralow-k dielectric film produce lower mechanical properties as well as incur electrical degradation during chip integration process because pore surface acts as a reactive path for moisture uptake or Cu diffusion. Furthermore, UV cure used in porogen removal simultaneously breaks the skeleton crosslinks in silica matrix. To overcome this issue, ultralow-k film with self-organized molecular pores due to steric hindrance is deposited by using particular precursors. Dielectric constant of ~2.1 with superior modulus (>13 GPa) is achieved by inducing

uniform distribution of porosity and lower polarizability, which modulus is significantly improved compared with that of porous SiCOH film fabricated by subtractive method with same k value. Also, it shows enhanced resistance against plasma-induced damage and thermally-induced film shrinkage. Analysis of the film structure indicates that symmetric linear Si–O molecular chains with $–CH_3$ terminal bonds are grown and cross-linked to each other in the film, leading to the decrease in dipole moment and improvement in the mechanical properties. It is achieved by incorporating the molecular pores in a uniform distribution manner into the backbone structure.

6.2 Future work

The subjects of this work are of technologic and scientific value. Although the work is extensive and detailed, it is far from complete and needs in-depth exploration. In many aspects, it may serve as a starting point for future work. The structure-property relationship is of fundamental interest in materials science and engineering. Advances in computational technology make it possible to model the microstructure of more realistic materials. Our quantitative structural analysis should come in handy in these simulations to the prediction of many properties such as modulus, hardness, viscoplasticity, dielectric constant, and so on. As the technology moves on, interlayer dielectrics will become increasingly porous. Therefore, pore structure including pore size, distribution, morphology, and connectivity should be carefully characterized and quantitatively analyzed to provide useful guidance for process optimization. The optimization of the matrix structure is a key factor in the manufacturing of viable ultralow-k dielectric films with robustness.

From these perspectives, characterization of pore morphology and its in-situ change with common BEOL integration processes is essential to develop and optimize both low-k dielectric films and processes. The structural parameters of interest include overall density, density of matrix material, pore size and pore distribution of periodicity. As reported in many

researches, cracking, fracture and delamination are still major concerns in implementation of ultralow-k dielectrics. Additionally, viscoplastic behavior is newly found at the relevant condition to BEOL integration process. It is obvious that these concerns will be more serious as porosity is increased, thus quantitative investigation of pore structure and its correlation to the property change is essential for reliable on-chip interconnect structure.

Structural information about pores gained from GISAXS or POSITRON beam technique can then be related to the change of thermo-mechanical stability of the film and also to the fundamental bond network of the film. The data will also help in differentiating between the effect of morphological change during pore formation (built-in change; pore incorporation inevitably reconfigures the chemical bond structure) and that during integration process (post-process change) on thermo-mechanical instability. In-situ observation in particular will enable us to track such mechanisms and provide an array of information useful for enhancing stability of the dielectrics in advanced microelectronics. Finally, the outcome of this study will demonstrate the usefulness of GISAXS to microelectronics community and may stimulate study of other planned materials with a similar scope.

References

[1] International Roadmap for Semiconductors (ITRS), Semiconductor Industry Association, 2009

[2] D. Edelstein, J. Heidenreich, R. Goldblatt, W. Cote, C. Uzoh, N. Lustig, P. Roper, T. McDevitt, A. Stamper, W. Motsiff, A. Simon, J. Dukovic, R. Wachnik, P. McLaughlin, T. Katsetos, H. Rathore, R. Schulz, L. Su, S. Luce, N. Rohrer, and J. Slattery, Tech. Dig. IEEE IEDM, 376 (1997)

[3] R. Rosenberg, D. C. Edelstein, C. –K. Hu, and K. P. Rodbell, "Copper metallization for high performance silicon technology", Annu. Rev. Mater. Sci. 30 229-62 (2000)

[4] Saraswat, K.C. and F. Mohammadi, Effect of Scaling of Interconnections on the Time-delay of VLSI Circuits, IEEE Transactions on Electron Devices, 1982. 29(4): p. 645-650

[5] Morgen, M., et al., Low dielectric constant materials for ULSI interconnects. Annual Review of Materials Science, 2000. 30: p. 645-680

[6] Bohr, Mark T., Interconnect scaling, The real limiter to high performance ULSI

[7] C. Kittel, Introduction to solid state physics. Wiley, 1996

[8] K. Maex, M. R. Baklanov, D. Shamiryan, F. Iacopi, S. H. Brongersma, and Z. S. Yanovitskaya, "Low dielectric constant materials for microelectronics", J. Appl. Phys. 93, 8793-8841 (2003)

[9] Grill, A. Journal of Applied Physics. 93, no. 3. 2003. p. 1785

[10] Kwak SI, Jeong KH, Rhee SW. 2004. Nanocomposite low-k SiCOH films by direct PECVD using vinyltrimethylsilane. J. Electrochem. Soc. 151:F11–16

[11] Tada M, Kawahara J, Hayashi Y. 2001. Characterization of plasma-polymerized divinylsiloxane benzocyclobutene (DVS-BCB) polymer film. Mater. Res. Soc. Conf. Proc. ULSI XVI: 579–85

[12] Tada M, Yamamoto H, Ito F, Takeuchi T, Furutake N, Hayashi Y. 2007. Chemical structure effects of ring-type siloxane precursor on properties of plasma-polymerized porous SiCOH films. J. Electrochem. Soc. 154: D354–61

[13] Kawahara J, Kinimi N, Kinoshita K, Nakano A, Komatsu M, et al. 2007. An organic low-k film deposited by plasma-enhanced copoloymerization. J. Electrochem. Soc. 154: H147–52

[14] Wu Q, Gleason KK. 2003. Plasma-enhanced CVD of organosilicate glass (OSG) films deposited from octamethyltrisiloxane, bis(trimethylsiloxy)methylsilanes, and 1,1,3,3-tetramethyldisiloxane. Plasmas Polym. 8:31-41

[15] R. M. A. Azzam, N. M. Bashara. Ellipsometry and Polarized Light. Elsevier, Amsterdam, 1977

[16] C. Le Cornec, F. Ciaramella, V. Jousseaume, P. Leduc, A. Zenasni, and G.Passemard. K Value Improvement of ULK Dielectrics by Wet Activation. Microelectronic engineering, Vol.83, No.11-12, 2006, p. 2122-2125

[17] W. Volksen, R. D. Miller, and G. Dubois, "Low dielectric constant materials", Chemical reviews, vol. 110, no. 1, pp. 56-110, Jan. 2010

[18] A. Grill, "Porous p-SiCOH Ultralow- k Dielectrics for Chip Interconnects Prepared by PECVD," Annual Review of Materials Research, vol. 39, no. 1, pp. 49-69, Aug. 2009

[19] G. Meggy, W.L. Peter, L. Xia, and E. Yieh. The Case for CVD Low-K Technology. Semiconductor Fabtech, 15th Edition, http://www.fabtech.org, 2005, p.179-183

[20] R. Vrtis, MRS Tutorial, Spring, 2003

[21] J.G. Ryan, Copper and Low-k Dielectric Integration Challenges, SEMICON West 2000

[22] K. Carter, The road to Low Dielectric Constant Materials, Proceedings from the Ninth Meeting of the Symposium on Polymers for microelectronics, Wilmington DE 2000

[23] National Technology Roadmap for Semiconductors, Semiconductor Industry Association (2004)

[24] S. Lin, et al., Proceedings of the Int. Interconnect Tech. Conf. (IITC 2001), p. 146-148

[25] S. J. Martin et al., Advanced Materials 12, 23 (2000) p. 1769-1778

[26] G. Wang, et al., IEEE Trans. Dev. Mat. Rel. 3, 4 (2003) p. 119-128

[27] F. Iacopi, et al., Microelectron. Eng. 75 (2004) p. 54-62

[28] C. Waldfried, et al., Proceedings of the Int. Interconnect Tech. Conf. (IITC 2002), p. 226-228

[29] H. Miyajima, et al., Proceedings of the Int. Interconnect Tech. Conf. (IITC 2004), p. 222-224

[30] E. Mickler, et al., Proceedings of the Int. Interconnect Tech. Conf. (IITC 2004), p. 190-192

[31] A. Delan, M. Rennau, S.E. Schulz and T. Gessner, Microelectron. Eng. 70 (2003) p. 280-284

[32] T.-Y. Chiang, K. Banerjee and K.C. Saraswat, Technical Digest. International Electron Devices Meeting, (IEDM 2000), p. 261-264

[33] H. Miyajima, R. Katsumata, Y. Nakasaki, Y. Nishiyama and N. Hayasaka. Water Absorption Properties of Fluorine-Doped SiO2 Films Using Plasma-Enhanced Chemical Vapor Deposition. Jpn. J. Appl. Phys, Vol.35, Part 1, No.12A., Dec. 1996, p.6217 - p.6225

[34] S. J. Martin, J. P. Godschalx, M. E. Mills, E. O. Shaffer II, P. H. Townsend. Development of a Low-Dielectric-Constant Polymer for the Fabrication of Integrated Circuit Interconnect, Adv. Mater. Vol.12, No.23, December, 2000, p.1769 - p.1778

[35] J. Yao, A. Iqbal, H. Juneja, and F. Shadman. Moisture Uptake and Outgassing in Patterned and Capped Porous Low-k Dielectric Films. Journal of The Electrochemical Society, Vol. 154, No.10, 2007, p.G199 - p.G206

[36] A. Iqbal, H. Juneja, J. Yao, and F. Shadman. Removal of Moisture Contamination from Porous Polymeric Low-k Dielectric Films. AICHE, Vol. 52, No.4, 2006, p.1586 - p.1593

[37] Shaw, T.M., et al. Advanced Metallization Conference 2003 Proceeding (AMC2003) 2003. Montreal, Quebec, Canada and Tokyo, Japan Materials Research Society, Warrendale, PA

[38] Guyer, E.P., J. Gantz, and R.H. Dauskardt, Aqueous solution diffusion in hydrophobic nanoporous thin-film glasses. Journal of Materials Research, 2007. 22(3): p. 710-718

[39] Tsui, T.Y., A.J. McKerrow, and J.J. Vlassak, The effect of water diffusion on the adhesion of organosilicate glass film stacks. Journal of the Mechanics and Physics of Solids, 2006. 54(5): p. 887-903

[40] Lin, Y.B., T.Y. Tsui, and J.J. Vlassak, Water diffusion and fracture in organosilicate glass film stacks. Acta Materialia, 2007. 55(7): p. 2455-2464

[41] H. Yanazawa, T. Fukuda, Y. Uchida, I. Katou. Water Sorbability of low-k Dielectrics Measured by Thermal Desorption Spectroscopy. Surface Science, Vol. 566–568, 2004, p. 566 - 570

[42] A.A. Kumbhar, S.K. Singh, and R.O. Dusane. Enhancement of Moisture Resistance of Spin-

on Low-k HSQ Films by Hot Wire Generated Atomic Hydrogen Treatment. Thin Solid Films, 501 (May, 2006) 329 – 331

[43] K. Yonekura, et al., J. Vac. Sci. Technol. B22, 2 (2004) p. 548-553

[44] D. Shamiryan, et al., J. Vac. Sci. Technol. B20, 5 (2002), p. 1923-1928

[45] E. Kondoh, et al., J. Vac. Sci. Technol. B18, 3 (2000), p. 1276-1280

[46] O. Louveau, et al., Microelectron. Eng. 73-74 (2004), p. 351-356

[47] Y. Furukawa, et al., Microelectron. Eng. 76 (2004), p. 25-31

[48] A. Matsushita, et al. Proceedings of the Int. Interconnect Tech. Conf. (IITC 2003), p.147-149

[49] W. Chen, et al., J. Electrochem. Soc. 151, 8 (2004), F182-F188

[50] M. Assous, et al., Proceedings of the Int. Interconnect Tech. Conf. (IITC 2003), p.97-99

[51] V. Arnal, et al., Proceedings of the Int. Interconnect Tech. Conf. (IITC 2004), p.202-204

[52] T. Furusawa, et al., Proceedings of the Int. Interconnect Tech. Conf. (IITC 2003), p.195-197

[53] O. Hinsinger, et al., Technical Digest. International Electron Devices Meeting, (IEDM 2004), p. 317-320

[54] B. Xie & A.J. Muscat, Microelectron. Eng. 76 (2004), p. 52-59

[55] B.P. Gorman, et al., J. Vac. Sci. Technol. B22, 3 (2004), p. 1210-1212

[56] Y.S. Mor, et al., J. Vac. Sci. Technol. B20, 4 (2002), p. 1334-1338

[57] C.N. Yeh, et al., Proceedings of the Int. Interconnect Tech. Conf. (IITC 2003), p. 192-194

[58] R. Kanamura, et al., Proc. VLSI (2003), p. 107-108

[59] A. Grill, S. Gates, C. Dimitrakopoulos, V. Patel, S. Cohen, Y. Ostrovski, E. Liniger, E. Simonyi, D. Restaino, S. Sankaran, S. Reiter, A. Demos, K. S. Yim, V. Nguyen, J. Rocha and D. Ho, Proc. IEEE Int. Interconnect Technol. Conf., 2008, 7, 28

[60] S. Nitta, et al., Technical Digest. International Electron Devices Meeting, (IEDM 2004), p. 321 –324

[61] S.H. Rhee, M.D. Radwin, M.F.ng, J.I. Martin, and D. Erb, Appl. Phys. Lett. 83, 2644 (2003)

[62] Y. Li, Z. Tokei, J. V. Aelst, L. Carbonell, H. R. Baklanov, O. Richard, H. Bender, G.

Groeseneken, K. Maex, Semicond. Sci. Technol. 22 (2007) 320-325

[63] E. Taglauer, Appl. Phys. A 51 (1990) 238

[64] D. Kim, Y. Lee, N. Park, Appl. Phys. Lett. 69 (1996) 2779

[65] S. Sugahara, K. Usami, M. Matsumura, Jpn. J. App. Phys. 38 (1999) 1428

[66] Michael S. Silverstein, Michal Shach-Caplan, Maria Khristosov, Tuval Harel, Plasma Process. Polym. 2007, 4, 789–796

[67] Sun, J.N., et al., Appl. Phys. Lett., 2002. 81(8) 1447-1449

[68] Lee, H.J., et al., Appl. Phys. Lett., 2007. 91(17)

[69] J.R. Combes, L.D. White, C.P. Tripp, Langmuir 15 (1999) 7870

[70] E. H. Zin, W.H. Bang, E. T. Ryan, S. King, and C.-U. Kim, Appl. Phys. Lett., 102, 221909 (2013)

[71] D. M. Meng, N. L. Michael, Y. J. Park, and C. U. Kim, *Appl. Phys. Lett*. 88, 261911 (2006)

[72] M. S. R. Heynes, H. Rawson, *Phys. Chem. Glass*. 2/1 (1961) 1

[73] R.W. Douglas, W.L. Armstrong, J.P. Edward and D. Hull, *Glass Technol*. 6 (1965) 52

[74] Smith, R.S., The Effect of Ultra-violet Light Curing on the Molecular Structure and Fracture Properties of an Ultra Low-k Material. Dissertation, The University of Texas at Austin, 2007

[75] Gunzler, H. and H.-U. Gremlich, IR Spectroscopy: An Introduction. WILEYVCH, 2002

[76] A. Grill and D.A. Neumayer, J. Appl. Phys., 94, 6697 (2003)

[77] Sen, P.N. and M.F. Thorpe, Physical Review B, 1977. 15 (8) 4030-4038

[78] Grill, A. and V. Patel, Appl. Phys. Lett., 2001. 79(6) 803-805

[79] M. P. Marder, “Condensed Matter Physics,” *John Wiley & Sons, Inc.*, 2000

[80] Rudawska, A. and E. Jacniacka, Analysis for determining surface free energy uncertainty by the Owen-Wendt method. International Journal of Adhesion and Adhesives, 2009, 29(4): p. 451-457

[81] Ohring, M., Materials Science of Thin Films. Academic Press, Inc., 2002

[82] Owens, D.K. and R.C. Wendt, *Estimation of Surface Free Energy of Polymers.* Journal of

Applied Polymer Science, 1969. 13(8): p. 1741

[83] http://www.ksvltd.com/content/index/keysfe, KSV Instruments Ltd., 2010

[84] O'Neill, Hardness measurement of metals and alloys, London, Chapman and Hall, 1967

[85] J.C. Hay, A. Bolshakov, G.M. Pharr, J Mater Res. 14, (1999) 2296

[86] I.N. Sneddon, Int. J.Eng. Sci., Vol 3, 1965, 47-56

[87] G.M. Pharr, Mater, Sci, Eng, A,, Vol 253, 1998, p 151-158

[88] E. Taglauer, Appl. Phys. A 51 (1990) 238

[89] E. Kondoh, M.R. Baklanov, H. Bender, K. Max, Electro-Chem. Solid State Lett. 1 (1998) 224

[90] A. Grill and V. Patel, J. Electrochem. Soc. 153, F169 (2006)

[91] E. T. Ryan, J. Martin, K. Junker, J. Wetzel, J. N. Sun, and D. W. Gidley, J. Mater. Res. 16, 3335 (2001)

[92] S. Sugahara, K. Usami, M. Matsumura, Jpn. J. App. Phys. 38 (1999) 1428

[93] J.R. Combes, L.D. White, C.P. Tripp, Langmuir 15 (1999) 7870

[94] Zenasni et al., J. Appl. Phys. 102, 094107 (2007)

[95] Y. Kikuchi, A. Wada, T. Kurotori, M. Sakamoto, T. Nozawa, S. Samukawa, J. Phys. D: Appl. Phys. 46 (2013) 395203 (7pp)

[96] Zhou, Y., et al., Correlation of surface and film chemistry with mechanical properties in interconnects. Characterization and Metrology for ULSI Technology, 2003, 683: p. 455-461

[97] Jacques, J.M., et al., Fracture property improvements of a nanoporous thin film via post deposition bond modifications. Materials, Technology and Reliability of Advanced Interconnects 2005, 2005. 863: p. 61-66

[98] Abell, T., et al., Solid state MAS NMR spectroscopic characterization of plasma damage and UV modification of low k dielectric films. Mater. Res. Soc. Symp. Proc., 2005, 863

[99] Hoofman, R.J.O.M., et al., Challenges in the implementation of low-k dielectrics in the back-end of line. Microelectronic Engineering, 2005, 80: p. 337-344

[100] Abell, T. and K. Maex, Damage minimized plasma pore sealing of microporous low-k

dielectrics. Microelectronic Engineering, 2004, 76(1-4): p. 16-19

[101] R.M. Rance, R.D. Short, J. Chem. Soc., Faraday Trans. 93 (1997) 3713

[102] Asefa. T et al. Angew. Chem. Int. Ed. (2000) 39, 1808

[103] K. P. Cheung, Plasma Charging Damage (Springer-Verlag, Berlin, Germany, 2000)

[104] D. Rats, V. Hajek, and L. Martinu, Thin Solid Films 340, 33 (1999)

[105] H. Chaabouni et al., Microelectronic Engineering 84 (2007) 2595-2599

[106] Jae Mok Jung et al., Microelectronic Engineering 87 (2010) 1680-1684

[107] A.M. Urbanowicz et al., Journal of Applied Physics 107, 104122 (2010)

[108] F. Iacopi et al., Journal of Applied Physics 99, 053511 (2006)

[109] Hatton, B.D., Landskron, K., Hunks, W.J., Bennett, M.R., Shukaris, D., Perovic, D.D. and Ozin, G.A. Materials chemistry for low-k materials. Mater. Today, 9, 22–31 (2006)

[110] V. Jousseaume, A. Zenasni, L. Favennec, G. Gerbaud, M. Bardet, J. P. Simon and A. Humbert, J. Electrochem. Soc., 2007, 154, G103

[111] D. D. Burkey and K. K. Gleason, J. Electrochem. Soc., 2004, 151, F105

[112] J. S. Rathore, L. V. Interrante and G. Dubois, Adv. Funct. Mater., 2008, 18, 4022

[113] G. Dubois, T. Magbitang, W. Volksen, E. Simonyi and R. D. Miller, Proc. IEEE Int. Interconnect Technol. Conf., 2005, 8, 226

[114] N. J. Trujillo, Q. Wu and K. K. Gleason, Adv. Funct. Mater., 2010, 20, 607

[115] W. Wang, D. Grozea, A. Kim, D. D. Perovic and G. A. Ozin, Adv. Mater., 2009, 21, 1

Biographical Information

Yoonki Sa gained the Bachelor's and Master's degree in the field of Materials Science & Engineering in Hongik University and his thesis is related to the superplastic behavior and mechanical properties of light metals such as Mg, Al alloy and bulk metallic glasses. He published 4 journal papers during his Master course and one of the papers was cited more than 70.

He has five and half years of industry experience in researches and developments of electronic packaging including Pb-free interconnects and its reliability evaluation test, alloy developments, high electro-migration resistant solder metallurgy, micro-bump formation and flip-chip bonding, TSV filling with molten solder. Especially, while he was working at KITECH funded by the government in Korea, he delivered more than 20 presentations.

During his PhD study at University of Texas at Arlington, he studied thermo-mechanical reliability of Cu/low-k interconnect structure and high reliable Pb-free solder alloy for flip chip application under the guidance of Prof. Choong-Un Kim. Also, he has strong background in assembly processing and equipment, integrated flow, reflow behaviors, surface finish, flux chemistry, mechanical characterizations and physics for improved solder joint integrity, failure analysis.

His sufficient career in microelectronics raised hands on skills with SEM/EDS, FTIR, SAM (Scanning Acoustic Microscopy), SMT process line (Screen printer, mounter, reflow), HALT (Highly Accelerated Life Test), Flip-chip bonder, Die saw machine, Reliability Chambers (Thermal Shock/Cycling, Vibration, HAST, etc.), XRD, GISAXS (Grazing-incidence small angle x-ray scattering), AFM, XPS, Nano-indentation, Ellipsometer, Optic profilometer, FIB, Ion-milling, Evaporator, Sputter, Shear tester (Dage 4000), Tensile tester (Instron), DSC, TMA, etc.